Doctoral Dissertation

Studies on Synthesis of New β-Cyclodextrin Dimers and their Molecular Recognition Ability in Organic Solvents

Chizuru Asahara

January 2021

Graduate School of Engineering,

Osaka University

Preface and Acknowledgements

The work of this thesis has been performed from 2012 to 2021 under the guidance of Prof. Dr. Toshiyuki Kida at Department of Applied Chemistry, Graduated School of Engineering, Osaka University. The thesis describes synthesis of new β-cyclodextrin dimers and their molecular recognition ability in organic solvents.

This thesis could not have been completed without the support from numerous people. Here, I wish to express my sincerest appreciation to all of them.

First and foremost, I would like to express my sincerest gratitude to Prof. Dr. Toshiyuki Kida for his precise guidance, helpful suggestions, educational philosophy, and hearty encouragements through this work.

I gratefully express acknowledgement to Prof. Dr. Mitsuru Akashi for his intimate guidance continuous advice and kind encouragement.

I would also like to thank Professors Dr. Michiya Matsusaki and Dr. Kazuya Kikuchi for their helpful advice and kind assistance.

I deeply appreciate Associate Prof. Dr. Tadashi Mori and Assistant Prof. Dr. Hajime Shigemitsu for their invaluable assistance based on their deeply understanding in chemistry.

I wish to appreciate Professor Dr. Hiroharu Ajiro (Nara Institute of Science and Technology), Professor Dr. Takami Akagi in the once Akashi group.

I would like to express my heartfelt thanks to Mr. Hiroshi Moriguchi, Dr. Kyoko Inoue and Dr. Hiroaki Tanaka for giving me analytic assistance at the analytical instrumentation facility.

I also with to acknowledge all the members of Kida group for their hearty encouragement and constant support.

I express special appreciation to the secretaries in out laboratory, including Ms. Yasuyo Watanabe and Ms. Kaori Matsumoto for their generous assistance.

I would like to express my sincere gratitude to Professor. Dr. Tomoko Fujiwara (The University of Memphis in USA) for accepting me as a visiting student for a month in 2013.

I would sincerely like to thank my bosses Dr. Masanobu Yoshikawa and Dr. Junichiro Sameshima (TORAY Research Center, Inc.) for giving me an opportunity to attend university and obtain a degree while working at the company.

At last but not least, I would like to express my thanks to my family, my husband Dr. Haruyasu Asahara and my cute daughter Ms. Mari Asahara for their continuous and kind support.

Chizuru Asahara

Department of Applied Chemistry
Graduate School of Engineering
Osaka University
2-1 Yamadaoka, Suita, Osaka, 565-0871, JAPAN
January, 2021

Contents

General Introduction

Molecular capsules and tubes are three-dimensional structures with an internal space isolated from the outside. Since such three-dimensional spaces exhibit unique properties, which can recognize other small molecules through non-covalent interactions, they have attracted much interest in diverse fields, including supramolecular chemistry, organic synthesis and biochemistry.[1] Using the inner three-dimensional spaces, they have been applied to separation,[2] molecular recognition,[3] reaction fields,[4] chemical sensors,[5] drug carriers,[6] and so on.

Molecular capsules possessing various internal environments have been synthesized utilizing covalent[7] or non-covalent bonds[8]. In 1983, D. J. Cram reported a molecular capsule *carcerand*,[9] which is a host molecule based on calixarene. Carcerand entraps its guests in non-equilibrium state so that they cannot escape even at high temperatures. They also developed *hemicarcerands*,[10] which encapsulate guest molecules in hydrophobic cavities, but the guests could be released without breaking any covalent bonds when the inclusion complexes were heated to a higher temperature. Since guest molecules within the inner phase of hemicarcerands are protected from the bulk phase, unstable compounds can be stabilized.[11] J. Rebek Jr. et al. reported that various molecular capsules can be formed by self-assembly. One was a supramolecular capsule like a 'soft ball' that self-assembled through inter molecular hydrogen bonding. Encapsulation of the reactants in this capsule accelerated the reaction rate of Diels–Alder reaction.[12]

Reported molecular tubes include carbon nanotubes,[13] organic molecular tubes composed of aromatic or aliphatic moieties.[14] M. Yoshizawa et al. reported the molecular tube which had a well-defined and open cylindrical cavity encircled by multiple polyaromatic panels. The molecular tube exhibited the selective recognition and binding of long hydrocarbons containing branched methyl groups and/or unsaturated carbon-carbon double bonds.[15] These previous studies have demonstrated that molecular capsules and molecular tubes realize unique and interesting functions, depending on their structures.

On the other hand, cyclodextrins (CDs), which are cyclic oligosaccharides composed of several glucose units, are common and useful hosts in host-guest chemistry and supramolecular chemistry (Fig. 1).[16] CDs form inclusion complexes with guest molecules with an appropriate size and shape in aqueous media[17] or certain polar organic media[18] via the incorporation of guests into their cavities. The molecular recognition ability of CDs has been applied to molecular sensors,[19] reaction fields,[20] drug carriers,[21] etc. In addition, because CDs also possess an asymmetric cavity derived from the constituent D-glucose units, they have enantioselective recognition ability of

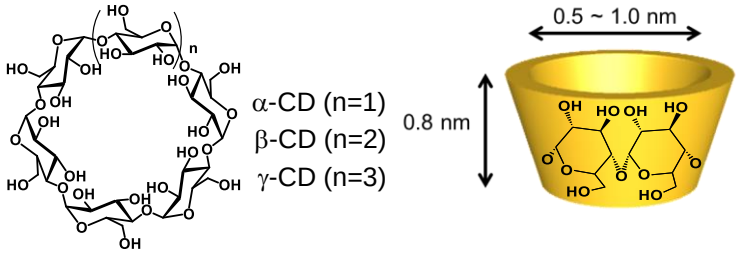

Figure 1. Chemical structures and schematic illustration of cyclodextrins (CDs).

specific chiral guests and are used as stereoselective reaction fields.[22] For example, Y. Inoue et al. reported enantio-differentiating [4 + 4] photocyclodimerization of 2-anthracenecarboxylate using a γ-CD cavity. The enantioselectivity of the photodimerization originated from the difference in the stability of the diastereomeric pair of the orientational isomers of the 1:2 inclusion complex in the ground state. These isomers were the precursors of the enantiomers of a specific chiral cyclodimer.[23]

Many kinds of CD derivatives have been synthesized to improve the ability of CDs.[24] For instance, CD dimers where two CD molecules were connected by the appropriate linkers showed a high inclusion ability toward bulky guests that were too large to fit well in the cavity of the original CD (Fig. 2a).[25] In addition, a stable inclusion complex could be formed by utilizing the interaction between an included guest into a CD dimer cavity and a linker connecting two CD molecules (Fig. 2b).[26] Thus, utilizing an appropriate linker can realize attractive functions in CD dimers, which cannot be achieved by a CD monomer.

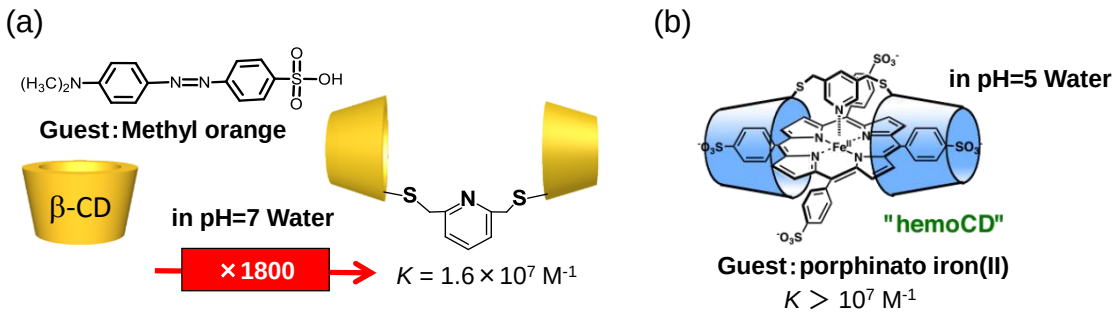

Figure 2. Reported examples of CD dimers. (a) ref. 25, (b) ref. 26.

However, conventional CD dimers have two serious limitations. First, previous research on CD dimers focused on the usage of CD dimers in aqueous media because inclusion complex formation between CD dimers and guest molecules in organic media was believed to be extremely difficult. Because the main driving force for inclusion of guest molecules within the CD dimer cavity is hydrophobic and/or van der Waals interactions between the guests and the CD dimer cavity, and an organic solvent was considered to be a strong competitor for inclusion within the CD dimer

cavity. Inclusion complexes are expected to form even in organic solvents through multiple interactions, including the van der Waals interaction and hydrogen bonding between CD dimers and guests. Successful guest inclusion in organic solvents by CD dimers will open new applications of CD dimers such as the development of adsorbents and sensors for removal and detection of harmful organic compounds in oils, the creation of a stereoselective reaction field in organic solvents, and the construction of supramolecular architectures in organic media.

The second limitation is the number of linkers connecting two CD rings. Most CD dimers consist of two CD rings and a single linker. Only a few studies reported CD dimers bearing multiple linkers[27] because such a modification process was believed to require many reaction steps and a troublesome purification. If a new methodology to facilely synthesize CD dimers bearing multiple linkers is developed, the resulting CD dimers possess a rigid skeleton and inner space. These CD dimers can precisely recognize the shape and size of guest molecules including chiral molecules.

Under these backgrounds, this study aims to construct new CD dimers using β-CD as building blocks.

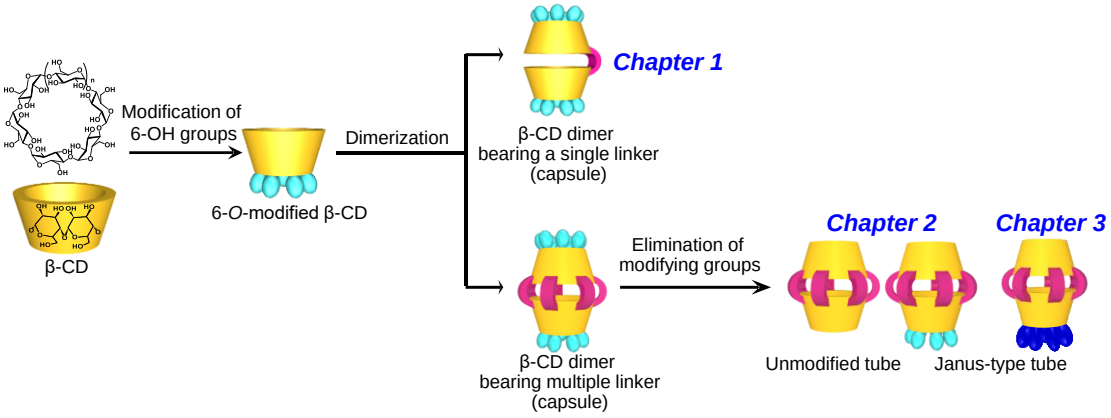

Figure 3. Over view of this study.

Chapter 1 details the synthesis of β-CD dimers in which two 6-*O*-modified β-CD molecules connected by a single linker (β-CD dimer capsule), their inclusion ability and chiral recognition ability for aromatic guests in organic solvents. The inclusion complex formation between 6-O-*tert*-butyldimethylsilylated β-CD (TBDMS-β-CD) dimers bearing a single xylylene linker and aromatic guest compounds, including pyrene, naphthalene, anthracene and chiral naphthalene derivatives, in nonpolar solvents is discussed. In addition, a kinetic resolution of racemic naphthylethylamine through the selective sequestration of one enantiomer by the TBDMS-β-CD dimer in the nonpolar solvent is examined.

Chapter 2 presents the facile synthesis of unmodified or Janus-type β-CD dimer bearing multiple linkers (β-CD dimer tubes). The inclusion ability of the Janus-typeβ-CD dimer toward various saturated and unsaturated long-chain fatty acid esters is examined. The inclusion ability of the

Janus-type β-CD dimer and the unmodified β-CD dimer is also compared.

Chapter 3 discusses the effect of 6-*O*-substituents in Janus-type β-CD dimers on inclusion ability toward long-chain unsaturated fatty acid esters. Regarding the formation of an inclusion complex with Janus-type β-CD dimer, the terminal TBDMS substituents of the Janus-type CD play an important role in enhancing the guest inclusion ability of the tubular host, possibly through changing the internal environment of the tubular cavity. The synthesis of Janus-type β-CD bearing 6-*O*-triisopropylsilyl (TIPS) groups at one end and the inclusion complex formation with unsaturated fatty acid esters is described. The inclusion ability of this Janus-type TIPS-β-CD with Janus-type TBDMS-β-CD synthesized in Chapter 2 is also compared.

References

1) a) M. Yoshizawa, J. K. Klosterman, M. Fujita, *Angew. Chem. Int. Ed.* **2009**, *48*, 3418–3438. b) R. Warmuth, J. Yoon, *Acc. Chem. Res.* **2001**, *34*, 95–105. c) T. Shimizu, W. Ding, N. Kameta, *Chem. Rev*. **2020**, *120*, 2347−2407. (d) L.-P. Yang, X. Wang, H. Yao, W. Jiang, *Acc. Chem. Res.* **2020**, *53*, 198−208.
2) a) D. M. Rudkevich, *Bull. Chem. Soc. Jpn.* **2002**, *75*, 393–413. b) P. Ballester, *Chem. Soc. Rev.* **2010**, *39*, 3810–3830. c) W. Jiang, D. Ajami, J. Rebek Jr., *J. Am. Chem. Soc.* **2012**, *134*, 8070–8073.
3) a) B. W. Smith, M. Monthioux, D. E. Luzzi, *Nature* **1998**, *396*, 323‑324. b) K. Suenaga, M. Tence, C. Mory, C. Colliex, H. Kato, T. Okazaki, H. Shinohara, K. Hirahara, S. Bandow, S. Iijima, *Science* **2000**, *290*, 2280–2282. c) K. Hirahara, K. Suenaga, S. Bandow, H. Kato, T. Okazaki, H. Shinohara, S. Iijima, *Phys. Rev. Lett.* **2000**, *85*, 5384–5387.
4) a) T. S. Koblenz, J. Wassenaar, J. N. H. Reek, *Chem. Soc. Rev.* **2008**, *37*, 247–262. b) T. Okazaki, K. Suenaga, K. Hirahara, S. Bandow, S. Iijima, H. Shinohara, *J. Am. Chem. Soc.* **2001**, *123*, 9673–9674.
5) J. Zhang, J. Wu, L, Wu, *J. Mol. Model.* **2020**, *26*, 276.
6) a) B. Therrien, *Top. Curr. Chem.* **2012**, *319*, 35–55. b) S. C. Larnaudie, J. Sanchis, T. –H. Nguyen, R. Peltier, S. Catrouillet, J. C. Brendel, C. J. H. Porter, K. A. Jolliffe, S. Perrier, *Biomaterials* **2018**, *178*, 570–582. c) V. V. Chaban, T. I. Savchenko, S. M. Kovalenko, O. V. Prezhdo, *J. Phys. Chem. B* **2010**, *114*, 13481−13486.
7) A. Jasat, J. C. Sherman, *Chem. Rev.* **1999**, *99*, 931–967.
8) a) O. Dumele, N. Trapp, F. Diederich, *Angew. Chem. Int. Ed.* **2015**, *54*, 12339 –12344. b) F. -U. Rahman, D. Tzeli, I. D. Petsalakis, G. Theodorakopoulos, P. Ballester, J. Rebek Jr., and Y. Yu, *J. Am. Chem. Soc.* **2020**, *142*, 5876–5883.
9) a) D. J. Cram, *Science* **1983**, 219, 1177−1183. b) D. J. Cram, S. Karbach, Y. H. Kim, L. Baczynskyj, G. W. Kalleymeyn, *J. Am. Chem. Soc.* **1985**, *107*, 2575−2576.

10) a) M. L. C. Quan, D. J. Cram, *J. Am. Chem. Soc.* **1991**, *113*, 2754–2755. b) D. J. Cram, M. E. Tanner, C. B. Knobler, *J. Am. Chem. Soc.* **1991**, *113*, 7717–7727.
11) D. J. Cram, M. E. Tanner, R. Thomas, *Angew. Chem, Int. Ed.* **1991**, *30*, 1024–1027.
12) J. Kang, J. Rebek Jr, *Nature* **1997**, *385*, 50–52.
13) S. Iijima, *Nature* **1991**, *354*, 56–58.
14) a) Z. Sun, K. Ikemoto, T. M. Fukunaga, T. Koretsune, R. Arita, S. Sato, H. Isobe, *Science* **2019**, *363*, 151–155. b) N. Kishi, M. Akita, M. Kamiya, S. Hayashi, H. –F. Hsu, M. Yoshizawa, *J. Am. Chem. Soc.* **2013**, *135*, 12976–12979. (c) A. Harada, J. Li, M. Kamachi, *Nature* **1993**, *364*, 516.
15) K. Yazaki, Y. Sei, M. Akita, M. Yoshizawa, *Nat. Commun.* **2014**, *5*, 5179.
16) a) G. Wenz, Angew. *Chem. Int. Ed.* **1994**, *33*, 803–822. b) K. A. Connors, *Chem. Rev.* **1997**, *97*, 1325–1358.
17) a) M. V. Resharsky, Y. inoue, *Chem. Rev.* **1998**, *98*, 1875–1918. b) R. Breslow, S. D. Dong, *Chem. Rev.* **1998**, *98*, 1997–2012.
18) a) B. Siegel, R. Breslow, *J. Am. Chem. Soc.* **1975**, *97*, 6869–6870. b) A. F. Daniel de Namor, R. Traboulssi, D. F. V. Lewis, *J. Am. Chem. Soc.* **1990**, *112*, 8442–8447. c) A. Harada, S. Takahashi, *Chem. Lett.* **1984**, *13*, 2089–2090.
19) A. Ueno, I. Suzuki, T. Osa, *Anal. Chem.* **1990**, *62*, 2461–2466.
20) K. Takahashi, *Chem. Rev.* **1998**, *98*, 2013–2034.
21) a) K. Uekama, F. Hirayama, T. Irie, *Chem. Rev.* **1998**, *98*, 2045–2076. b) F. Yhaya, J. Lim, Y. Kim, M. Liang, A. M. Gregory, M. H. Stenzel, *Macromolecules* **2011**, *44*, 8433–8445.
22) M. Rekharsky, Y. Inoue, *J. Am. Chem. Soc.* **2000**, *122*, 4418–4435.
23) A. Nakamura, Y. Inoue, *J. Am. Chem. Soc.* **2003**, *125*, 966–972.
24) a) F. Venema, C. M. Baselier, E. v. Dienst, B. H. M. Ruël, M. C. Feiters, J. F. J. Engbersen, D. N. Reinhoudt, R. J. M. Nolte, *Tetrahedron Lett.* **1994**, *35*, 1773–1776. b) R. Breslow, S. Halfon, B. Zhang, *Tetrahedron* **1995**, *51*, 377–388. c) F. Hamon, C. Blaszkiewicz, M. Buchotte, E. Banaszak-Léonard, H. Bricout, S. Tilloy, E. Monflier, C. Cézard, L. Bouteiller, C. Len, F. Djedaini-Pilard, *Beilstein J. Org. Chem.* **2014**, *10*, 2874–2885. d) Y. Isihimaru, Y. Kojo, T. Masuda, S. Saito, Y. Yue, Y. Fujisaki, *Tetrahedron Lett.* **2014**, *55*, 2438–2441.
25) K. Fujita, S. Ejima, T. Imoto *J. Chem. Soc., Chem. Commun.* **1984**, 1277−1278.
26) K. Watanabe, H. Kitagishi, K. Kano, *Angew. Chem. Int. Ed.* **2013**, *52*, 6894 –6897.
27) a) L. Krejčí, M. Buděšínský, I. Císařováb, T. Kraus, *Chem. Commun.* **2009**, 3557–3559. b) A. Wang, W. Li, P. Zhang, C. C. Ling, *Org. Lett.* **2011**, *13*, 3572–3575.

Chapter 1

Molecular Recognition Ability of β-CD Dimers Bearing a Single Linker toward Aromatic Guest Molecules in Organic Solvents

1.1 Introduction

In most cases, the inclusion complex formation between CDs and organic guest molecules has been achieved in water[1] or in polar organic solvents.[2] It has been believed that inclusion complex formation between CDs and guest molecules in nonpolar solvents would be extremely difficult, because the main driving force for the inclusion of guest molecules within the CD cavity is hydrophobic interactions and/or van der Waals interactions between the guests and the CD cavity, and the enormous amount of nonpolar solvents become a strong competitor for inclusion within the CD cavity. Recently, the author's research group found that 6-*O*-modified β-CDs, such as heptakis(6-*O*-*tert*-butyldimethylsilyl)-β-CD (TBDMS-β-CD) and heptakis(6-*O*-triisopropylsilyl)-β-CD (TIPS-β-CD), effectively formed inclusion complexes with chlorinated benzenes[3] and pyrene[4] in nonpolar solvents. In particular, TIPS-β-CD forms 2:1 inclusion complexes with pyrene in benzene and cyclohexane with high association constants. Moreover, the research group reported the extremely high chiral recognition of an aromatic amine in cyclohexane can be achieved by a supramolecular dimer of TIPS-β-CD.[5] These finding prompted us to explore the inclusion ability of 6-*O*-modified β-CD dimers, in which two 6-*O*-modified β-CD molecules are covalently connected by an appropriate single linker, towards aromatic guest

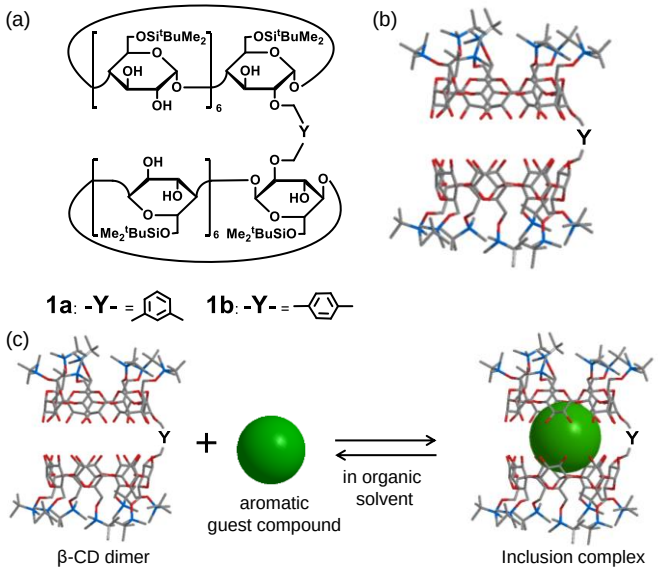

Figure 1-1. (a) Chemical structure and (b) schematic illustration of β-CD dimers **1a** and **1b**. (c) Schematic illustration of 1:1 inclusion complex formation between **1a** (or **1b**) and an aromatic guest compound in organic solvents.

molecules in nonpolar solvents. Such β-CD dimers can be expected to act as more effective and selective hosts as compared with the corresponding 6-*O*-modified β-CD monomers and their supramolecular dimers by utilizing more confined guest-inclusion space.

The author reports herein the inclusion complex formation between TBDMS-β-CD dimers bearing a single linker and aromatic guest compounds including pyrene, napthalene, anthracene, and chiral naphthalene derivatives in nonpolar solvents (Fig. 1-1). In addition, a kinetic resolution of racemic naphthylethylamine through the selective sequestration of the one enantiomer by the TBDMS-β-CD dimers in the nonpolar solvent was examined.

1.2 Results and Discussion

1.2.1 Synthesis

TBDMS-β-CD dimers **1a** and **1b**, where two TBDMS-β-CD molecules are covalently connected in a head-to-head fashion by *m*-xylylene (**1a**) and *p*-xylylene (**1b**) linkers, were chosen as host molecules. **1a** and **1b** were prepared by reacting TBDMS-β-CD with *m*-xylylene dibromide and *p*-xylylene dibromide using a previously reported method, respectively.[6] The resulting products were purified by silica-gel column chromatography using methanol/chloroform (1: 9) as an eluent.

1.2.2 Inclusion of Aromatic Guests

Pyrene, naphthalene, and anthracene were used as guest molecules. Fig. 1-2 shows the fluorescence spectral changes of pyrene against **1a** and **1b** concentrations in cyclohexane and

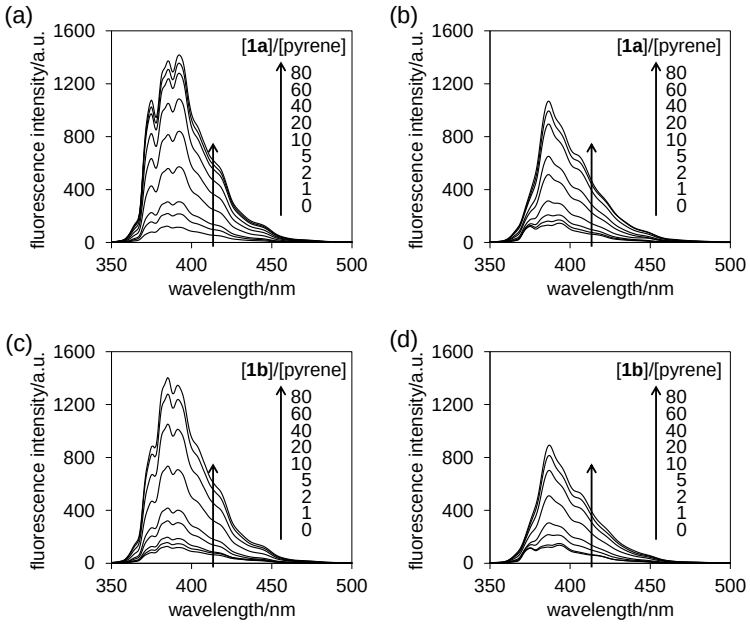

Figure 1-2. Fluorescence spectral changes of pyrene (1.0×10^{-6} M) upon the addition of increasing amounts of β-CD dimers **1a** and **1b** (a, c) in cyclohexane and (b, d) in benzene at 25 °C. λ_{ex}=340 nm and 336 nm for the cyclohexane and benzene solution, respectively.

benzene. The fluorescence intensity of pyrene increases as the ratio of [CD host]/[pyrene] increases, suggesting that these β-CD dimers and pyrene form inclusion complexes in both solvents. The addition of **1a** induces a larger increase in the fluorescence intensity of pyrene compared to **1b** in these solvents, implying that the linker length affects complexation between the β-CD dimer and pyrene in nonpolar solvents. The Job plots indicate that these β-CD dimers form a 1:1 complex with pyrene (Figs. 1-3 and 1-22).

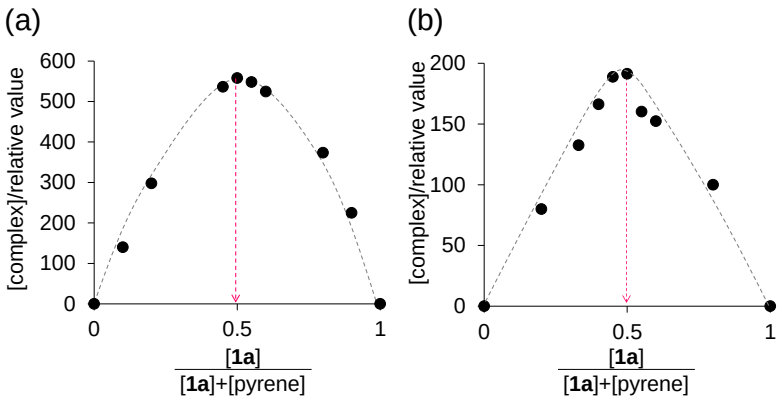

Figure 1-3. Job plots for the complexes between β-CD dimer **1a** and pyrene in (a) cyclohexane and (b) benzene at 25 °C. (a) λ_{ex}= 340 nm; λ_{em}= 384 nm. (b) λ_{ex} = 336 nm; λ_{em} = 386 nm.

Table 1-1. Association Constants between TBDMS-β-CD Dimers **1a** and **1b** (or TBDMS-β-CD monomer) and Aromatic Guests (Pyrene and Naphthalene) in Organic Solvents at 25 °C.

		Association constant (M^{-1})	
Host	Solvent	Pyrene	Naphthalene
1a	cyclohexane	$(9.6 \pm 0.68) \times 10^4$	$(6.8 \pm 2.9) \times 10^3$
	benzene	$(4.0 \pm 0.18) \times 10^4$	$(2.1 \pm 0.16) \times 10^3$ [a]
	THF	$(6.7 \pm 0.35) \times 10^2$ [a]	
1b	cyclohexane	$(1.9 \pm 0.27) \times 10^4$	$(1.7 \pm 0.57) \times 10^3$
	benzene	$(2.3 \pm 0.24) \times 10^4$	$(1.6 \pm 0.47) \times 10^3$ [a]
TBDMS-β-CD	cyclohexane	$K = (1.3 \pm 0.42) \times 10^8\ M^{-2}$ [b] $\sqrt{K_1K_2} = 9.1 \times 10^3$ $K_1 = (3.1 \pm 0.81) \times 10^3$ [b] $K_2 = (2.7 \pm 0.38) \times 10^4$ [b]	$(1.0 \pm 0.34) \times 10^8\ M^{-2}$ [a]
	benzene	$K = (6.1 \pm 1.6) \times 10^7\ M^{-2}$ [b] $\sqrt{K_1K_2} = 7.1 \times 10^3$ $K_1 = (2.8 \pm 0.49) \times 10^3$ [b] $K_2 = (1.8 \pm 0.37) \times 10^4$ [b]	$(1.7 \pm 0.98) \times 10^7\ M^{-2}$ [a]
	THF	6.8 ± 1.4 [a]	

[a] Determined by the NMR titration method. [b] Ref. 4a.

Table 1-1 shows the association constants *K*, which were estimated from the fluorescence spectral changes of pyrene upon the addition of the CD dimers. The association constants *K* (K_1 and K_2) between two TBDMS-β-CD monomers and one pyrene molecule are shown for comparison. Here, K_1 and K_2 denote the association constants between the TBDMS-β-CD monomer and one pyrene molecule and between the TBDMS-β-CD monomer–pyrene (1 : 1) complex and one TBDMS-β-CD monomer, respectively. **1a** showed higher inclusion ability toward pyrene as compared with the TBDMS-β-CD monomer ($\sqrt{K_1 K_2}$). This result suggests that the two TBDMS-β-CD molecules in **1a**, which are connected by a *m*-xylylene linker, cooperatively work for pyrene inclusion in nonpolar solvents. **1a** shows a higher inclusion ability toward pyrene than **1b** in these solvents, indicating that the *m*-xylylene linker is more effective for cooperation of the two CD rings in guest inclusion than the *p*-xylylene linker. These results reveal that the linker length connecting the two β-CD rings remarkably affects the cooperation of the two TBDMS-β-CD rings for the guest inclusion, and consequently, the inclusion ability of the TBDMS-β-CD dimer toward guests in nonpolar solvents. **1a** shows a higher association constant with pyrene in cyclohexane than in benzene, suggesting that there should be a difference in the inclusion mode of pyrene into the CD dimer cavity between these solvents. On the other hand, the solvent has a negligible effect on the complexation behavior of **1b** with pyrene.

It is noteworthy that **1a** realizes effective guest inclusion even in polar organic solvents such as tetrahydrofuran (THF). Fig. 1-4 shows the ^{1}H NMR spectral changes of **1a** upon the addition of pyrene in THF-d_8. The clear shift of the ^{1}H signals of **1a** upon the addition of pyrene suggests that **1a** forms an inclusion complex with pyrene in this solvent. The association constant between **1a** and pyrene is 98-fold higher than that between the TBDMS-β-CD monomer and pyrene in THF-d_8. This result indicates that **1a** functions as a more powerful host than the corresponding monomer in both polar and nonpolar solvents.

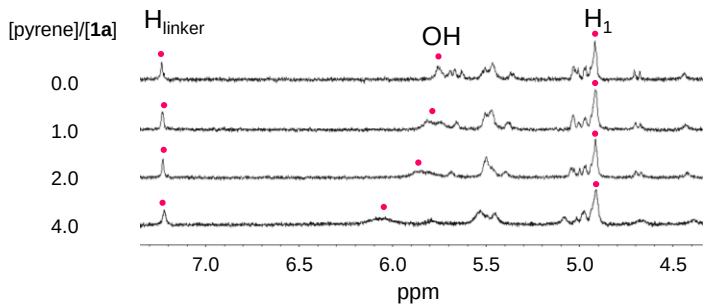

Figure 1-4. ^{1}H NMR spectral changes of **1a** (1.0×10^{-3} M) upon the addition of increasing amounts of pyrene in THF-d_8 at 25 °C.

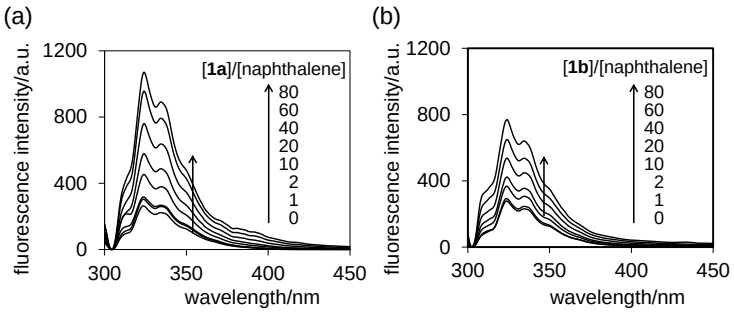

Figure 1-5. Fluorescence spectral changes of naphthalene (1.0×10^{-6} M) upon the addition of increasing amounts of β-CD dimers (a) **1a** and (b) **1b** in cyclohexane at 25 °C. λ_{ex}=278 nm.

Fig. 1-5 shows the fluorescence spectral changes of naphthalene against **1a** and **1b** concentrations in cyclohexane. Similar to the cases of pyrene, the fluorescence intensity of naphthalene increases as the ratio of [β-CD dimer]/[naphthalene] increases, suggesting inclusion complexes are formed between the β-CD dimers and naphthalene in cyclohexane.

On the other hand, when benzene is used as the solvent, clear fluorescence spectral changes of naphthalene are not observed upon the addition of the β-CD dimers, implying that the association

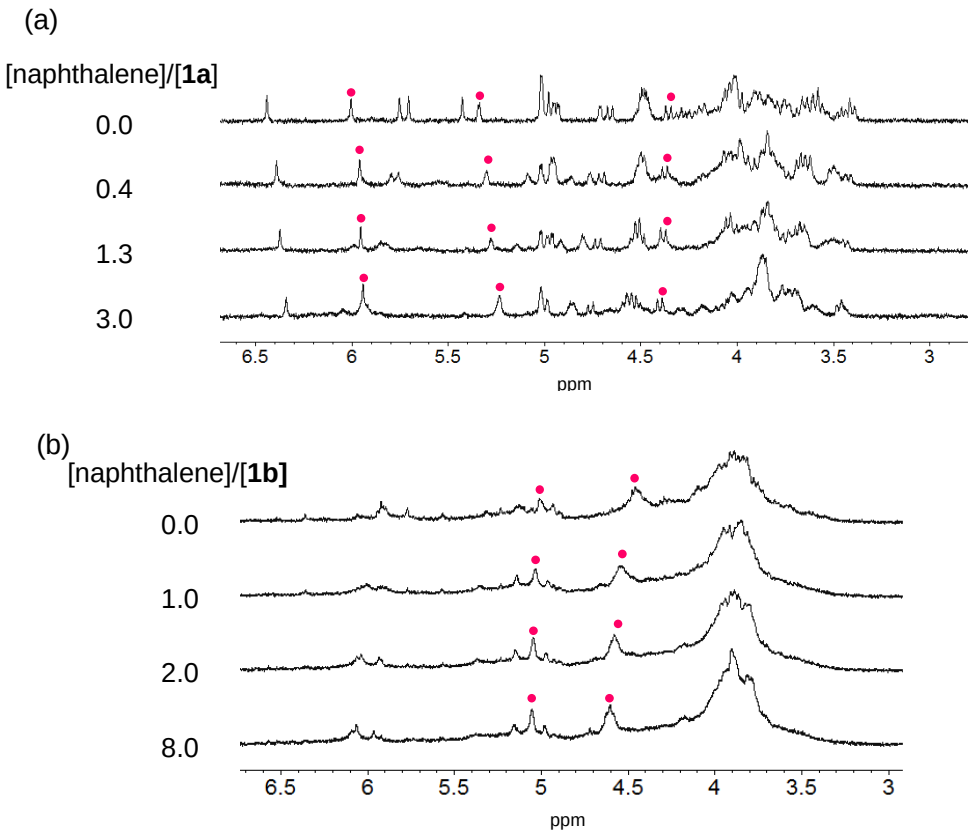

Figure 1-6. ^{1}H NMR spectral changes of (a) **1a** (1.0×10^{-3} M) and (b) **1b** (1.0×10^{-3} M) upon addition of increasing amounts of naphthalene in benzene-d_6 at 25 °C.

constants between the β-CD dimers and naphthalene in benzene may be lower than these in cyclohexane. Thus, the ^{1}H NMR titration method was employed to study the complexation behavior between the β-CD dimers and naphthalene guest in benzene. Fig. 1-6 show the changes in the ^{1}H NMR signals of β-CD dimers **1a** and **1b** upon the addition of naphthalene in benzene-d_6, respectively. The clear shift in the proton signals of these β-CD dimers upon the addition of naphthalene suggests that the naphthalene guest is incorporated within the cavities of these hosts. The association constants were determined based on these ^{1}H NMR spectral changes. Similar to the cases of the pyrene guest, **1a** bearing a *m*-xylylene linker shows a higher association with naphthalene in cyclohexane and benzene solvents compared to **1b** bearing a *p*-xylylene linker (Table 1-1). **1a** shows higher association constants with naphthalene in cyclohexane than in benzene. In contrast, the solvent has a negligible effect on the association constants in the case of host **1b**, which is similar to the case of the pyrene guest. Both **1a** and **1b** show about a 10-fold higher association constant with pyrene than naphthalene, indicating that inclusion complex formation between the TBDMS-β-CD dimers and the aromatic guest in the nonpolar solvents is very sensitive to the steric fit of the guest into the host cavity.

In sharp contrast to the pyrene and naphthalene guests, fluorescence spectral changes of the anthracene guest against the concentrations of **1a** and **1b** in cyclohexane are not observed (Fig. 1-7), indicating that anthracene hardly forms complexes with these TBDMS-β-CD dimers in cyclohexane. This interesting finding reveals that the size and shape of the guest molecule are important for inclusion within the TBDMS-β-CD dimer cavity in cyclohexane.

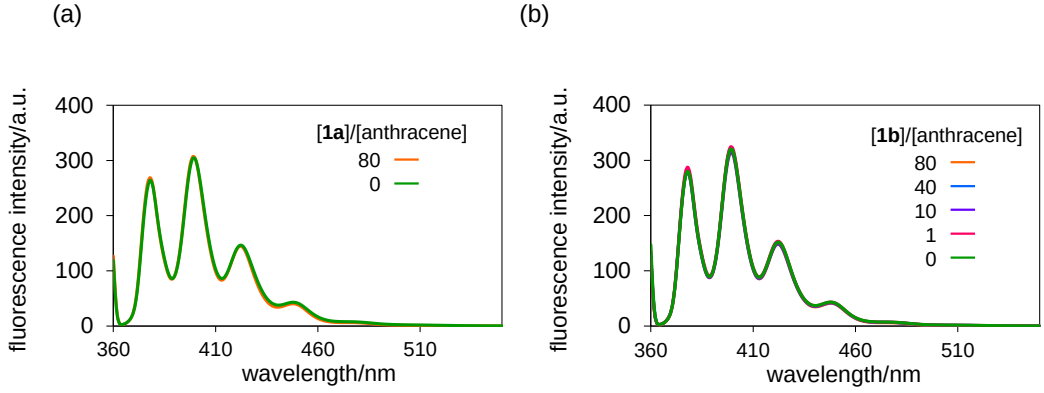

Figure 1-7. Fluorescence spectral changes of anthracene (1.0×10^{-6} M) upon addition of increasing amounts of β-CD dimers (a) **1a** and (b) **1b** in cyclohexane at 25 °C. λ_{ex}=356 nm.

The thermodynamic parameters for complexation between the TBDMS-β-CD dimers and pyrene in cyclohexane, which were determined by fluorescence titration at different temperatures, reveals that complexation is enthalpy-driven (ΔH=-37 kJmol^{-1} and ΔS=-28 Jmol^{-1}K^{-1} for **1a**, ΔH=-33 kJmol^{-1} and ΔS=-30 Jmol^{-1}K^{-1} for **1b**) (Tables 1-2 and 1-3). This result supports that the

interactions between the host cavity and the guest molecule, which may include the interaction between the guest molecule and the solvent incorporated inside the CD cavity, play an important role in inclusion complex formation in cyclohexane.

Table 1-2. Association constants between TBDMS-β-CD dimers (or TBDMS-β-CD) and pyrene in cyclohexane at different temperatures.

host	T (˚C)	*K* (M^{-1})
1a	1	$(1.6\pm0.021)\times10^5$
	25	$(9.6\pm0.68)\times10^4$
	35	$(6.5\pm0.044)\times10^4$
	45	$(3.5\pm0.043)\times10^4$
1b	15	$(2.6\pm0.032)\times10^4$
	25	$(1.9\pm0.27)\times10^4$
	35	$(1.2\pm0.010)\times10^4$
	45	$(7.1\pm0.011)\times10^3$
TBDMS-β-CD	15	$(2.4\pm1.6)\times10^8\ M^{-2}$
	25	$(1.3\pm0.42)\times10^8\ M^{-2}$
	40	$(3.2\pm1.8)\times10^7\ M^{-2}$
	55	$(5.5\pm2.7)\times10^8\ M^{-2}$

Table 1-3. Thermodynamic parameters for inclusion complex formation between β-CD dimers (or TBDMS-β-CD) and pyrene in cyclohexane at 25 ˚C.

host	ΔH (kJ/mol)	ΔS (J/molK)	ΔG (kJ/mol)
1a	-37	-28	-28
1b	-33	-30	-24
TBDMS-β-CD	-75	-96	-46

1.2.3 NMR Studies on the Inclusion Complex Structure

Two-dimensional NMR studies effectively provide useful information on the inclusion complex structure in solution. The NOESY spectra of the inclusion complex between **1a** and pyrene in cyclohexane-d_{12} and benzene-d_6 show remarkable correlations between the protons of pyrene and the H_3 and/or H_5 protons of **1a** (Figures 1-8), confirming that pyrene is incorporated within the cavity of **1a** in these solvents. In benzene-d_6, clear cross peaks between the H_3 protons of the host and all of the pyrene protons are observed, whereas the cross peaks between the H_5 protons of the host and the pyrene protons are barely observed, suggesting that a pyrene molecule is included with its long axis almost perpendicular to the axis of **1a**. In cyclohexane-d_{12}, cross peaks are observed between the H_5 protons as well as the H_3 protons of the host and all of the pyrene protons, suggesting that the long axis of the incorporated pyrene molecule is tilted toward the main axis

of **1a** cavity. Thus, the pyrene molecule penetrates more deeply into the CD cavity compared to the case of benzene-d_6. These results reveal that there is a clear difference in the inclusion mode of pyrene between benzene-d_6 and cyclohexane-d_{12} solvents. This finding is consistent with the results observed in the cases of complexes between the TBDMS-β-CD monomer and pyrene.[5]

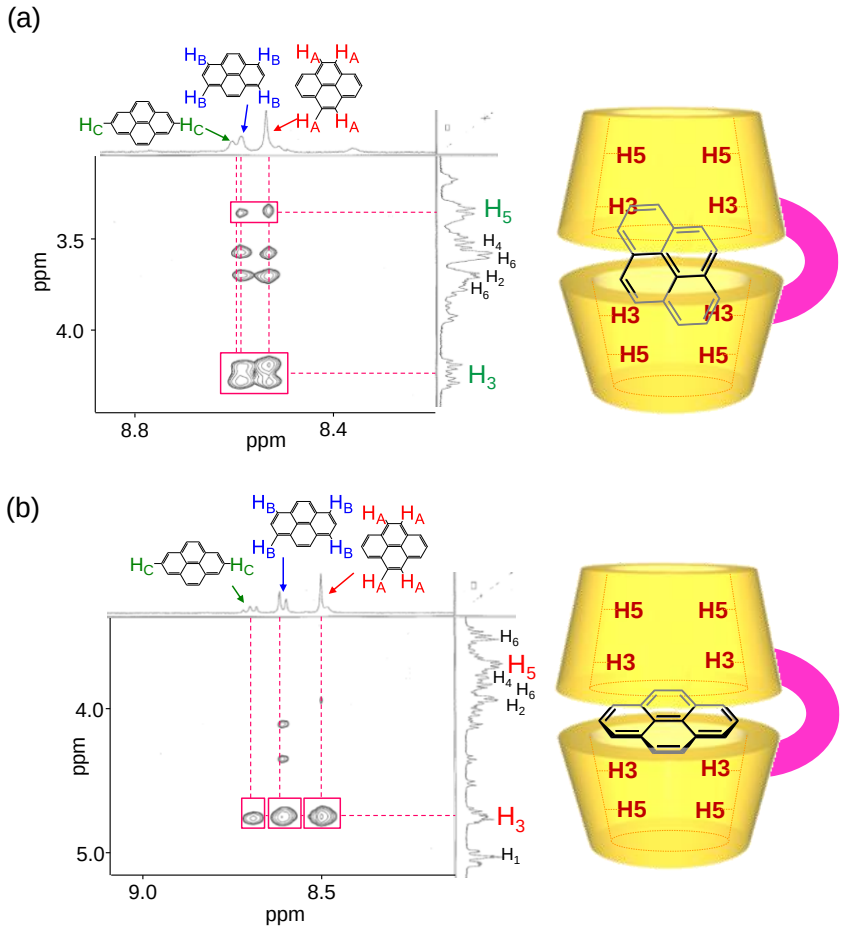

Figure 1-8. Partical NOESY spectrum and proposed structure of the complex between **1a** and pyrene (a) in cyclohexane-d_{12} (b) in benzene-d_6 .

1.2.4 Inclusion of Chiral Aromatic Guests

We also examined the chiral recognition abilities of **1a** and **1b**. A supramolecular dimer of TIPS-β-CD has been reported to show a high chiral recognition ability toward aromatic amines in nonpolar solvents. Based on this report, (*R*)- and (*S*)-1-(1-naphthyl)ethylamine [(*R*)- and (*S*)-1-NEA], (*R*)- and (*S*)-1-(1-naphthyl)-ethanol [(*R*)- and (*S*)-1-NET], and (*R*)- and (*S*)-1-(2-naphthyl)ethylamine [(*R*)- and (*S*)-2-NEA] were chosen as chiral guests (Fig. 1-9). The chiral recognition ability toward these guests was evaluated on the basis of the association constants (*K*) between the dimers and the chiral guest in cyclohexane, which were determined by the fluorescence titration method. Fig. 1-10 shows the fluorescence spectral changes of (*R*)-and (*S*)-

1-NEA against the TBDMS-β-CD dimer concentration in cyclohexane. The fluorescence intensity of (*R*)- and (*S*)-1-NEA increases as the ratio of [TBDMS-β-CD dimer]/[(*R*)- or (*S*)-1-NEA] increases, suggesting inclusion complexes are formed between the CD dimer and these guests in cyclohexane. A larger increase in the fluorescence intensity of (*S*)-1-NEA is observed upon the addition of **1a** compared to the case of (*R*)-1-NEA, implying that **1a** may selectively bind (*S*)-1-NEA over (*R*)-1-NEA in cyclohexane. The fluorescence intensities of (*R*)- and (*S*)-1-NET and (*R*)- and (*S*)-2-NEA in cyclohexane also increase as the ratio of [TBDMS-β-CD dimer]/[guest] increases (Figs. 1-24 and 1-25). In the cases of 1-NET, the fluorescence intensity of the (*S*)-isomer has a larger increase upon the addition of **1a** compared to that of the (*R*)-isomer. This is similar to the cases of 1-NEA, suggesting that **1a** shows a high chiral recognition ability toward 1-NET as well as 1-NEA in cyclohexane.

Table 1-4 summarizes the association constants between the TBDMS-β-CD dimers and the chiral aromatic guests in cyclohexane at 25°C, which were estimated from the fluorescence spectral changes of the guests upon the addition of the TBDMS-β-CD dimers. **1a** shows a clear binding selectivity for (*S*)-1-NEA over (*R*)-1-NEA. It is noteworthy that an extremely high chiral selectivity of more than 30 is achieved by **1a**, which is much higher than the chiral selectivity of

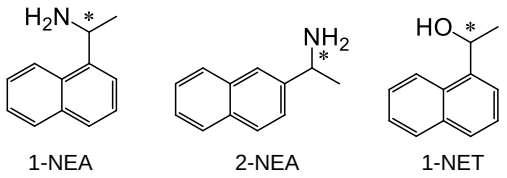

Figure 1-9. Chemical structures of 1-NEA, 2-NEA and 1-NET.

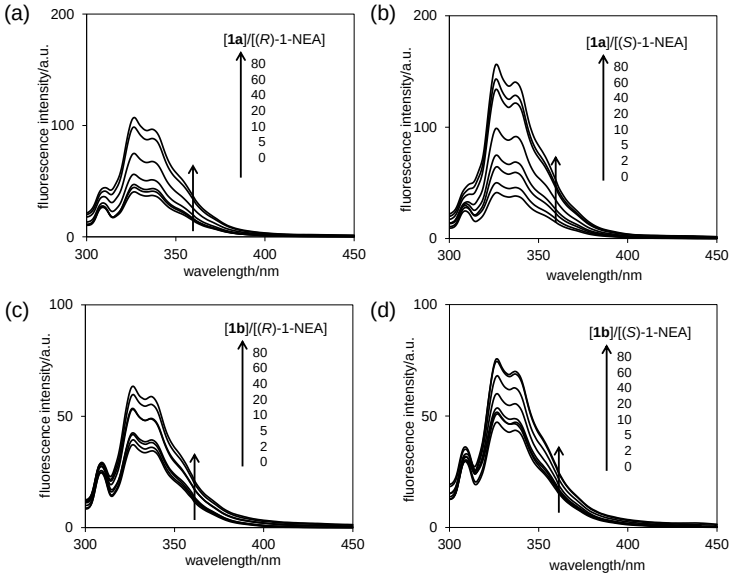

Figure 1-10. Fluorescence spectral changes of (a, c) (*R*)-1-NEA and (b, d) (*S*)-1-NEA (1.0×10^{-6} M) upon addition of increasing amount of (a, b) **1a** and (c, d) **1b** in cyclohexane at 25 °C. λ_{ex} =283 nm.

the TBDMS-β-CD monomer toward the corresponding chiral guest (K_S/K_R=6.1). **1a** also shows a considerably high binding selectivity for (*S*)-1-NET over the corresponding (*R*) isomer. These results demonstrate that **1a** is highly effective for chiral recognition of 1-NEA and 1-NET in cyclohexane. On the other hand, **1b** shows a lower chiral selectivity for guests 1-NEA and 1-NET compared to **1a**. In particular, the chiral selectivity for 1-NEA decreases significantly. These results clearly indicate that the distance between two TBDMS-β-CD rings largely affects the chiral discrimination ability toward 1-NEA. Thus, the appropriate cooperation of the two TBDMS-β-CD rings, which can be realized with a *m*-xylylene linker, is essential for a high chiral recognition by the TBDMS-β-CD dimers. On the other hand, the chiral recognition ability of **1a** and **1b** toward 2-NEA is much lower compared to the case of 1-NEA. These results reveal that the substitution position of the 1-aminoethyl group on the naphthalene ring of the guest significantly influences the chiral recognition by the TBDMS-β-CD dimers in cyclohexane.

Table 1-4. Association constants between β-CD dimers and chiral aromatic guests in cyclohexane at 25 °C.

		Association constant (M^{-1})		Selectivity
Host	Guest	K_R	K_S	K_S/K_R
1a	1-NEA	$(8.9\pm0.73)\times10^2$	$(2.9\pm0.77)\times10^4$	33±3.1
	1-NET	$(1.4\pm0.26)\times10^3$	$(5.2\pm0.27)\times10^4$	37±8.6
	2-NEA	$(6.2\pm1.2)\times10^3$	$(9.6\pm2.7)\times10^3$	1.5±0.2
1b	1-NEA	$(8.7\pm0.67)\times10^3$	$(1.6\pm0.69)\times10^4$	1.8±0.1
	1-NET	$(2.2\pm0.68)\times10^3$	$(1.6\pm0.37)\times10^4$	7.3±1.9
	2-NEA	$(1.4\pm0.10)\times10^4$	$(6.8\pm0.13)\times10^3$	0.5±0.0
TBDMS-β-CD	1-NEA	$(1.8\pm0.40)\times10^5$ M^{-2}	$(1.2\pm0.33)\times10^6$ M^{-2}	6.1±1.6

1.2.5 Kinetic Resolution of an Aromatic Amine

Utilizing the high chiral recognition ability of **1a** toward 1-NEA in cyclohexane, a non-enzymatic kinetic resolution of 1-NEA via enantioselective *N*-acylation should proceed. The selective inclusion of (*S*)-1-NEA over the (*R*)-isomer within the dimer cavity should predominantly shield the (*S*)-isomer from the reaction with acylation reagents in a bulk solution, resulting in the kinetically preferential *N*-acylation of the (*R*)-isomer over the (*S*)-isomer.

Based on this hypothesis, we examined the enantioselective *N*-acylation of racemic 1-NEA with benzoic anhydride in the presence of **1a** in cyclohexane. The enantioselective *N*-acylation of 1-NEA with benzoic anhydride in the presence of **1b** and the TBDMS-β-CD monomer as a control was also examined. A mixture of racemic 1-NEA and **1a** (2.5 eq.) in cyclohexane was stirred for 1 h to reach complexation equilibrium. Then benzoic anhydride was added at 10 or 25°C. The mixture was subsequently stirred at 10 or 25°C for 2 h.

Table 1-5 summarizes the conversion of 1-NEA, the enantiomer excess (*ee*, %) of the resulting

N-benzoyl-(*R*)-1-NEA as functions of the amount of added benzoyl anhydride. Enantioselective *N*-benzoylation of (*R*)-1-NEA exceeds 45% *ee* in the presence of **1a**. The enantioselectivity is enhanced as the amount of benzoyl anhydride decreases (entries 2–5). Reducing the reaction temperature from 25 to 10°C also increases the enantioselectivity. In particular, the highest enantioselectivity for *N*-acylation of (*R*)-1-NEA occurs using 2.5 eq. of **1a** and 0.10 eq. of benzoic anhydride at 10°C (87% *ee*). On the other hand, when **1b** is used as the host, the enantioselectivity is lower than **1a**. Considering that the chiral recognition ability of **1a** toward 1-NEA is higher than that of **1b**, it is clear that the chiral recognition ability of the TBDMS-β-CD dimers toward 1-NEA is closely related to the enantioselective *N*-acylation of the guest. Compared to the TBDMS-β-CD monomer, the presence of **1a** results in a higher enantioselectivity. This result strongly supports that dimerization of TBDMS-β-CD with an appropriate linker is an effective approach to construct enantioselective reaction fields. Generally, it is considered that the nonenzymatic kinetic resolution of racemic primary amino compounds is difficult due to the higher reactivity of the primary amino groups.[7] Thus, this TBDMS-β-CD dimer should be a powerful tool for non-enzymatic kinetic resolution of racemic amino compounds.

Table 1-5. Kinetic resolution of 1-NEA via enantioselective *N*-acylation with benzoic anhydride in the presence of **1a** or **1b** in cyclohexane [a].

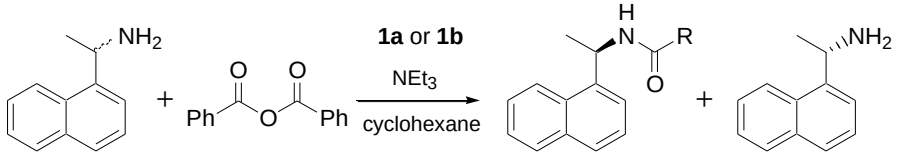

1-NEA benzoic anhydride *N*-benzoyl-(*R*)-1-NEA (*S*)-1-NEA

entry	CD	temp. (°C)	benzoic anhydride (eq.)	conversion[b] (%)	*ee*[b] (%)
1	none	25	0.50	50	-
2	**1a**	25	0.10	8.6	79
3	**1a**	25	0.50	50	49
4	**1a**	10	0.10	7	87
5	**1a**	10	0.50	46	55
6	**1b**	25	0.10	6.8	42
7	**1b**	25	0.50	50	24
8	**1b**	10	0.10	9	45
9	**1b**	10	0.50	43	28
10	TBDMS-β-CD	25	0.10	6.3	60
11	TBDMS-β-CD	25	0.50	50	47

[a] Acylation of 1-NEA (2.0×10^{-4} mmol) was carried out with benzoic anhydride in cyclohexane (0.2 mL) at 10 °C or 25 °C for 2h in the presence of triethylamine (1.0 eq.) and a CD dimer (2.5 eq.) [or TBDMS-β-CD (5.0 eq.)]. [b] Conversion of 1-NEA and enantiomeric excess of *N*-benzoyl-(*R*)-1-NEA were determined by HPLC.

1.3 Conclusions

The author has demonstrated that TBDMS-β-CD dimer **1a** bearing a *m*-xylylene linker effectively forms inclusion complexes with pyrene and naphthalene in nonpolar solvents such as cyclohexane and benzene. The association constants between **1a** and pyrene in nonpolar solvents are higher than those between **1b** bearing a *p*-xylylene linker and pyrene due to the larger cooperation of the two TBDMS-β-CD rings in **1a** for pyrene inclusion. **1a** also shows a remarkable inclusion ability toward pyrene in THF. The association constant between **1a** and pyrene in THF is 98-fold higher than that between the corresponding TBDMS-β-CD monomer and pyrene. This result indicates that the TBDMS-β-CD dimer works as an effective host even in polar organic solvents. A high chiral recognition of aromatic amines and alcohol is realized by utilizing inclusion within the cavity of **1a** in cyclohexane. In particular, an extremely high binding selectivity for (*S*)-1-(1-naphthyl)ethylamine ((*S*)-1-NEA) and (*S*)-1-(1-naphthyl)ethanol ((*S*)-1-NET) over the corresponding (*R*)-isomers is achieved. Moreover, by utilizing chiral recognition with **1a** in cyclohexane, a kinetic resolution of racemic 1-NEA via enantioselective *N*-benzoylation is attained with an enantiomer excess of up to 87%. **1a** should be applicable as a powerful chiral selector and a potent reaction tool for various enantioselective reactions.

1.4 Experimental Section

1.4.1 Materials and Methods

Heptakis(6-*O*-*tert*-butyldimethylsilyl)-β-cyclodextrin (TBDMS-β-CD) was prepared by referencing the literature.[8] α,α'-Dibromo-*m*-xylene and 1,4-dioxane were purchased from Wako Pure Chemical Industries (Japan). α,α'-Dibromo-*p*-xylene and sodium hydride (60% content) were purchased from Tokyo Chemical Industry (Japan). The ^{1}H and ^{13}C NMR spectra were recorded on a JEOL NMR system (400 MHz). Infrared (IR) spectra were obtained with a 100FT-IR spectrometer (Perkin Elmer). MALDI-TOF mass spectra were measured by Bruker Autoflex III.

1.4.2 Synthesis of α, α'-Bis[2-*O*-(heptakis(6-*O*-*tert*-butyldimethylsilyl)-β-cyclodextrin)]-*m*-xylene (1a)

Under a N_2 atmosphere, heptakis(6-*O*-*tert*-butyldimethylsilyl)-β-cyclodextrin (TBDMS-β-CD) (2.9 g, 1.5 mmol) and sodium hydride (180 mg, 4.5 mmol, 60%) were added in THF (60 mL), and the mixture was heated to reflux for 1 h. Into this solution, was added α, α'-dibromo-*m*-xylene (82 mg, 0.3 mmol) in THF (20 mL) dropwise under stirring, and the resulting mixture was stirred overnight under reflux. The reaction was quenched with methanol (100 mL). After evaporation of the solvent, the residue was dissolved in chloroform (200 mL) and washed twice with saturated aqueous NaCl (2 × 100 mL). The resulting chloroform solution was dried over anhydrous $MgSO_4$.

After the solvent was removed in vacuo, the residue was purified by silica gel column chromatography (chloroform/methanol, in a gradient from 19:1 to 9:1) to give α, α'-bis[2-*O*-(heptakis(6-*O*-*tert*-butyldimethylsilyl)-β-cyclodextrin)]-*m*-xylene as a white solid (327 mg, 27%). R_f 0.72 ($CHCl_3$/MeOH = 4/1); mp 275 °C (decomp); ^{1}H NMR (400 MHz, tetrahydrofuran-d_8) δ 0.09 (s, 84H), δ 0.92 (s, 126H), δ 3.36-4.15 (m, 84H), δ 4.70 (d, 2H), δ 4.92-5.04 (m, 16H), δ 5.36-5.76 (m, 26OH), δ 7.24 (m, 3H), δ 7.65 (s, 1H); ^{13}C NMR (100 MHz, tetrahydrofuran-d_8) δ 19.1, 26.5, 63.0, 73.2, 73.5, 74.1, 74.3, 74.4, 82.2, 82.4, 82.8, 103.2, 103.3, 103.5, 128.2, 128.7, 129.3, 129.7, 131.6, 139.3; MALDI-TOF MS (*m/z*) 3998 $[M+Na]^+$, 4013 $[M+K]^+$; FT-IR (cm^{-1}) ν_{C-H} = 2900, ν_{C-O-C} = 1050, ν_{Si-O} = 800; Anal. Calcd for $C_{176}H_{342}O_{70}Si_{14}\bullet 2H_2O$: C, 52.75; H, 8.70; O, 28.74; Si, 9.81. Found: C, 52.48: H, 8.57.

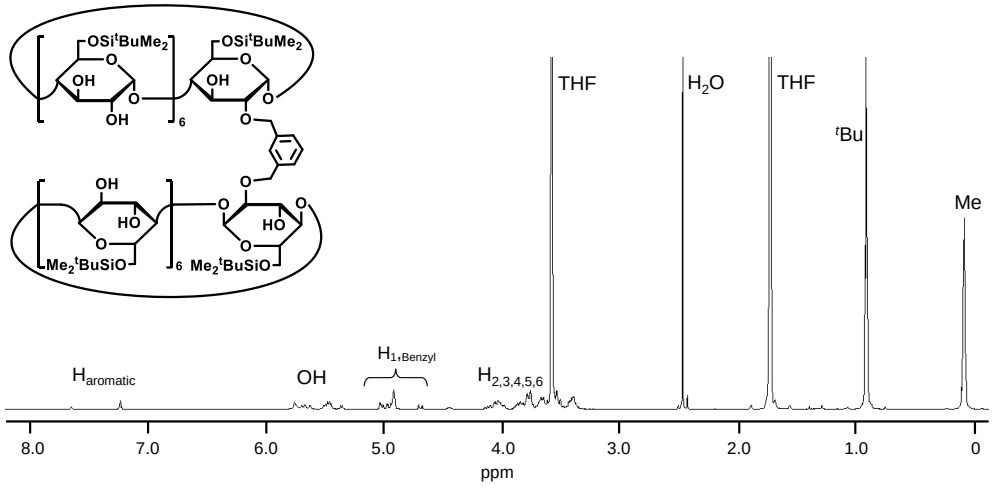

Figure 1-11. ^{1}H NMR spectrum of α,α'-bis[2-*O*-(heptakis(6-*O*-*tert*-butyldimethylsilyl)- β-cyclodextrin)]-*m*-xylene in THF-d_8.

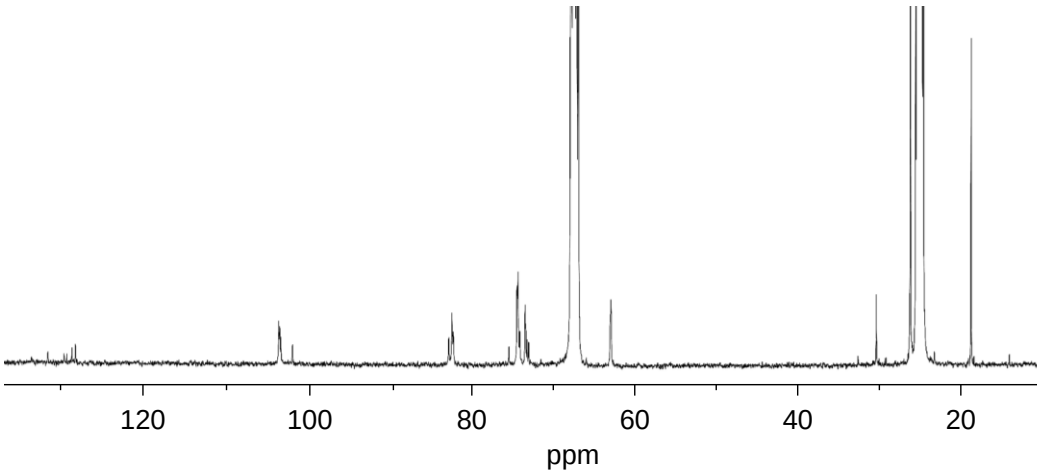

Figure 1-12. ^{13}C NMR spectrum of α,α'-bis[2-*O*-(heptakis(6-*O*-*tert*-butyldimethylsilyl)- β-cyclodextrin)]-*m*-xylene in THF-d_8.

1.4.3 Synthesis of α, α'-Bis[2-*O*-(heptakis(6-*O*-*tert*-butyldimethylsilyl)-β-cyclodextrin)]-*p*-xylene (1b)

Compound **1b** was synthesized in the same manner to **1a** to give a white solid (14% yield). R_f 0.72 ($CHCl_3$/MeOH = 4/1); mp: 273 °C (decomp); ^{1}H NMR (400 MHz, tetrahydrofuran-d_8) δ 0.09 (s, 84H), δ 0.92 (s, 126H), δ 3.37-4.08 (m, 84H), δ 4.76 (d, 2H), δ 4.91-5.05 (m, 16H), δ 5.41-5.68 (m, 26OH), δ 7.38 (s, 4H); ^{13}C NMR (100 MHz, tetrahydrofuran-d_8): δ 19.1, 26.5, 63.0, 73.1, 73.5, 74.2, 74.3, 74.4, 82.2, 82.5, 83.2, 102.2, 103.3, 128.7; MALDI-TOF MS (*m/z*) 4010 $[M+K]^+$; FT-IR (cm^{-1}): ν_{C-H} = 2900, ν_{C-O-C} = 1050, ν_{Si-O} = 800; Anal. Calcd for $C_{176}H_{342}O_{70}Si_{14}\bullet H_2O$: C, 52.98; H, 8.69; O, 28.47; Si, 9.85. Found: C, 52.74: H, 8.34.

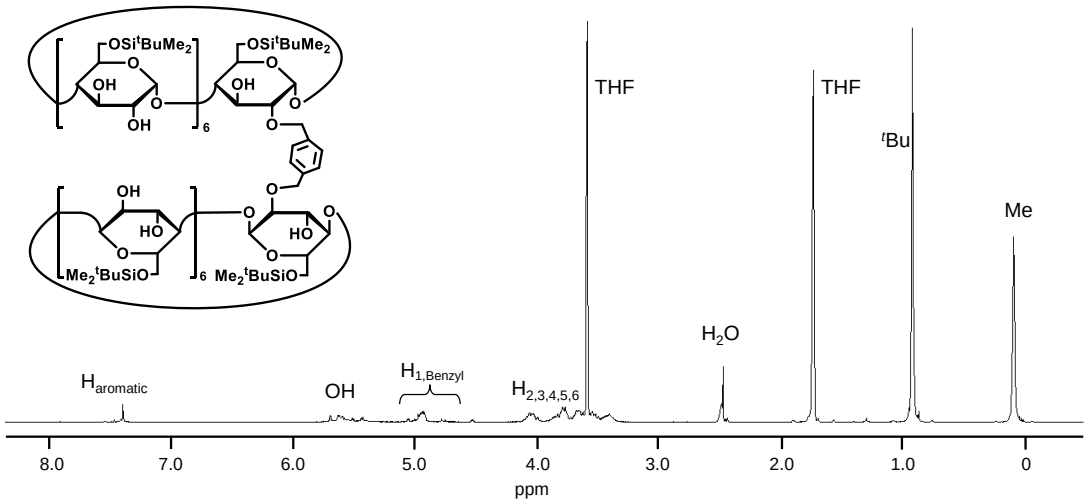

Figure 1-13. ^{1}H NMR spectrum of α,α'-bis[2-*O*-(heptakis(6-*O*-*tert*-butyldimethylsilyl)-β-cyclodextrin)]-*p*-xylene in THF-d_8.

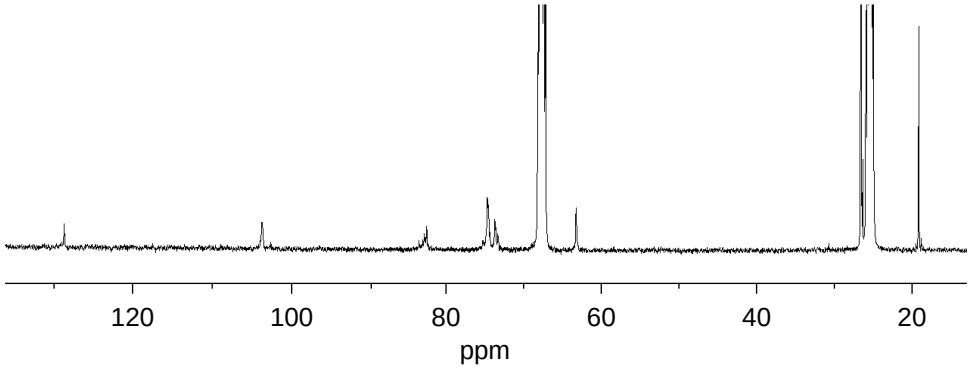

Figure 1-14. ^{13}C NMR spectrum of α,α'-bis[2-*O*-(heptakis(6-*O*-*tert*-butyldimethylsilyl)-β-cyclodextrin)]-*p*-xylene in THF-d_8.

1.4.4 Experimental Procedure for Fluorescence Titration and Job Plots

A guest solution (0.5 mL, 1×10^{-6} M) was titrated with increasing amounts of the host (0 ~ 8.0×10^{-5} M) at 25 °C. The titration curves (changes in the fluorescence intensity of the guest against the host concentration) were analyzed by a non-linear least-squares curve fitting method to generate the association constant (K) of the host-guest complex. The Job plots were acquired by monitoring the changes in the fluorescence intensity of the guest in a series of solutions with varying host/guest ratios where the total concentration of the host and guest remained constant (1×10^{-5} M). The relative concentration of the host-guest complex estimated from the fluorescence intensity of the guest was plotted against ([guest]/{[host] + [guest]}).

1.4.5 Experimental Procedure for NMR Titration and Job Plots

The ^{1}H-NMR titrations were performed at 25 °C in cyclohexane-d_{12}, benzene-d_6, and tetrahydrofuran (THF)-d_8. A solution of the host molecule (0.5 mL, 1.0 mM) was titrated in an NMR tube with increasing amounts of the guest stock solution (150 mM). The titration curves [changes in the chemical shift of the host protons (Δδ) against the guest/host concentration ratio] were analyzed by the nonlinear least-squares curve fitting method to generate the association constants of the host-guest complexes. The Job plots were acquired by monitoring the changes in the chemical shift of the host protons (Δδ) in a series of solutions with varying host/guest ratios where the total concentrations of the host and guest remained constant (2.0 mM). The relative concentration of the host-guest complex estimated from the Δδ · [host] value was plotted against ([guest]/{[host] + [guest]}).

1.4.6 Determination of Association Constants

The association constants (K) between β-CD dimers (host) and each guest in cyclohexane (cyclohexane-d_{12}) and benzene (benzene-d_6) were determined by a fluorescence titration or ^{1}H NMR titration method. For a 1:1 host-guest complex, the following expression can be written:

$$\text{host} + \text{guest} \rightleftharpoons \text{host•guest}$$

The association constant is given by eq 1

$$K = [\text{host} \bullet \text{guest}]/[\text{host}][\text{guest}] \qquad (1)$$

where [host], [guest], and [host•guest] are equilibrium concentrations.

For a 2:1 host-guest complex, the following expression can be written:

$$2\ \text{host} + \text{guest} \overset{K}{\rightleftharpoons} (\text{host})_2 \bullet \text{guest}$$

$$\text{host} + \text{guest} \overset{K_1}{\rightleftharpoons} \text{host} \bullet \text{guest}$$

$$\text{host} \bullet \text{guest} + \text{host} \overset{K_2}{\rightleftharpoons} (\text{host})_2 \bullet \text{guest}$$

The association constant is given by eq 2

$$K = [(\text{host})_2 \cdot (\text{guest})]/[\text{host}]^2[\text{guest}] = K_1 \cdot K_2 \qquad (2)$$

where [host], [guest], and $[(\text{host})_2 \cdot (\text{guest})]$ are equilibrium concentrations.

1.4.7 ^{1}H NMR Spectral Changes Observed for TBDMS-β-CD upon Addition of Naphthalene in Nonpolar Solvents

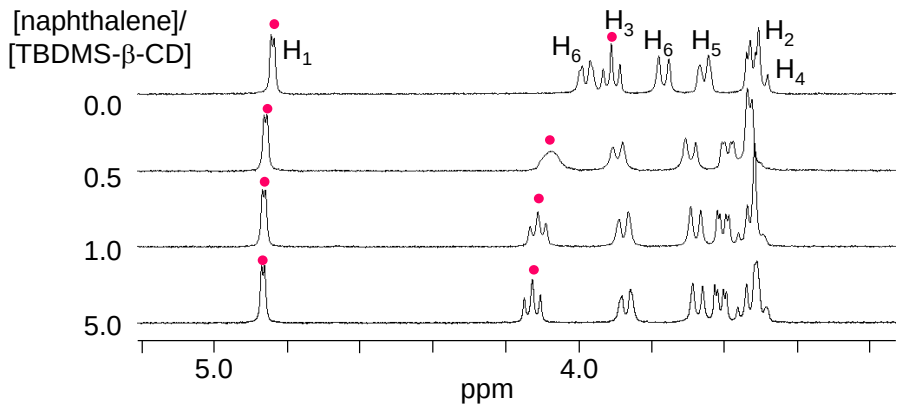

Figure 1-15. ^{1}H NMR spectral changes of TBDMS-β-CD (1.0×10^{-3} M) upon addition of increasing amounts of naphthalene in cyclohexane-d_{12} at 25 °C.

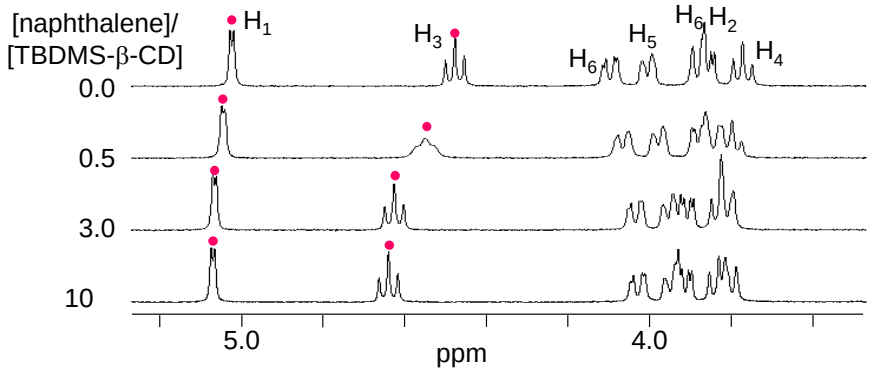

Figure 1-16. ^{1}H NMR spectral changes of TBDMS-β-CD (1.0×10^{-3} M) upon addition of increasing amounts of naphthalene in benzene-d_6 at 25 °C.

1.4.8 ^{1}H NMR Spectral Changes Observed for TBDMS-β-CD upon Addition of Pyrene in THF

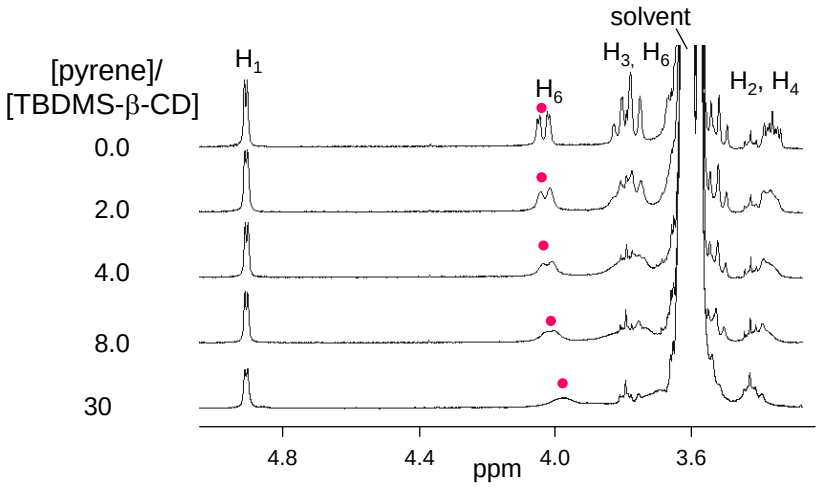

Figure 1-17. ^{1}H NMR spectral changes of TBDMS-β-CD (1.0×10^{-3} M) upon addition of increasing amounts of pyrene in THF-d_8 at 25 °C.

1.4.9 Titration Curves

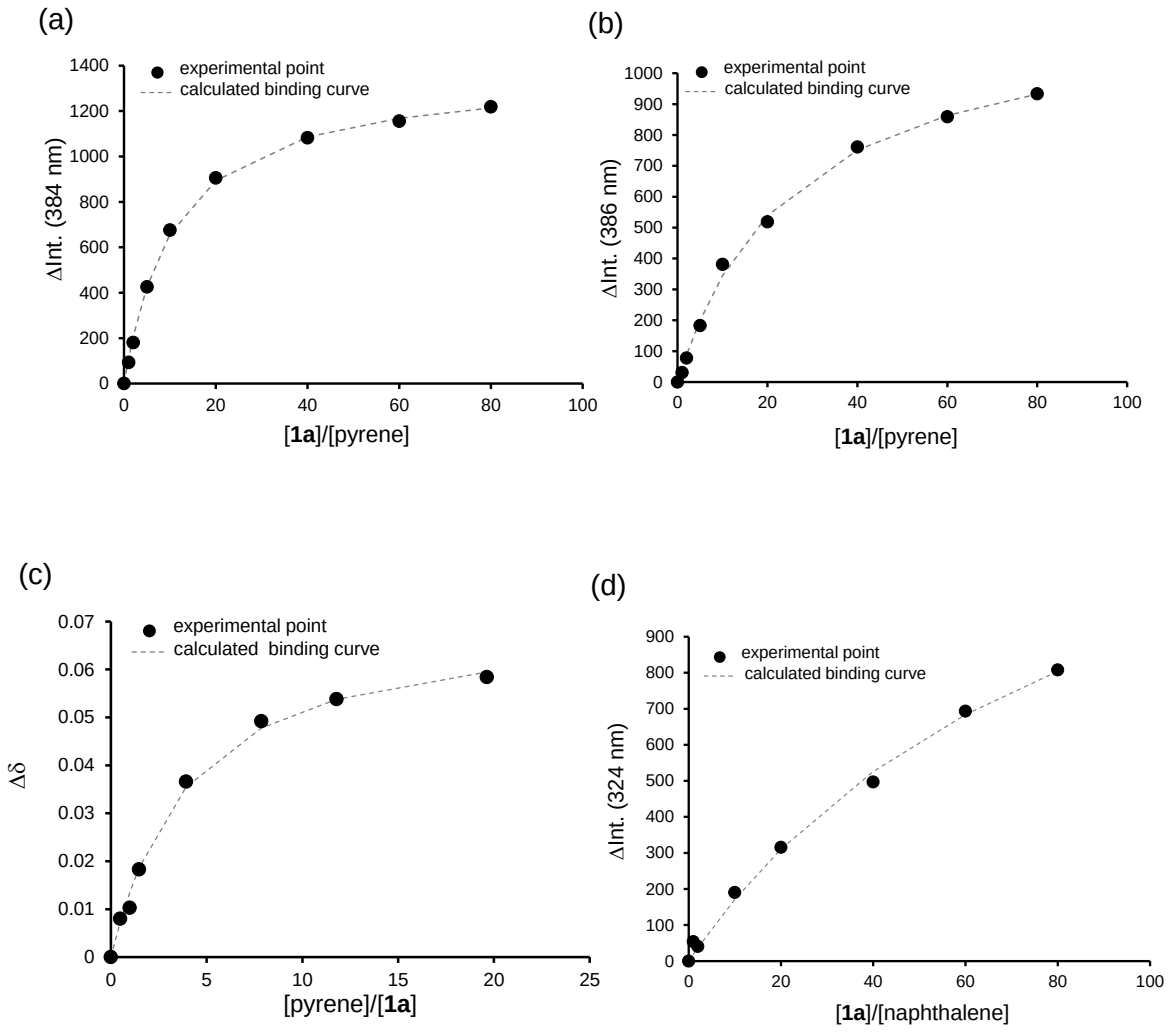

Figure 1-18. Titration curves for complex formation between β-CD dimer **1a** and aromatic guests in organic solvents. (a) Fluorescence titration curve for complex formation between **1a** and pyrene in cyclohexane. [pyrene] = 1.0×10^{-6} M. At 25 °C. (b) Fluorescence titration curve for complex formation between **1a** and pyrene in benzene.[pyrene] = 1.0×10^{-6} M. At 25 °C. (c) ^{1}H NMR titration curve for complex formation between **1a** and pyrene in THF-d_8. [**1a**] = 1.0×10^{-3} M. At 25 °C. The proton signal of **1a** at 7.22 ppm was used for titration. (d) Fluorescence titration curve for complex formation between **1a** and naphthalene in cyclohexane. [naphthalene] = 1.0×10^{-6} M. At 25 °C.

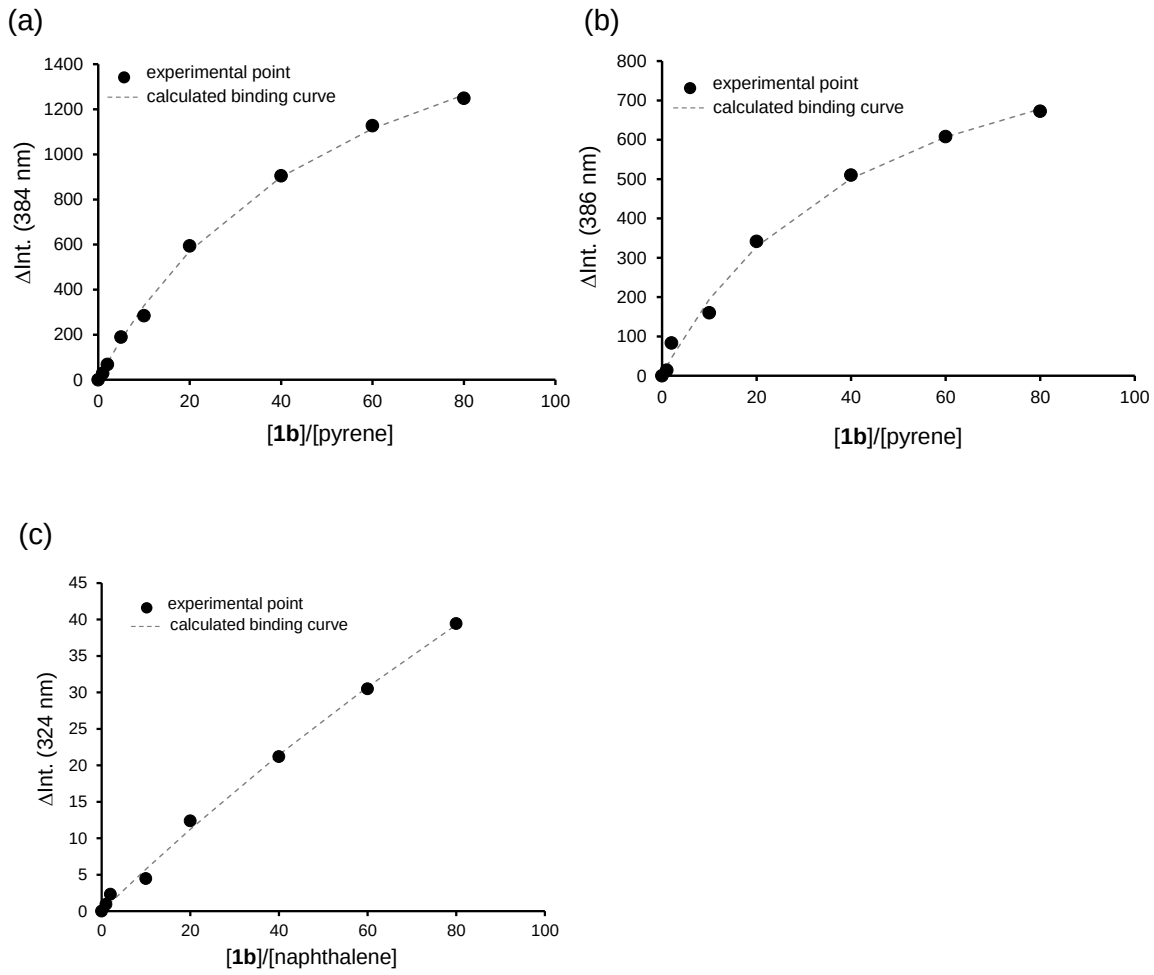

Figure 1-19. Titration curves for complex formation between β-CD dimer **1b** and aromatic guests in organic solvents. (a) Fluorescence titration curve for complex formation between **1b** and pyrene in cyclohexane. [pyrene] = 1.0×10^{-6} M. At 25 °C. (b) Fluorescence titration curve for complex formation between **1b** and pyrene in benzene. [pyrene] = 1.0×10^{-6} M. At 25 °C. (c) Fluorescence titration curve for complex formation between **1b** and naphthalene in cyclohexane. [naphthalene] = 1.0×10^{-6} M. At 25 °C.

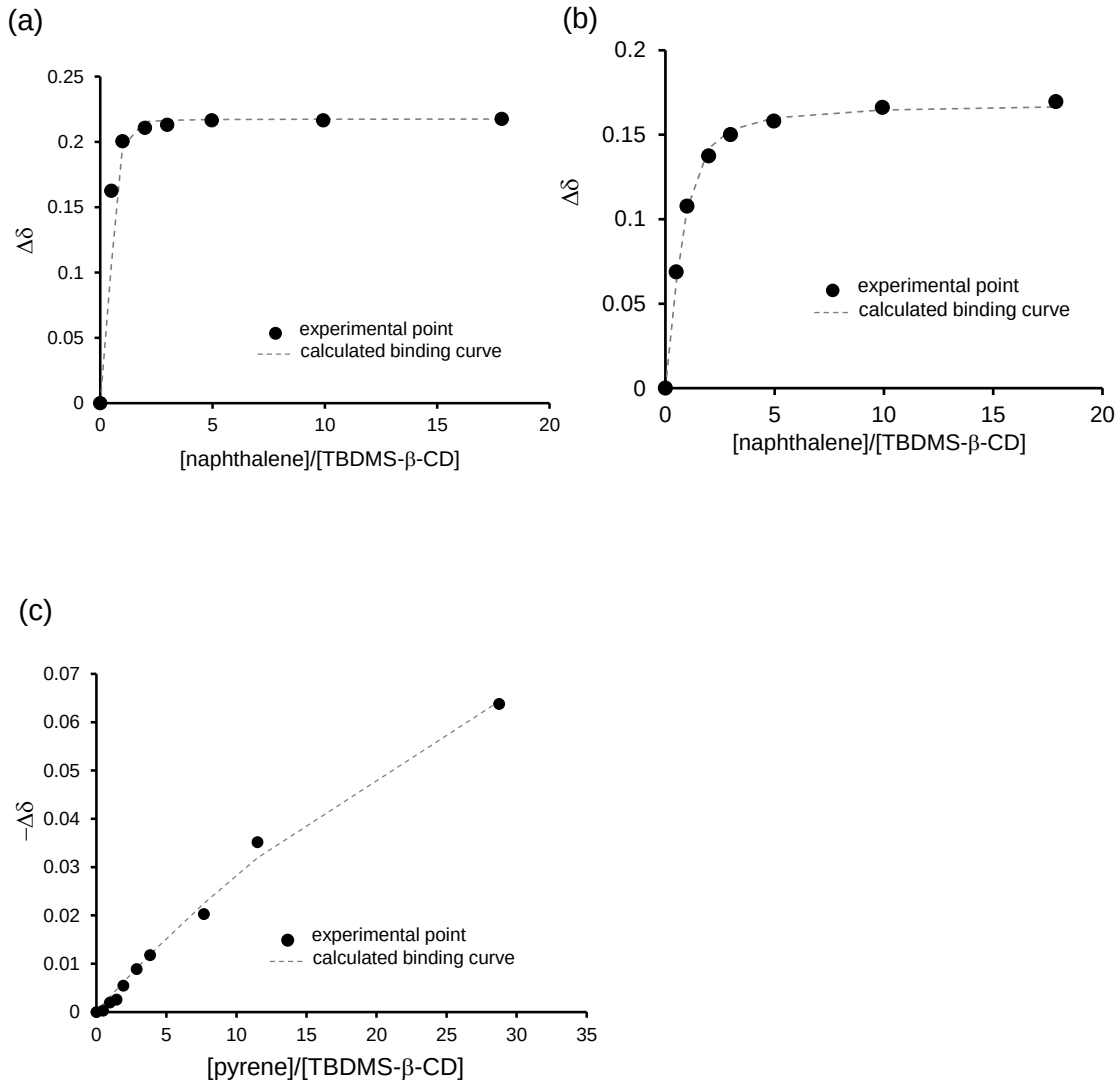

Figure 1-20. Titration curves for complex formation between TBDMS-β-CD and aromatic guests in organic solvents. (a) ^{1}H NMR titration curve for complex formation between TBDMS-β-CD and naphthalene in cyclohexane-d_{12}. [TBDMS-β-CD] = 1.0×10^{-3} M. At 25 °C. The proton signal of TBDMS-β-CD at 4.83 ppm was used for titration. (b) ^{1}H NMR titration curve for complex formation between TBDMS-β-CD and naphthalene in benzene-d_6. [TBDMS-β-CD] = 1.0×10^{-3} M. At 25 °C. The proton signal of TBDMS-β-CD at 5.02 ppm was used for titration. (c) ^{1}H NMR titration curve for complex formation between TBDMS-β-CD and pyrene in THF-d_8. [TBDMS-β-CD] = 1.0×10^{-3} M. At 25 °C. The proton signal of TBDMS-β-CD at 4.02 ppm was used for titration.

1.4.10 Job Plot for Complex Formation between β-CD dimers or TBDMS-β-CD and Aromatic Guests in Organic Solvents

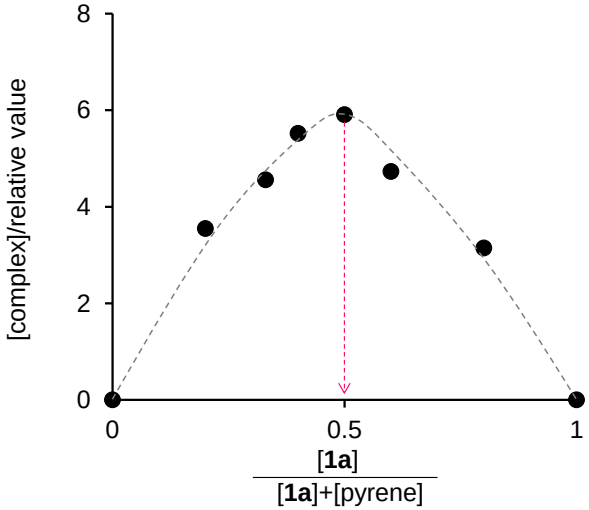

Figure 1-21. Job plot for the complex between **1a** and pyrene in THF-d_8 at 25 °C.

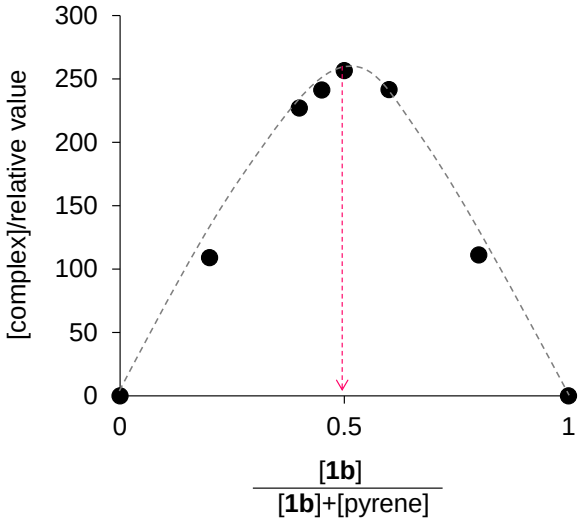

Figure 1-22. Job plot for the complex between **1b** and pyrene in cyclohexane at 25 °C. λ_{ex}=340 nm. λ_{em}= 384 nm.

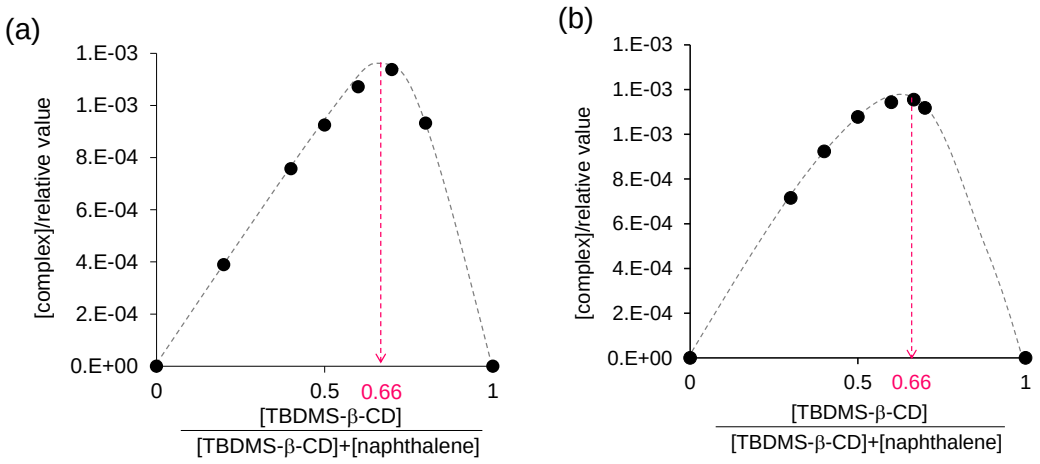

Figure 1-23. Job plot for the complex between TBDMS-β-CD and naphthalene (a) in cyclohexane-d_{12} (b) in benzene-d_6 at 25 °C.

1.4.11 Fluorescence Spectral Changes of (*R*)- or (*S*)-1-NET upon Addition of β-CD Dimers in Cyclohexane

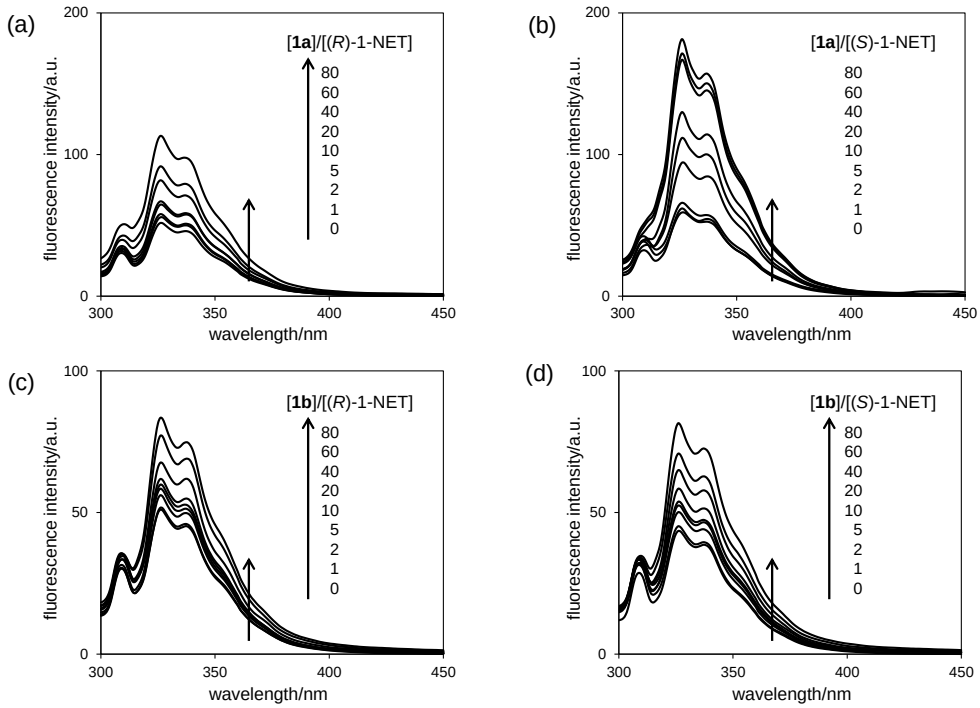

Figure 1-24. Fluorescence spectral changes of (a, c) (*R*)-1-NET (b, d) (*S*)-1-NET (1.0×10^{-6} M) upon addition of increasing amount of (a, b) **1a** and (c, d) **1b** in cyclohexane at 25 °C. λ_{ex} =283 nm.

1.4.12 Fluorescence Spectral Changes of (*R*)- or (*S*)-2-NEA upon Addition of β-CD Dimers in Cyclohexane

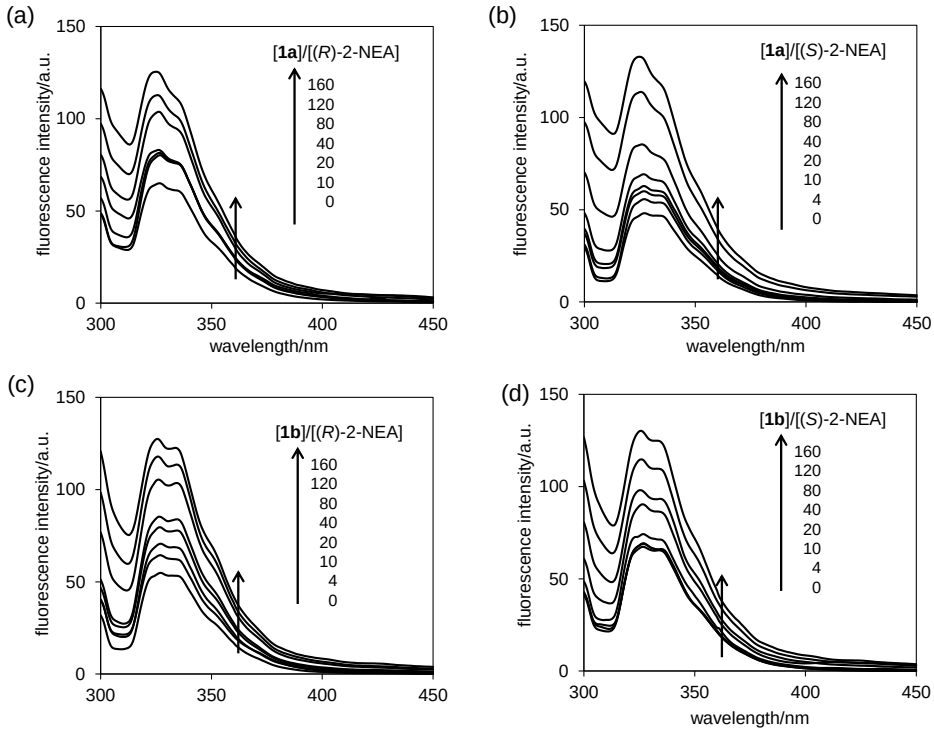

Figure 1-25. Fluorescence spectral changes of (a, c) (*R*)-2-NEA (b, d) (*S*)-2-NEA (1.0×10^{-6} M) upon addition of increasing amount of (a, b) **1a** and (c, d) **1b** in cyclohexane at 25 °C. λ_{ex} =275 nm.

1.4.13 ^{1}H NMR Spectral Changes Observed for TBDMS-β-CD upon Addition of (*R*)- or (*S*)-1-NEA in Cyclohexane

(a)

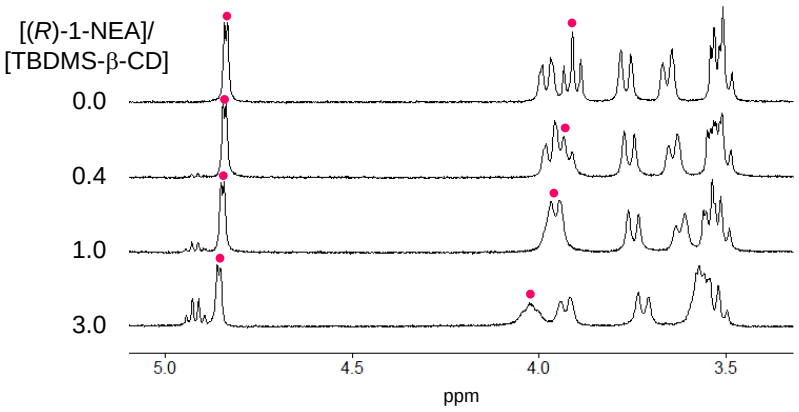

(b)

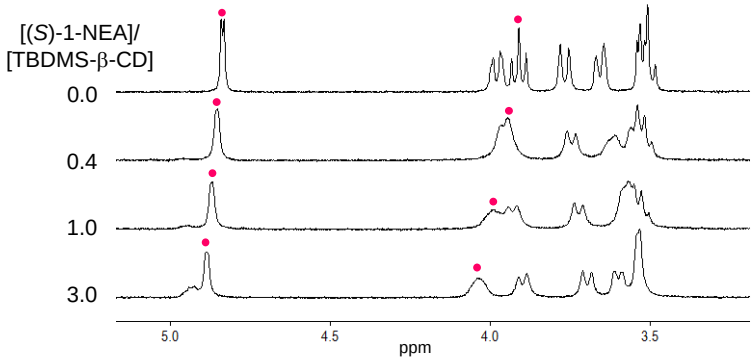

Figure 1-26. ^{1}H NMR spectral changes of TBDMS-β-CD (1.0×10^{-3} M) upon addition of increasing amounts of (a) (*R*)-1-NEA (b) (*S*)-1-NEA in cyclohexane-d_{12} at 25 °C.

1.4.14 Titration Curves for Complex Formation between β-CD Dimer 1a and Aromatic Chiral Guests in Cyclohexane

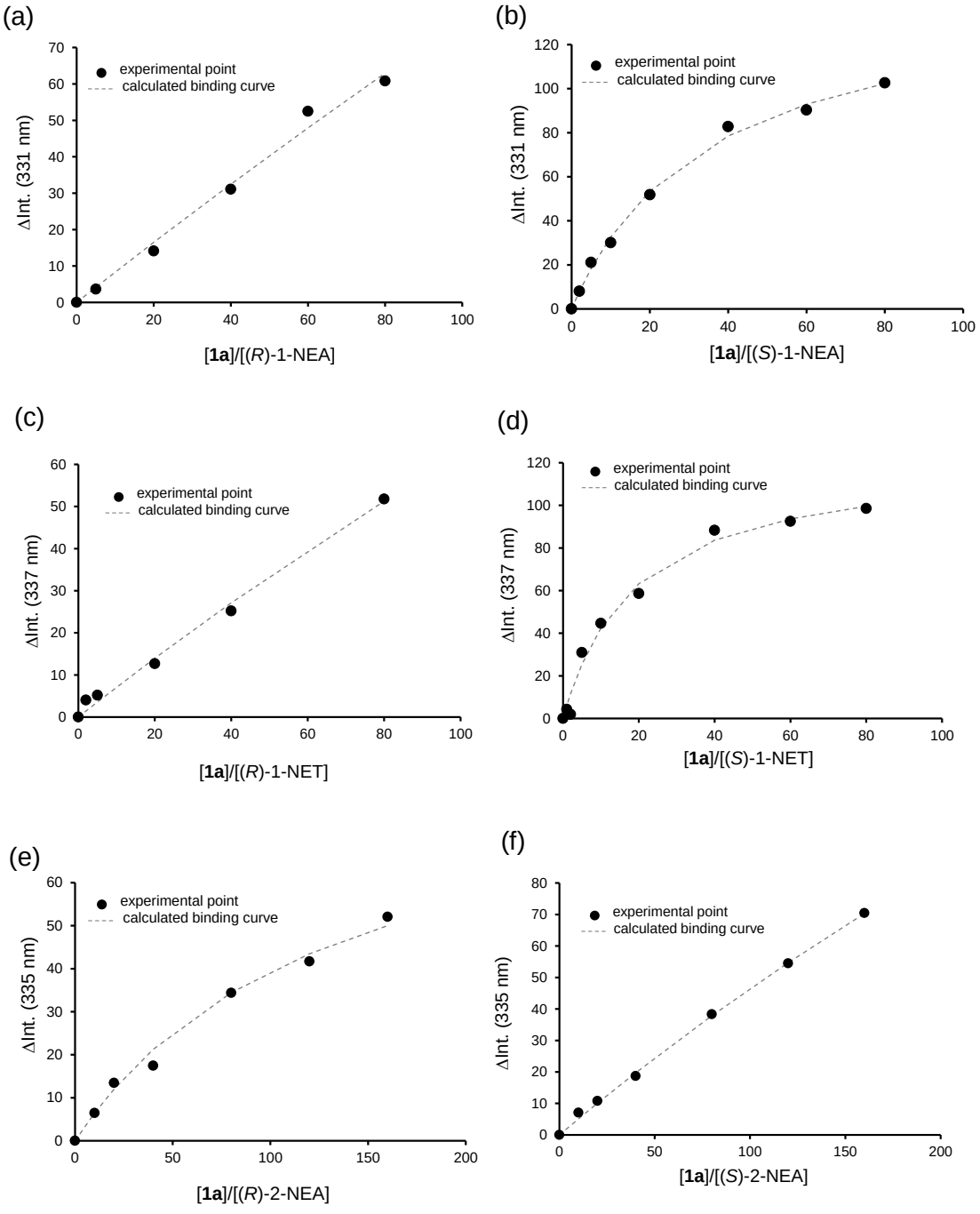

Figure 1-27. Fluorescence titration curve for complex formation between **1a** and (a) (*R*)-1-NEA (b) (*S*)-1-NEA (c) (*R*)-1-NET (d) (*S*)-1-NET (e) (*R*)-2-NEA (f) (*S*)-2-NEA in cyclohexane. [Guests] = 1.0×10^{-6} M. At 25 °C.

1.4.15 Titration Curves for Complex Formation between β-CD Dimer 1b and Aromatic Chiral Guests in Cyclohexane

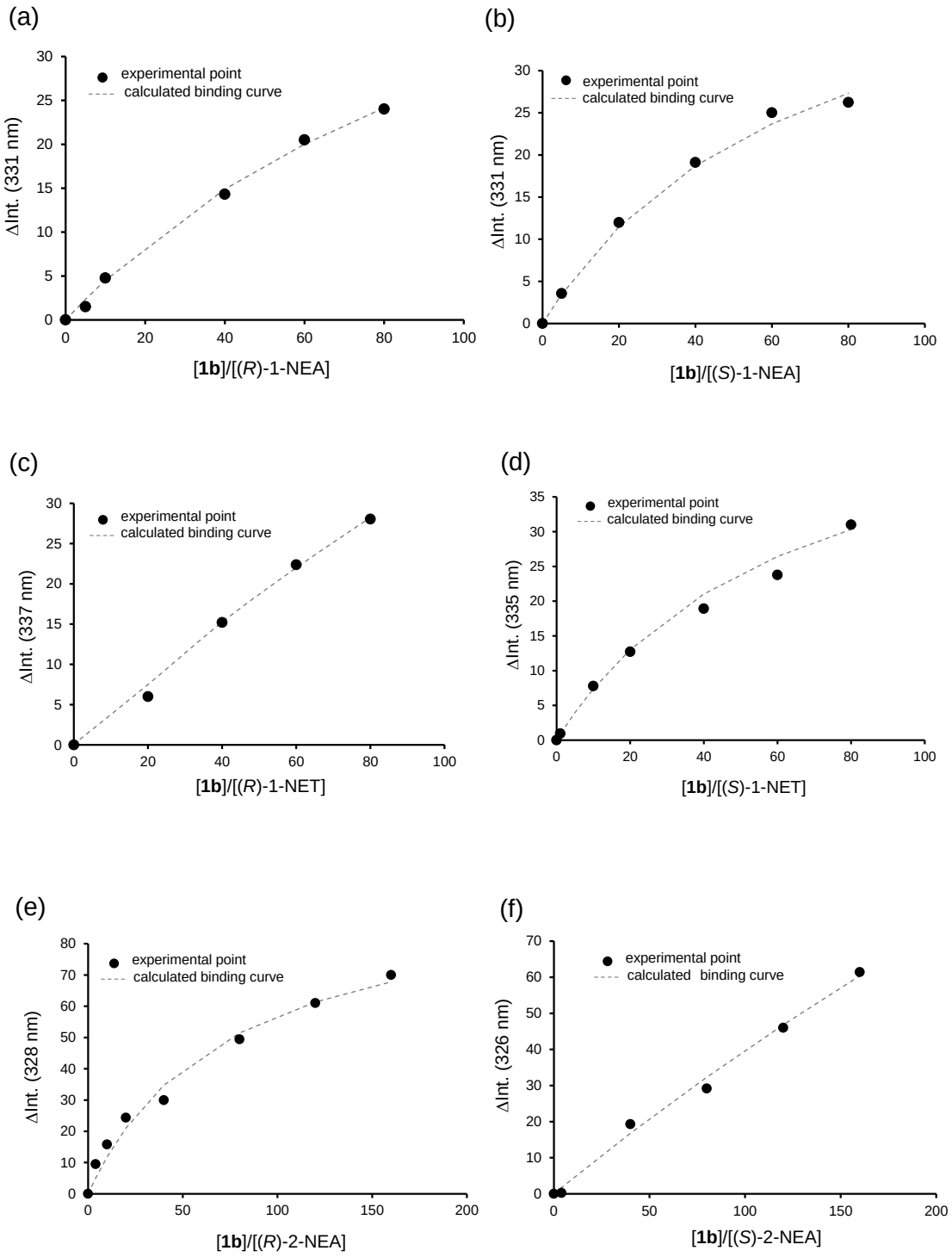

Figure 1-28. Fluorescence titration curve for complex formation between **1b** and (a) (*R*)-1-NEA (b) (*S*)-1-NEA (c) (*R*)-1-NET (d) (*S*)-1-NET (e) (*R*)-2-NEA (f) (*S*)-2-NEA in cyclohexane. [Guests] = 1.0×10^{-6} M. At 25 °C.

1.4.16 Titration Curves for Complex Formation between TBDMS-β-CD and Aromatic Chiral Guests 2a in Cyclohexane

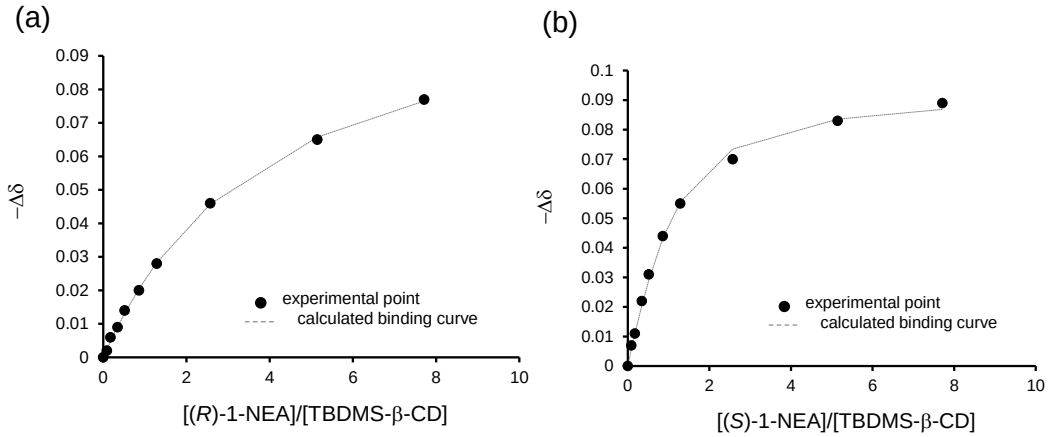

Figure 1-29. NMR titration curve for complex formation between TBDMS-β-CD and (a) (*R*)-1-NEA (b) (*S*)-1-NEA in cyclohexane. [TBDMS-β-CD] = 1.0×10^{-3} M. At 25 °C. The proton signal of TBDMS-β-CD at 4.83 ppm was used for titration.

1.4.17 Job Plots for Complexes between TBDMS-β-CD and Aromatic Chiral Guests 2a in Cyclohexane

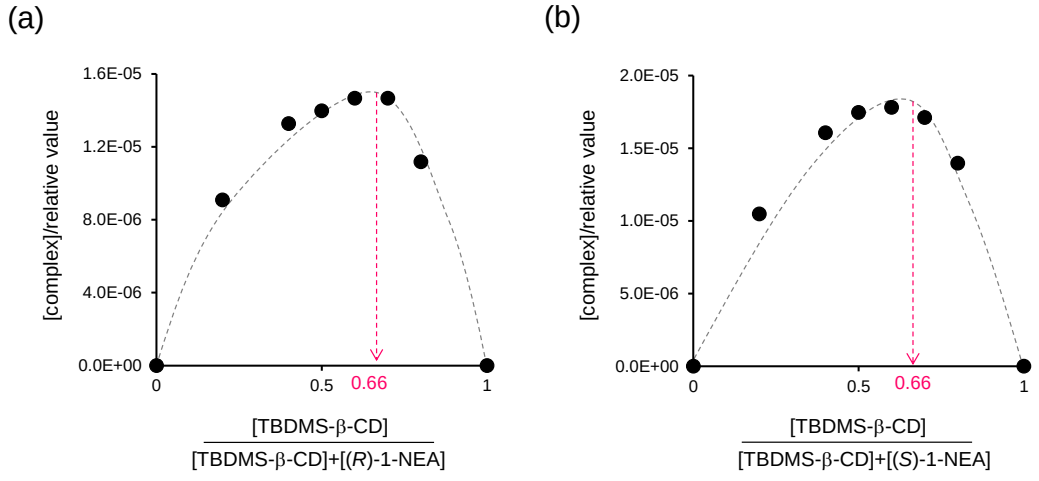

Figure 1-30. Job plots for the complexes of TBDMS-β-CD with (a) (*R*)-1-NEA and (b) (*S*)-1-NEA in cyclohexane-d_{12} at 25 °C.

1.4.18 Enantioselective *N*-Benzoylation of 1-(1-Naphthyl)ethylamine

N-Benzoylation of racemic 1-NEA was carried out with benzoic anhydride as an acylating reagent and triethylamine as a base in cyclohexane in the presence and absence of TBDMS-β-CD dimers **1a** and **1b**. After a mixture of racemic 1-NEA (2.0×10^{-4} mmol) and a TBDMS-β-CD dimer was stirred for 1 h in cyclohexane (200 μL) to reach the complexation equilibrium between 1-NEA and TBDMS-β-CD dimer, triethyamine (2.0×10^{-4} mmol) and then benzoic anhydride were added at 10 or 25 °C. The mixture was stirred at 10 or 25 °C for 2 h. The resulting products were analyzed by HPLC using a chiral phase column Diacel Chiralcel OD-H (250 mm × 4.6 mm i.d.) using hexane/2-propanol = 95/5 as an eluent at a flow rate of 1.5 ml min^{-1} using UV detection (254 nm).

HPLC charts of the products obtained after *N*-benzoylation of 1-NEA (2.0×10^{-4} mmol) with benzoic anhydride (1.0×10^{-4} mmol) in cyclohexane (200 μL) including triethyamine (2.0×10^{-4} mmol) in the absence and presence of TBDMS-β-CD dimer **1a** (5.0×10^{-4} mmol) are shown in Fig. 1-31.

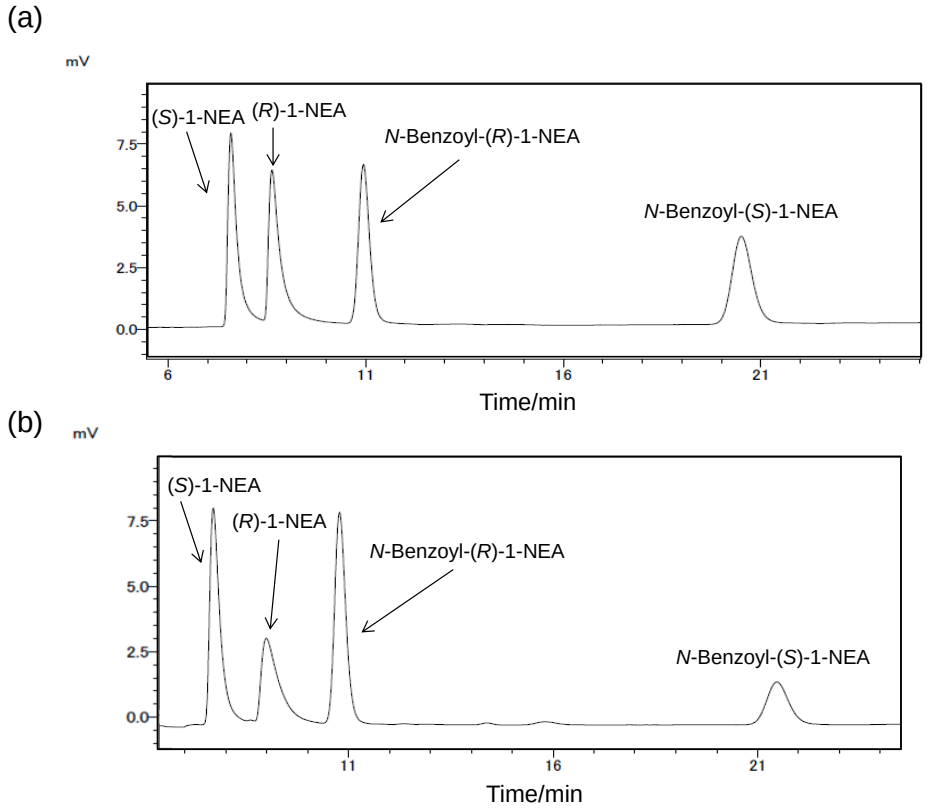

Figure 1-31. HPLC chromatogram of the products obtained after *N*-benzoylation of 1-NEA (2.0×10^{-4} mmol) with benzoic anhydride (1.0×10^{-4} mmol) in cyclohexane (200 μL) including triethyamine (2.0×10^{-4} mmol) in (a) the absence of (b)the presence of TBDMS-β-CD dimer **1a** (5.0×10^{-4} mmol). Column: Daicel Chiralcel OD-H (250 mm × 4.6 mm i.d.); mobile phase: hexane/2-propanol = 95/5; flow rate: 0.5 ml min^{-1}; temperature: 40 °C; detector: UV (254 nm).

References

1) M. V. Resharsky, Y. Inoue, *Chem. Rev.* **1998**, *98*, 1875‑1918.
2) a) B. Siegel, R. Breslow, *J. Am. Chem. Soc.* **1975**, *97*, 6869–6870; b) A. F. Daniel de Namor, R. Traboulssi, D. F. V. Lewis, *J. Am. Chem. Soc.* **1990**, *112*, 8442–8447.
3) T. Kida, Y. Fujino, K. Miyawaki, E. Kato, M. Akashi, *Org. Lett.* **2009**, *11*, 5282–5285.
4) T. Kida, T. Iwamoto, Y. Fujino, N. Tohnai, M. Miyata, M. Akashi, *Org. Lett.* **2011**, *13*, 4570–4573.
5) a) T. Kida, T. Iwamoto, H. Asahara, T. Hinoue, M. Akashi, *J. Am. Chem. Soc.* **2013**, *135*, 3371–3374; b) H. Asahara, T. Kida, T. Iwamoto, T. Hinoue, M. Akashi, *Tetrahedron* **2014**, *70*, 197–203.
6) E. v. van Dienst, B. H. M. Snellink, I. von Piekartz, M. H. B. G. Gansey, F. Venema, M. C. Feiters, R. J. M. Nolte, J. F. J. Engbersen, D. N. Reinhoudt, *J. Org. Chem.* **1995**, *60*, 6537–6545.
7) a) For selected examples, see: S. Das, N. Majumdar, C. Kanta De, D. S. Kundu, A. Döhring, A. Garczynski, B. List, *J. Am. Chem. Soc*. **2017**, *139*, 1357–1359; b) N. Mittal, D. X. Sun, D. Seidel, *Org. Lett.* **2012**, *14*, 3084–3087; c) A. Kolleth, S. Christoph, S. Arseniyadis, J. Cossy, *Chem. Commun.* **2012**, *48*, 10511–10513; d) C. Min, N. Mittal, C. K. De, D. Seidel, *Chem. Commun.* **2012**, *48*, 10853–10855; e) V. P. Krasnov, D. A. Gruzdev, G. L. Levit, *Eur. J. Org. Chem.* **2012**, 1471–1493.
8) a) A. Shitangkoon, G. Vigh, *J. Chromatogr. A.* **1996**, *738*, 31–42; b) K. Takeo, H. Mitoh, K. Uemura, *Carbohydr. Res.* **1989**, *187*, 203–221; c) P. R. Ashton, R. Koniger, J. F. Stoddart, *J. Org. Chem.* **1996**, 61, 903–908.

Chapter 2

Molecular Recognition Ability of β-CD Dimers Bearing Multiple Linkers toward Long-Chain Fatty Acid Esters in Organic Solvents

2.1 Introduction

To date, there are only two examples of CD dimers constructed via covalent bonds by more than three linkers[1], which may be due to the considerably difficult synthesis. Regarding guest inclusion ability, it is only reported that α-CD dimer with three disulfide linkers includes long-chain alcohols in water[1a]. Recently we reported the facile synthesis of β-CD dimers with seven xylylene linkers via a one-step reaction of 6-*O*-tert-butyldimethylsilylated β-CD (TBDMS-β-CD) with xylylene dibromide[2]. Although these TBDMS-β-CD dimers form inclusion complexes with aromatic guests such as phenol and aniline in nonpolar solvents, the types of incorporated guests are limited to small aromatic molecules because the bulky TBDMS groups at both ends of the CD dimer inhibit the incorporation of guest molecules into the CD dimer cavity from the ends. In the course of our studies on the synthesis of open-ended β-CD dimer from TBDMS-β-CD dimers via the elimination of the TBDMS groups, we found that a Janus-type TBDMS-β-CD dimer is selectively synthesized with tetramethylammonium fluoride (TMAF) as a desilylation reagent to give one fully modified end by TBDMS groups and one unmodified end. This interesting finding prompted us to explore the desilylation of the TBDMS-β-CD dimer under various conditions and to study the mechanism of selective elimination of the TBDMS groups from only one side of the CD rings in the TBDMS-β-CD dimer.

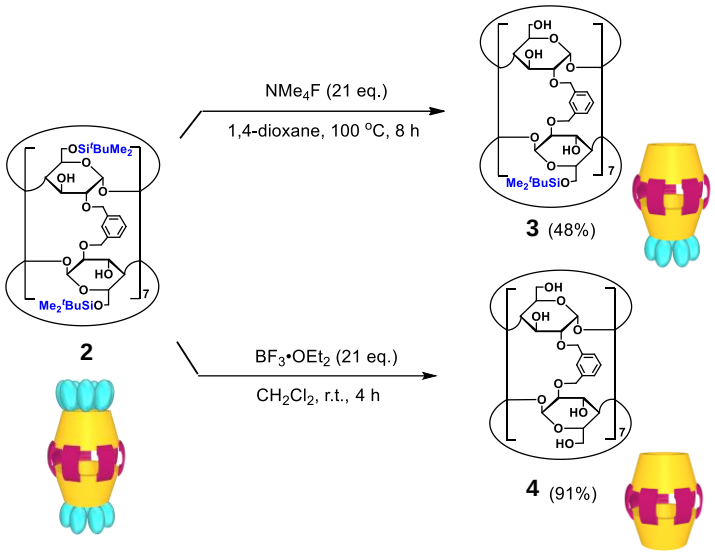

Scheme 2-1. Synthesis of β-CD **3** and **4**.

Herein we report the facile synthesis of a Janus-type TBDMS-β-CD dimer tube and unmodified β-CD dimer tube, respectively. The inclusion ability of these β-CD dimer tubes for long-chain fatty acid esters was examined.

2.2 Results and Discussion

2.2.1 Synthesis

Based on our initial finding, we chose TBDMS-β-CD dimer **2** bearing seven *m*-xylylene linkers as the starting material to synthesize the desired CD dimer (Scheme 2-1). **2** was synthesized by a one-step reaction of TBDMS-β-CD with *m*-xylylene dibromide using the previously reported method.[2] Reacting **2** with TMAF[3] (21 eq.) in 1,4-dioxane for 8 h at 100 °C gives a strong peak

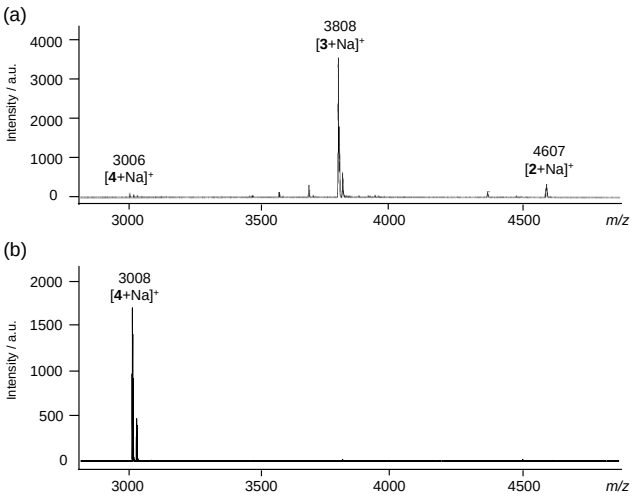

Figure 2-1. MALDI-TOF MS spectra of the products obtained by the reaction of **2** (a) with TMAF in 1,4-dioxane for 8 h at 100 °C and (b) with $BF_3{\cdot}OEt_2$ in CH_2Cl_2 for 4 h at room temperature.

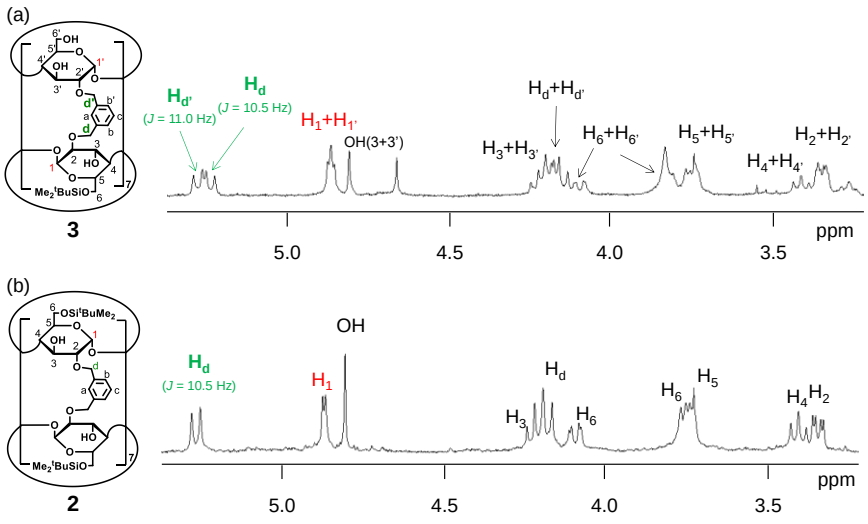

Figure 2-2. ^{1}H NMR spectra of (a) **3** and (b) **2** in acetone-d_6 at 25 °C.

corresponding to **3**, which is formed by the elimination of seven TBDMS groups from **2**, in the MALDI-TOF MS spectrum of the reaction mixture (Fig. 2-1a). **3** was isolated by silica gel column chromatography using methanol/chloroform (1:10 to 1:6) as an eluent.

Figure 2-2 shows the ^{1}H NMR spectra of **3** and **2**. The spectrum of **3** contains a set of CD and linker proton signals similar to that of **2** as well as another set of CD and linker proton signals whose integral ratio with the former set is 1:1. This result confirms that **3** is composed of two types of CD rings in different chemical environments, that is, TBDMS-β-CD and unmodified β-CD. Thus, using TMAF as a desilylation reagent selectively eliminates seven TBDMS groups from one side of the CD ring of **2** to give a Janus-type TBDMS-β-CD dimer **3**.

On the other hand, the reaction of **2** with $BF_3{\cdot}OEt_2$ (21 eq.) as another desilylation reagent[4] in dichloromethane for 4 h at room temperature (Scheme 2-1) gives **4** in 91% yield (Fig. 2-1b). This result suggests that the conditions completely eliminate the TBDMS groups from **2**.

To gain insight into the selective elimination mechanism of the TBDMS groups from only one side of CD rings in **2** using TMAF, the desilylation of **2** with TMAF was monitored by MALDI-

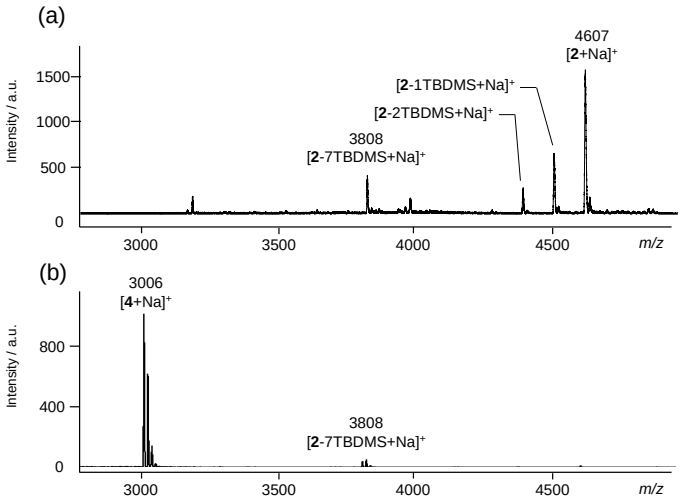

Figure 2-3. MALDI-TOF MS spectra of the products of the desilylation of **2** with TMAF in 1,4-dioxane at 100 °C for (a) 2 h and (b) 18 h.

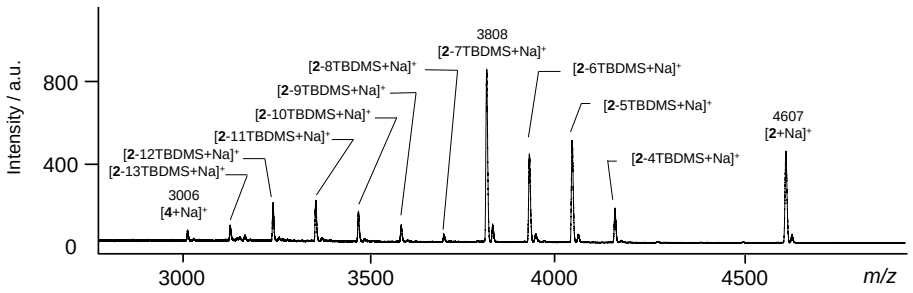

Figure 2-4. MALDI-TOF MS spectrum of the product of the desilylation of **2** with TBAF (14 eq.) in THF for 8 h at 60 ºC.

TOF MS spectroscopy. After 2 h, the spectrum contains peaks attributed to the elimination of one, two, and seven TBDMS groups from **2** along with unreacted **2** (Fig. 2-3a). However, the spectrum after 18 h contains the peak of **4** without the TBDMS group while that of **3** is negligible (Fig. 2-3b). These results suggest that **3** is a kinetically trapped intermediate in the desilylation process of **2** to produce **4**. Using tetra(*n*-butyl)ammonium fluoride (TBAF),[4] which has a more reactive F^- ion than TMAF,[5] as a desilylation reagent selectively eliminates seven TBDMS groups from **2**, but at a much lower selectivity (Fig. 2-4).

The selective elimination of the TBDMS groups on one side of the two CD rings with TMAF is attributed to two factors. One is the low reactivity of the F^- ion of TMAF, which may suppress the random elimination of the TBDMS groups from the two CD rings. The other is the hindrance due to the many bulky TBDMS groups on the CD rings. These bulky groups sterically inhibit the attack of the F^- ion on the Si atoms of the TBDMS groups in the early stages of the reaction. However, once one or two TBDMS groups are removed by a successful attack of the F^- ion on the Si atom, the generated space decreases the steric hindrance. Consequently, it is easier for the F^- ion to attack the next Si atom on the same CD ring. Thus, the subsequent elimination of the TBDMS groups on the same CD ring occurs rapidly to give **3**.

2.2.2 Inclusion of Long-chain Fatty Acid Esters

3 shows a good solubility in polar organic solvents, including methanol, THF, and chloroform. In contrast, **4** has a low solubility in all solvents except for DMSO. We evaluated the inclusion ability of **3** toward various long-chain fatty acid esters by the ^{1}H NMR titration method using methanol-d_4 as the solvent. Fig. 2-5 shows the changes in the ^{1}H NMR signals of **3** induced by the addition of methyl oleate in methanol-d_4 at 25 °C. Adding the guest shifts the signal of H_3 protons directed inside the cavity, suggesting an inclusion complex between **3** and methyl oleate is formed in methanol-d_4. In the cases of other guests, the H_3 proton signal of **3** also shifts upon the addition of the guests (Figs. 2-14–2-22). Job plots using the NMR method has a maximum at

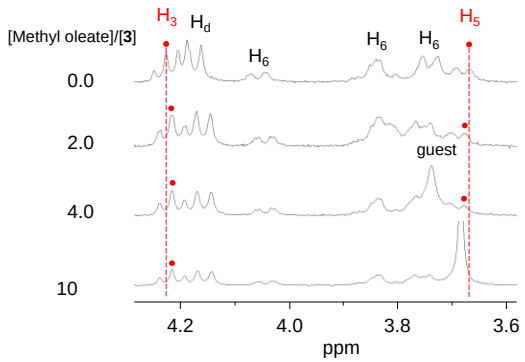

Figure 2-5. ^{1}H NMR spectral changes observed for **3** (5.0×10^{-4} M) upon the addition of methyl oleate in methanol-d_4 at 25 ºC .

a [**3**]/[guest] molar ratio of 1 : 1, indicating that **3** forms a 1 : 1 inclusion complex with guests in methanol-d_4 (Figs. 2-23 – 2-26). The nuclear overhauser effect spectrum (NOESY) of a 2-methyllinoleate inclusion complex in methanol-d_4 confirms that the resonances of the H_3 and H_5 protons of **3** are correlated to the CH_3 protons (H_A) and CH_2 protons (H_B) of methyl linoleate (Fig. 2-6a). In addition, in the NOESY spectrum of the inclusion complex of **3** with DHA methyl ester, the cross-peak between the H_3 protons of **3** and the methyl protons (H_G) of DHA methyl ester was clearly observed (Fig. 2-6b). These results indicate that these guests are included inside the cavity of **3**.

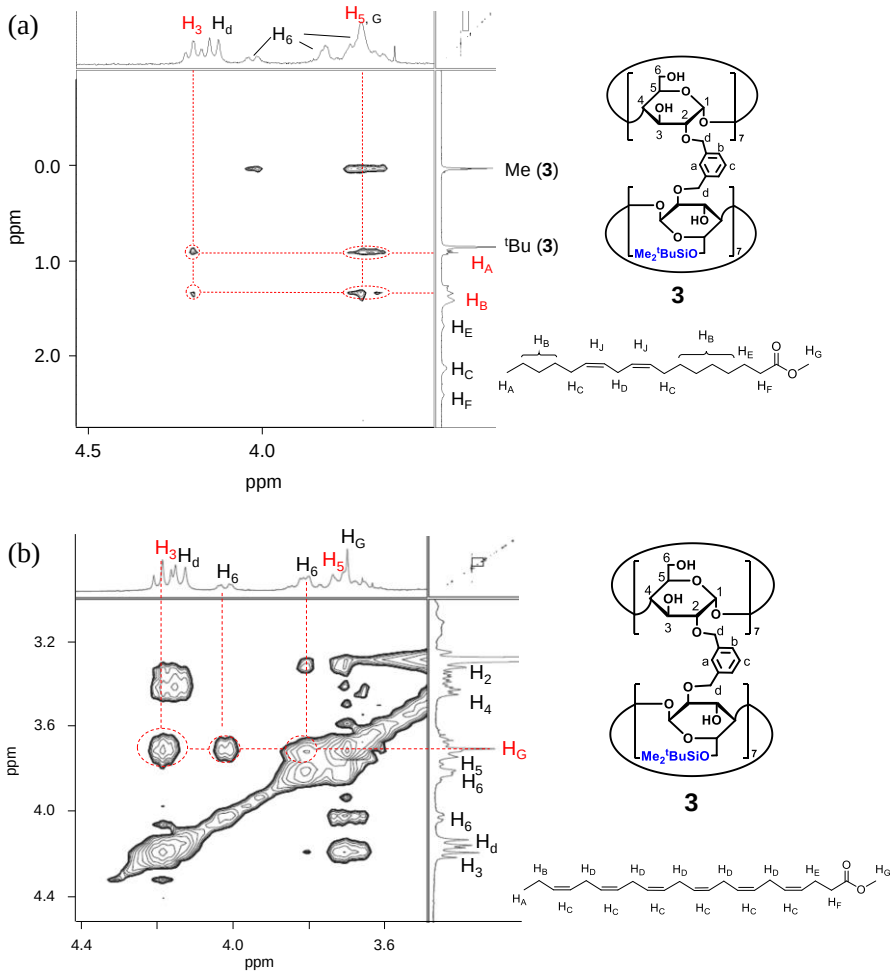

Figure 2-6. The partial 400 MHz NOESY spectrum of a complex of **3** with (a) methyl linoleate (b) methyl docosahexaenoate in methanol-d_4 at 25 ºC.

Table 2-1 summarizes the association constants between **3** and various long-chain fatty acid esters. **3** shows a moderate to high inclusion ability toward these fatty acid esters in methanol-d_4. The association constant between **3** and saturated fatty acid esters increases as the alkyl chain length increases (entries 1–3). The association constant with methyl stearate (C18) is five times higher than that with methyl myristate (C14). This result suggests that the solvophobic interactions or van der Waals interactions between **3** and these lipids affect inclusion complex formation. The association constant with methyl elaidate possessing a C18 chain and one *trans* double bond is almost the same as that with methyl stearate, whereas the association with methyl linoelaidate with the same carbon number and two *trans* double bonds is much lower than those association constants. The inclusion ability of **3** decreases as the linearity of the lipid structure increases. On the other hand, the association constant with methyl oleate with one cis double bond is more than twice those with methyl elaidate and methyl stearate. Consequently, **3** exhibits a selective inclusion ability for *cis*-unsaturated fatty acid esters compared to the corresponding *trans*-unsaturated fatty acid esters and saturated fatty acid esters in methanol-d_4. Interestingly, increasing the number of *cis* double bonds in the carbon chain of the guest remarkably increases the association constant with **3**. The association constant with methyl linoleate possessing two *cis* double bonds is three times higher than that with methyl oleate possessing one cis double bond. Further increasing the number of cis double bonds and the alkyl chain length increases the association constant. In particular, an extremely high inclusion ability toward methyl docosahexaenoate (DHA) with a C22 chain and six *cis* double bonds (1.2×10^5 M^{-1}) is observed. Thermodynamic parameters for complexation between **3** and methyl linoleate in methanol-d_4, which were determined by ^{1}H NMR titration at different temperatures, revealed the complexation

Table 2-1. Association constants between **3** and various long-chain fatty acid methyl esters in methanol-d_4 at 25 °C.

Entry	Guest		Association constant (M^{-1})
1	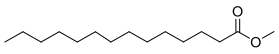	Methyl myristate (14:0)	$(4.8 \pm 0.48) \times 10^2$
2	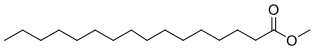	Methyl palmitate (16:0)	$(8.6 \pm 0.95) \times 10^2$
3	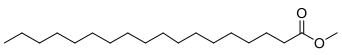	Methyl stearate (18:0)	$(2.5 \pm 0.60) \times 10^3$
4	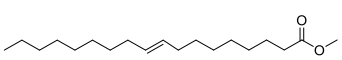	Methyl elaidate (18:1 *trans*)	$(3.0 \pm 0.46) \times 10^3$
5	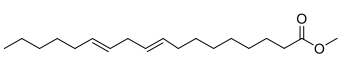	Methyl linoelaidate (18:2 *trans*)	$(3.1 \pm 0.42) \times 10^2$
6	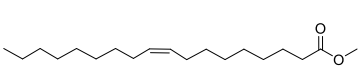	Methyl oleate (18:1 *cis*)	$(6.7 \pm 0.71) \times 10^3$
7	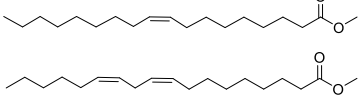	Methyl linoleate (18:2 *cis*)	$(2.0 \pm 0.80) \times 10^4$
8	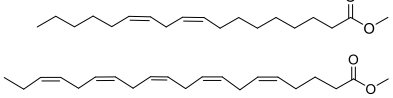	EPA methyl ester (20:5 *cis*)	$(5.8 \pm 0.41) \times 10^4$
9	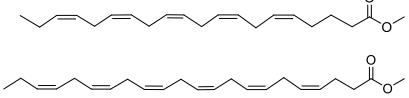	DHA methyl ester (22:6 *cis*)	$(1.2 \pm 0.49) \times 10^5$

is driven by both enthalpy and entropy (ΔH = -6.5 kJ mol^{-1} and ΔS = 60 J $mol^{-1}K^{-1}$), suggesting that solvophobic interactions in addition to van der Waals interactions between the host and the guest molecule work as driving forces for inclusion complex formation.

2.2.3 Inclusion Complex Structure by Calculation

3 possesses a selective inclusion ability for cis double bond rich fatty acid esters, suggesting that a *cis*-specific bent structure fits well into the cavity of the β-CD dimer. The optimized structure of the inclusion complex between **3** and DHA methyl ester indicates that the spiral form of DHA methyl ester is incorporated within the internal space of **3** (Fig. 2-7). Such a good fit of DHA methyl ester into the cavity may lead to the high association constant between **3** and DHA methyl ester. Although DHA is an essential oil, its use has been limited due to the susceptibility to oxidation in air. The CD molecular tube **3** should act as an effective antioxidant for DHA through incorporation into the cavity.

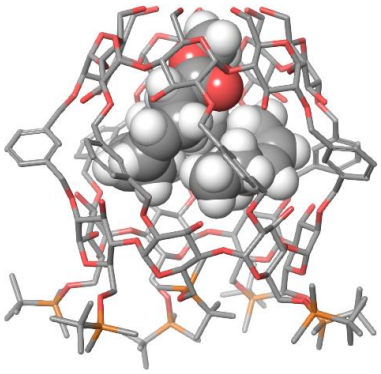

Figure 2-7. Optimized structure of the inclusion complex between **3** and methyl docosahexaenoate (DHA methyl ester) as obtained from Macromodel calculations (Monte Carlo Conformational Search, OPLS 2005 force fields). [6] **3** is shown with a cylinder representation, whereas DHA methyl ester is shown with a space-filling representation. H atoms except for DHA methyl ester have been omitted for clarity. Color labels: gray, carbon; red, oxygen; orange, silicon; white, hydrogen in DHA methyl ester.

2.2.4 Comparison between Janus-type and Unmodified β-CD dimers

We also compared the inclusion ability of β-CD dimer tubes **3** and **4** toward long-chain fatty acid esters. A mixture of methanol-d_4 and DMSO-d_6 was used as the solvent because it sufficiently dissolves methyl elaidate and methyl oleate as guests as well as **3** and **4**. Upon the addition of these guests, the proton signals of the xylylene linker of **3** and **4** remarkably shift downfield (Figs. 2-27–2-30), suggesting the formation of host–guest inclusion complexes. Table 2-2 shows the association constants estimated from these ^{1}H NMR spectral changes. Similar to **3**, **4** shows a clear binding selectivity for methyl oleate with a *cis* double bond. These hosts have almost the same *cis*/*trans* selectivity, indicating that the cavity of the β-CD dimer tubes plays an important role in the selective inclusion of *cis*-unsaturated fatty acid ester over the *trans* isomer. Interestingly,

Janus-type **3** shows a two-fold higher inclusion ability toward these guests than **4**. This result can be explained by considering that the bulky TBDMS groups at one end of **3** act like a cap to enhance the inclusion ability toward these guest molecules by expanding the hydrophobic space of the tubular cavity, as observed in previously reported capped cyclodextrins.[7] By changing the TBDMS groups to other substituents with different size and hydrophobicity, the inclusion ability of the Janus-type host will be effectively tuned.

Table 2-2. Association constants between **3** or **4** and various long-chain fatty acid methyl esters in methanol-d_4/DMSO-d_6 (7/3) at 25 °C.

Entry	Host	Guest	Association constant (M^{-1})
1	**3**	methyl elaidate	$(7.4 \pm 1.7) \times 10^2$
2		methyl oleate	$(2.1 \pm 0.69) \times 10^3$
3	**4**	methyl elaidate	$(4.2 \pm 0.27) \times 10^2$
4		methyl oleate	$(1.1 \pm 0.075) \times 10^3$

2.3 Conclusions

In conclusion, a novel β-CD dimer tube with one end fully modified and the other end unmodified is facilely synthesized from the TBDMS-β-CD dimer by controlling the elimination conditions of the TBDMS groups. The obtained Janus-type β-CD dimer exhibits inclusion selectivity for *cis*-unsaturated fatty acid esters over the corresponding *trans* isomers and saturated fatty acid esters, which has not been achieved by conventional CD derivatives. In particular, the Janus-type β-CD dimer shows an extremely high inclusion ability toward DHA ester in methanol-d_4. This Janus-type β-CD dimer can serve as a powerful molecular selector and molecular container. In addition, it can be used as a synthetic precursor for structurally well-defined molecular tubes with different functional groups at both ends. These applications will greatly expand the scope of molecular tubes.

2.4 Experimental Section

2.4.1 Materials and Methods

Boron trifluoride diethyl ether complex and dichloromethane were purchased from Tokyo Chemical Industry Co., Ltd. (Japan). Tetrabutylammonium fluoride was purchased from Sigma-Aldrich (Japan). Tetramethylammonium fluoride and 1,4-dioxane were purchased from Wako Pure Chemical Industries, Ltd. (Japan). These reagents were used without further purification. 1H and 13C NMR spectra were recorded on a JEOL NMR system (400 MHz). The following abbreviations were used for chemical shift multiplicities: s = singlet, d = doublet, t = triplet, q =

quartet, m = multiplet. NMR signal assignments were based on additional 2D-NMR spectroscopy (e.g., COSY and HSQC). Infrared (IR) spectra were obtained with a Spectrum 100FT-IR spectrometer (Perkin Elmer). MALDI-TOF MS spectra were measured by Bruker Autoflex III. Melting points were measured with BUCHI Melting point B-545. Elemental analysis was performed with Perkin Elmer 240C. HPLC was performed using a Shimadzu Prominence HPLC system equipped with a Soft 400 ELSD detector.

2.4.2 Synthesis of TBDMS-β-CD dimer 2

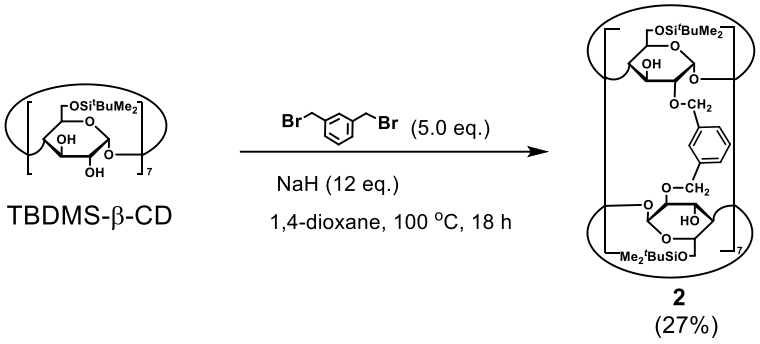

Scheme 2-2. Synthesis of **2**.

2 was prepared according to our previously reported method.[2] The structure was confirmed by the ^{1}H NMR spectrum.

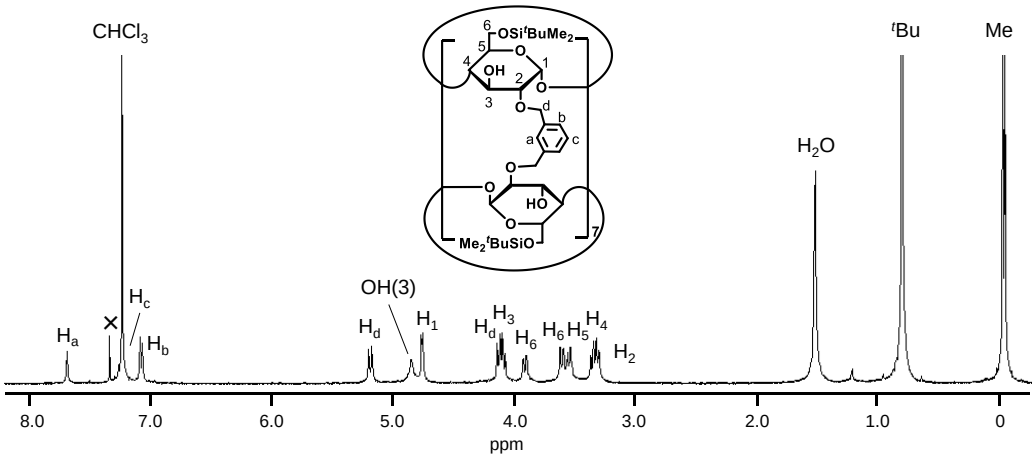

Figure 2-8. ^{1}H NMR spectrum of **2** in chloroform-*d* at 25 °C.

2.4.3 Synthesis of Janus-type TBDMS-β-CD dimer 3

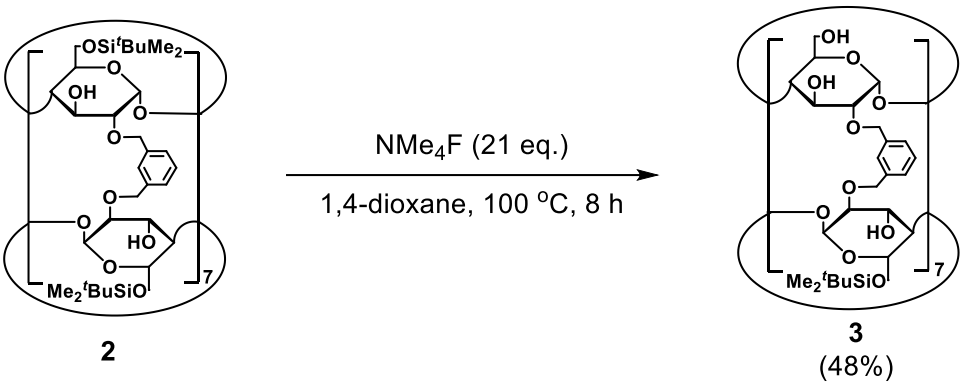

Scheme 2-3. Synthesis of **3**.

2 (20 mg, 4.4 μmol) and tetramethylammonium fluoride (TMAF, 8.6 mg, 92 μmol) were dissolved in 1,4-dioxane (2.0 mL). The reaction mixture was stirred for 8 h at 100 °C. After the solvent was removed in vacuo, the resulting solid was purified by silica gel column chromatography (chloroform/methanol, in a gradient 10:1 to 6:1) to give compound **3** (8.0 mg, 48% yield). R_f 0.5 ($CHCl_3$/MeOH = 4/1); mp: 273 °C (decomp); ^{1}H NMR (400 MHz, methanol-d_4): δ 0.07 (d, J = 2.8 Hz, 42H), δ 0.88 (s, 63H), δ 3.34-3.46 (m, 28H), δ 3.63-3.85 (m, 35H), δ 4.07 (d, J = 8.8 Hz, 7H), δ 4.15-4.25 (m, 28H), δ 4.93 (m, 28H), δ 5.21-5.25 (m, 28H), δ 7.14-7.18 (m, 14H), δ 7.23-7.27 (m, 7H), δ 7.66 (s, 7H); ^{13}C NMR (100 MHz, methanol-d_4): δ -5.74, -4.47, 19.26, 26.63, 61.84, 72.90, 73.18, 75.33, 75.43, 77.44, 77.50, 83.22, 83.45, 84.34, 85.00, 103.76, 129.19, 129.64, 129.82, 131.38, 138.99, 139.01; MALDI-TOF MS: m/z = 3808 $[M+Na]^+$; Anal. Calcd for $C_{152}H_{280}O_{70}Si_7$•$6H_2O$: C, 56.15; H, 7.56. Found: C, 56.24: H, 7.59; FT-IR (cm^{-1}): 3406, 2926, 2855, 1462, 1360, 1251, 1158, 1083, 1039, 833, 777.

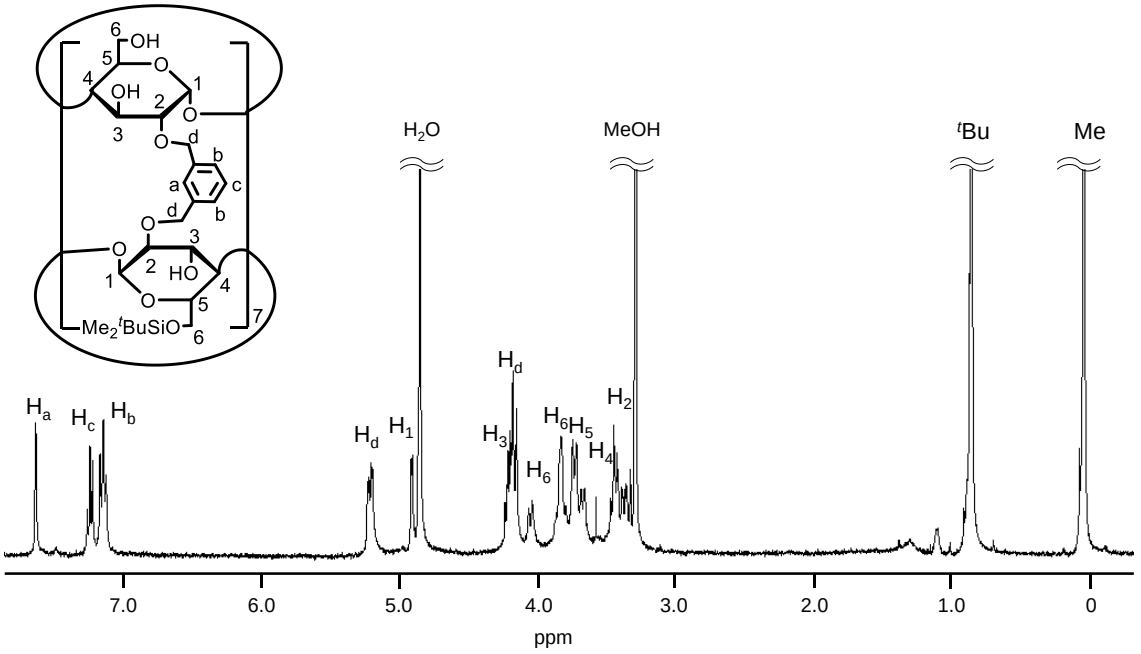

Figure 2-9. ^{1}H NMR spectrum of **3** in methanol-d_4 at 25 °C.

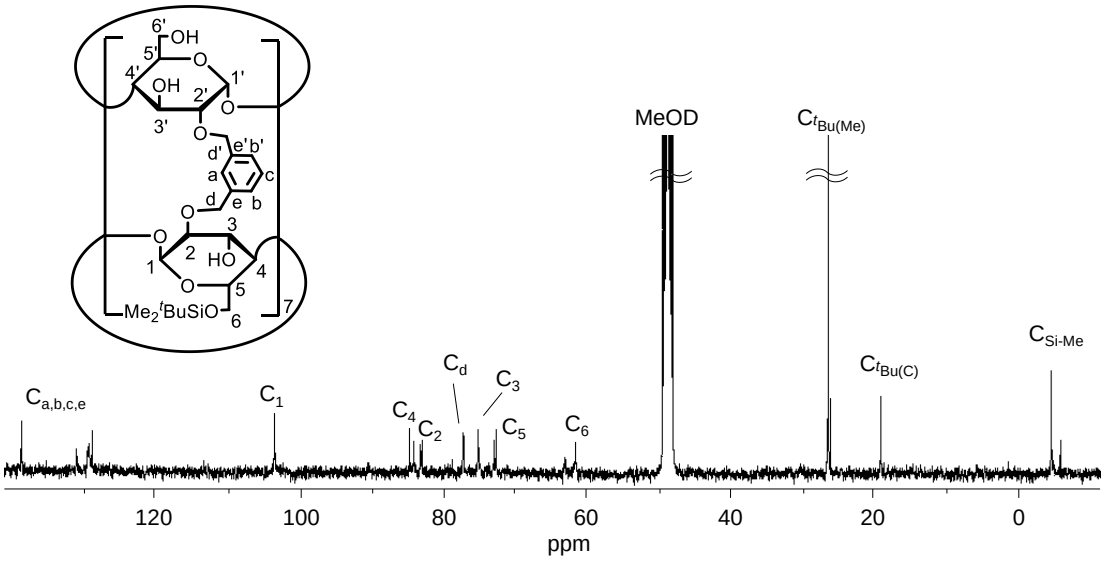

Figure 2-10. ^{13}C NMR spectrum of **3** in methanol-d_4 at 25 °C.

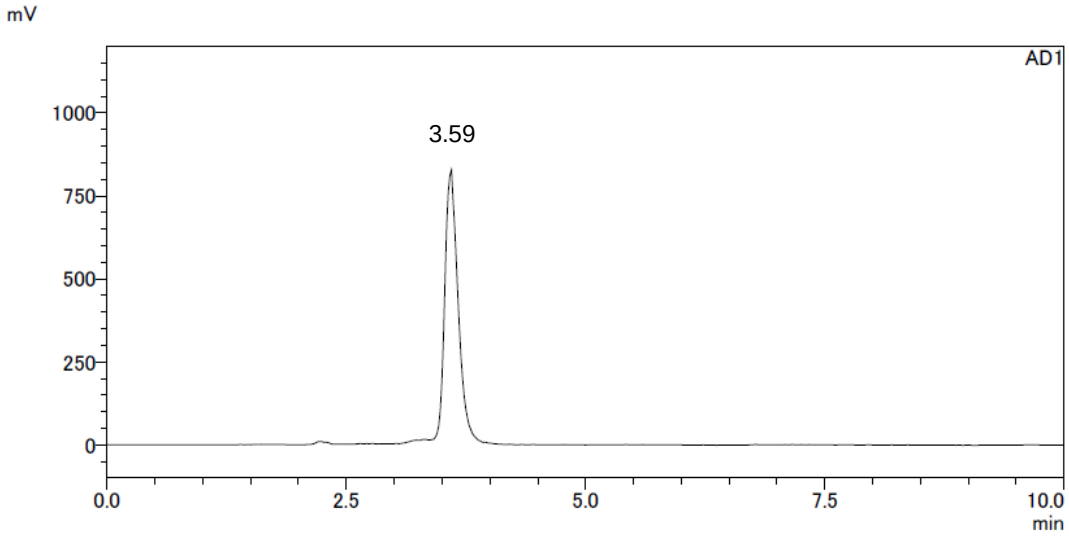

Figure 2-11. HPLC chromatogram of **3**. Column: NACALAI TESQUE, COSMOSIL 5SL-II Packed Column (250 mm × 4.6 mm i.d.); mobile phase: chloroform/methanol = 2/1 (v/v); flow rate: 1.5 ml min^{-1}; temperature: 25 °C; detector: ELSD.

2.4.4 Synthesis of Unmodified β-CD dimer 4

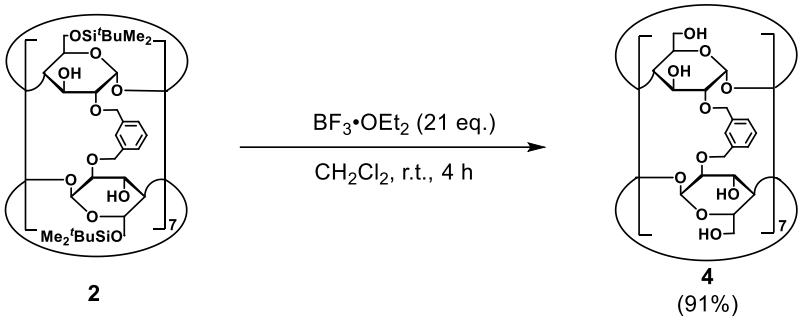

Scheme 2-4. Synthesis of **4**.

2 (0.1 g, 22 μmol) was dissolved in dichloromethane (10.0 mL). Into this solution, boron trifluoride diethyl ether complex (60 μL, 0.48 mmol) was added, and the reaction mixture was stirred for 4 h at room temperature. After the solvent was removed in vacuo, the resulting solid was washed with acetone (10 mL×3) and hexane (10 mL×3), and dried at 80 °C in vacuo to give compound **4** (60 mg, 91% yield). mp: 270 °C (decomp); ^{1}H NMR (400 MHz, DMSO-d_6): δ 3.26-3.41 (m, 28H), δ 3.58-3.70 (m, 28H), δ 4.02 (t, J = 9.6 Hz, 14H), δ 4.21 (d, J = 9.6 Hz, 14H), δ 4.63 (s, 14H), δ 4.84 (m, 14H), δ 5.04 (d, J = 9.6 Hz, 14H), δ 7.13 (d, J = 8.0 Hz, 14H) , δ 7.22 (t, J = 7.2 Hz, 7H) , δ 7.52 (s, 7H); ^{13}C NMR (100 MHz, DMSO-d_6): δ 59.91, 71.32, 73.58, 75.20,

81.68, 83.14, 101.42, 127.80, 128.20, 137.55; MALDI-TOF MS: *m/z* = 3008 $[M+Na]^+$; Anal. Calcd for $C_{140}H_{182}O_{70}•9H_2O$: C, 53.43; H, 6.41. Found: C, 53.43: H, 6.44; FT-IR (cm^{-1}): 3389, 2920, 1360, 1322, 1247, 1155, 1083, 1010, 948, 854, 754, 700.

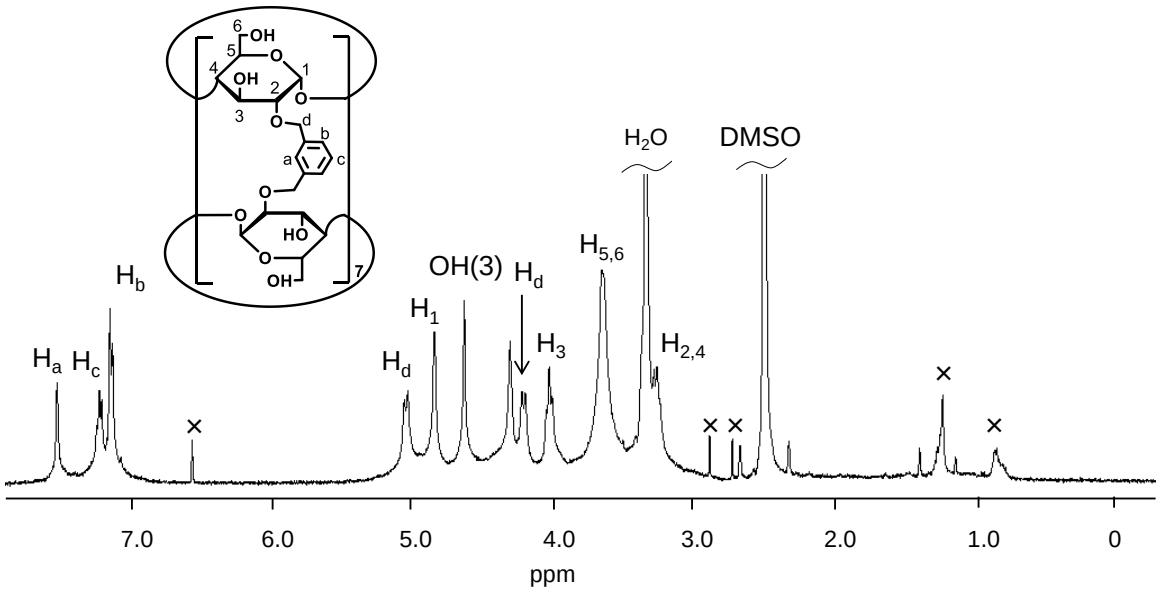

Figure 2-12. ^{1}H NMR spectrum of **4** in DMSO-d_6 at 25 °C.

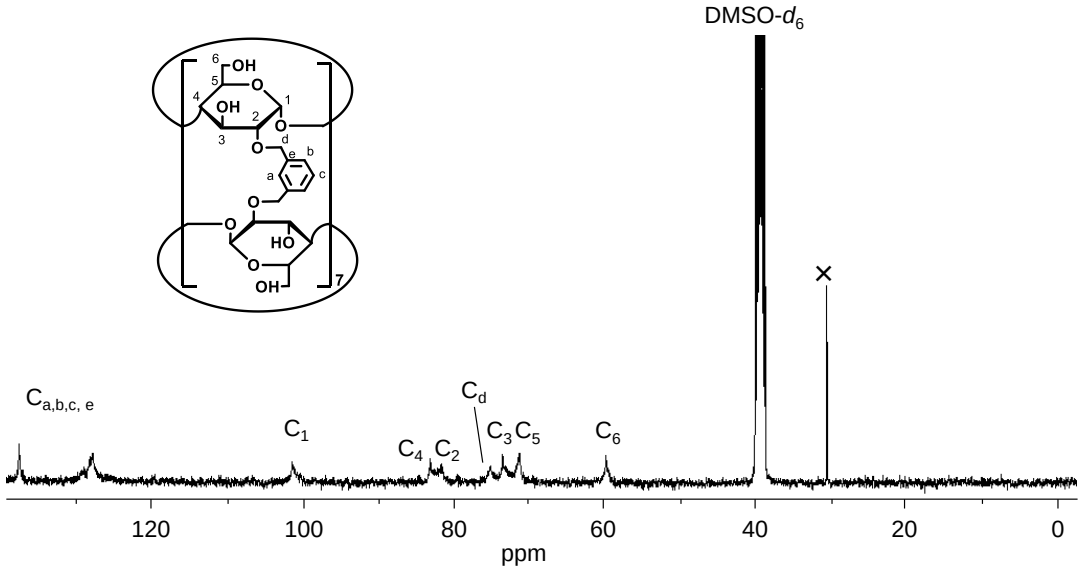

Figure 2-13. ^{13}C NMR spectrum of **4** in DMSO-d_6 at 25 °C.

2.4.5 Determination of Association Constants by NMR Titration

A solution of the host molecule (5.0×10^{-4} M, 0.5 mL) was titrated in a NMR tube with increasing amounts of guest stock solution (200 mM). 6 or more solutions with different host-guest concentration ratios were analyzed. Four of ^{1}H NMR spectra obtained are shown in each figure. The titration curves (changes in the chemical shift of the host protons ($\Delta\delta$) against the guest/host concentration ratio) were analyzed by a non-linear least-squares curve fitting method to give the association constants between the hosts and the guests.

2.4.6 Experimental Procedure for Job Plots

Job plots were carried out by monitoring the changes in the chemical shift of the host protons ($\Delta\delta$) in a series of solutions with varying host/guest ratios but the total concentrations of the host and guest being kept constant (0.4 or 2.0 mM). The relative concentration of the host-guest complex estimated from the $\Delta\delta \cdot$[host] value was plotted against ([host]/{[host] + [guest]}).

2.4.7 ^{1}H-NMR Spectral Changes Observed for 3 upon Addition of Long-Chain Fatty Acid Esters in Methanol-d_4 and Titration Curves for Their Complex Formation

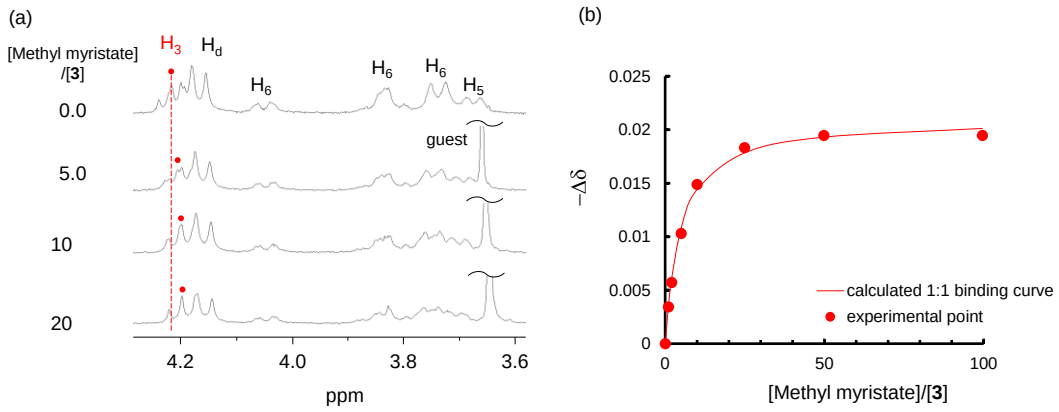

Figure 2-14. (a) ^{1}H NMR spectral changes observed for **3** (5.0×10^{-4} M) upon addition of methyl myristate in methanol-d_4 at 25 ºC. (b) ^{1}H NMR titration curve for complex formation between **3** and methyl myristate in methanol-d_4 at 25 ºC. The proton signal of **3** at 4.2 ppm was used for titration.

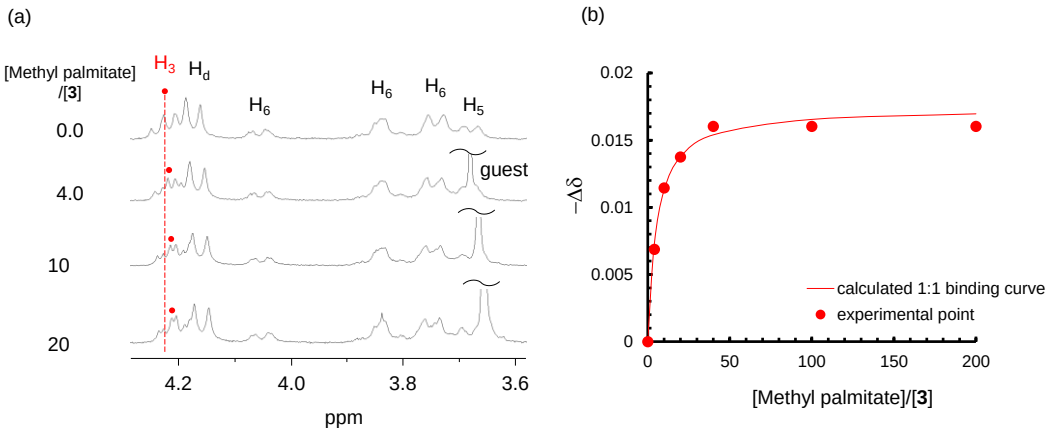

Figure 2-15. (a) ^{1}H NMR spectral changes observed for **3** (5.0×10^{-4} M) upon addition of methyl palmitate in methanol-d_4 at 25 ºC. (b) ^{1}H NMR titration curve for complex formation between **3** and methyl palmitate in methanol-d_4 at 25 ºC. The proton signal of **3** at 4.2 ppm was used for titration.

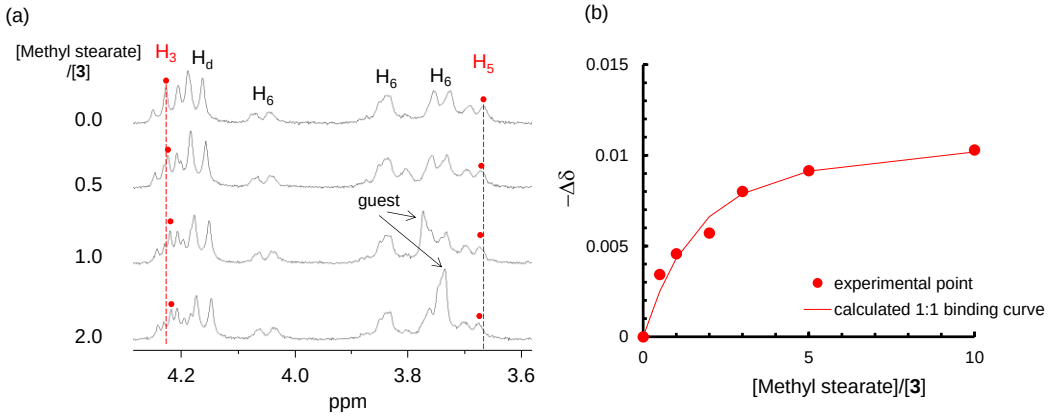

Figure 2-16. (a) ^{1}H NMR spectral changes observed for **3** (5.0×10^{-4} M) upon addition of methyl stearate in methanol-d_4 at 25 ºC. (b) ^{1}H NMR titration curve for complex formation between **3** and methyl stearate in methanol-d_4 at 25 ºC. The proton signal of **3** at 4.2 ppm was used for titration.

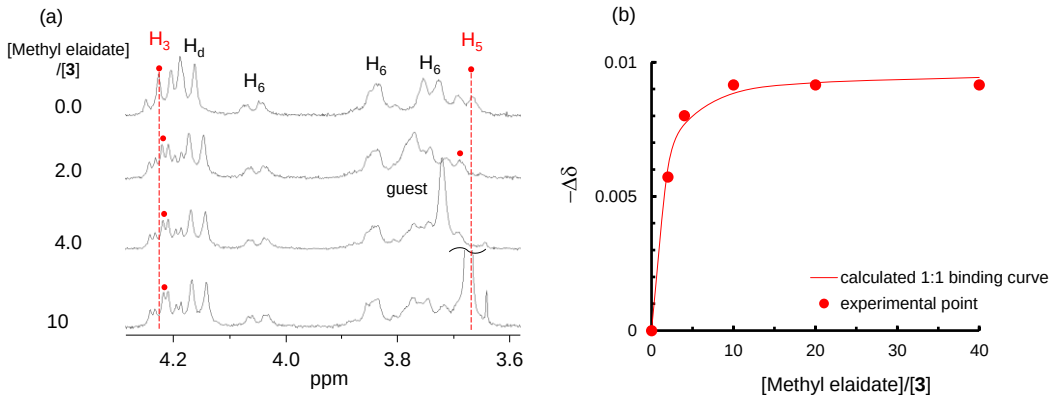

Figure 2-17. (a) ^{1}H NMR spectral changes observed for **3** (5.0×10^{-4} M) upon addition of methyl elaidate in methanol-d_4 at 25 ºC. (b) ^{1}H NMR titration curve for complex formation between **3** and methyl elaidate in methanol-d_4 at 25 ºC. The proton signal of **3** at 4.2 ppm was used for titration.

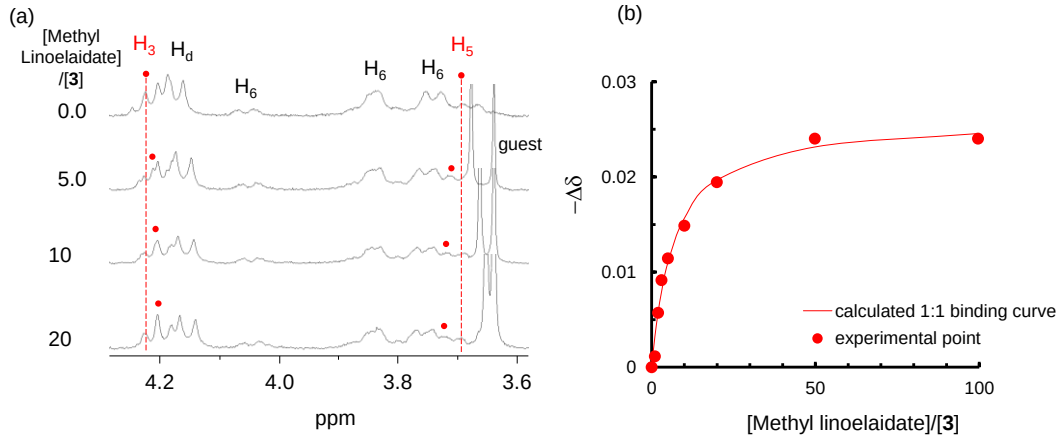

Figure 2-18. (a) ^{1}H NMR spectral changes observed for **3** (5.0×10^{-4} M) upon addition of methyl linoelaidate in methanol-d_4 at 25 ºC. (b) ^{1}H NMR titration curve for complex formation between **3** and methyl linoelaidate in methanol-d_4 at 25 ºC. The proton signal of **3** at 4.2 ppm was used for titration.

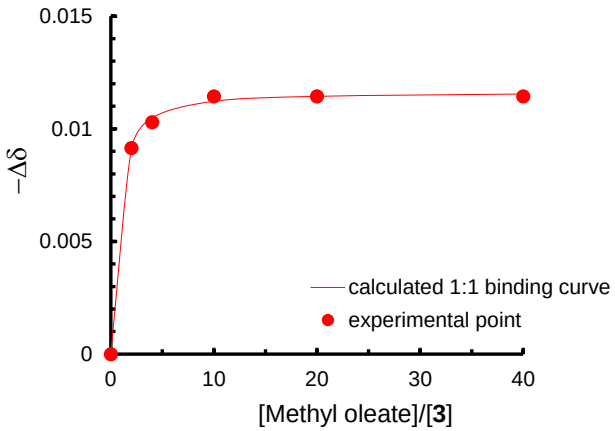

Figure 2-19. ^{1}H NMR titration curve for complex formation between **3** and methyl oleate in methanol-d_4 at 25 ºC. The proton signal of **3** at 4.2 ppm was used for titration.

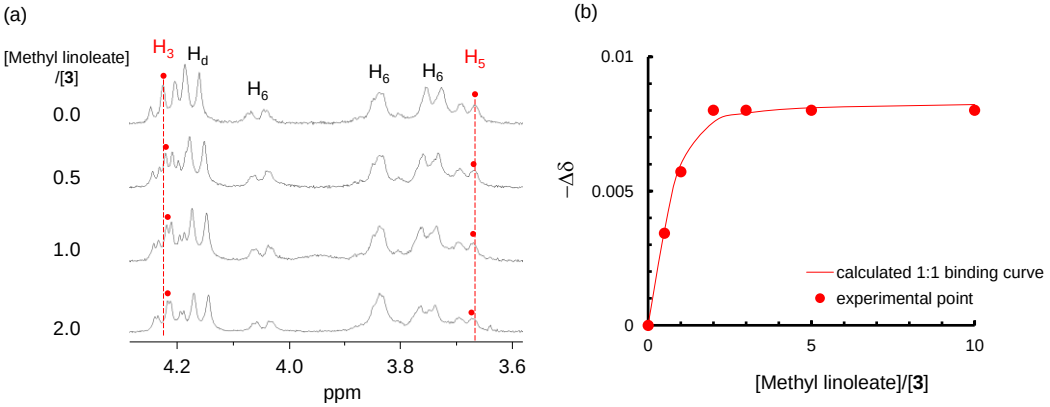

Figure 2-20. (a) ^{1}H NMR spectral changes observed for **3** (5.0×10^{-4} M) upon addition of methyl linoleate in methanol-d_4 at 25 ºC. (b) ^{1}H NMR titration curve for complex formation between **3** and methyl linoleate in methanol-d_4 at 25 ºC. The proton signal of **3** at 4.2 ppm was used for titration.

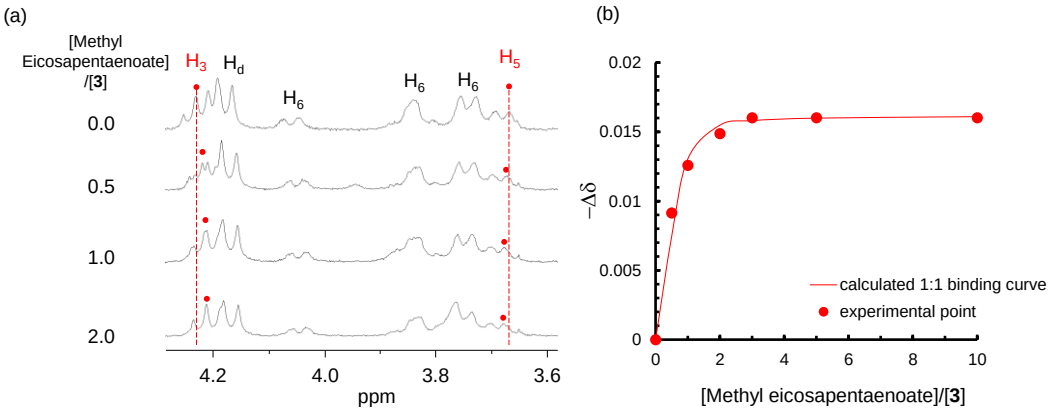

Figure 2-21. (a) ^{1}H NMR spectral changes observed for **3** (5.0×10^{-4} M) upon addition of methyl eicosapentaenoate in methanol-d_4 at 25 ºC. (b) ^{1}H NMR titration curve for complex formation between **3** and methyl eicosapentaenoate in methanol-d_4 at 25 ºC. The proton signal of **3** at 4.2 ppm was used for titration.

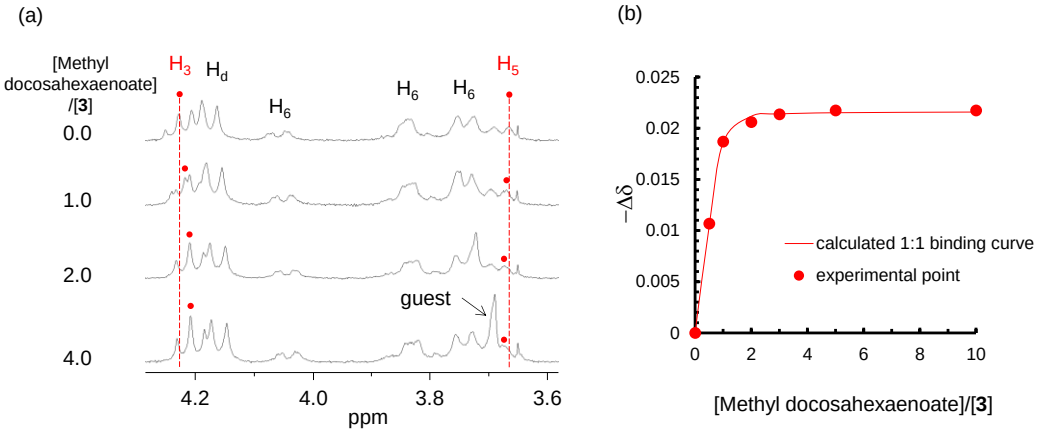

Figure 2-22. (a) ^{1}H NMR spectral changes observed for **3** (5.0×10^{-4} M) upon addition of methyl docosahexaenoate in methanol-d_4 at 25 ºC. (b) ^{1}H NMR titration curve for complex formation between **3** and methyl docosahexaenoate in methanol-d_4 at 25 ºC. The proton signal of **3** at 4.2 ppm was used for titration.

2.4.8 Job Plots for Complexes between 3 and Long-Chain Fatty Acid Esters in Methanol-d_4

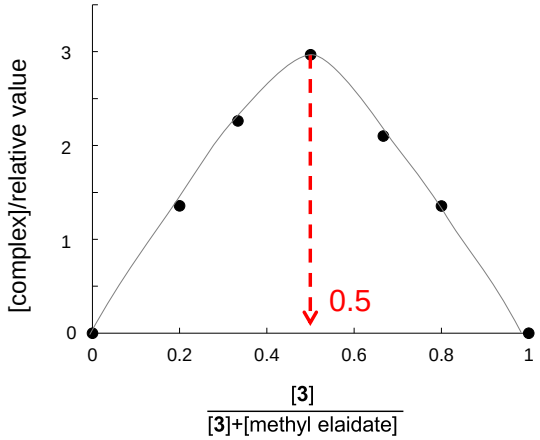

Figure 2-23. Job plot for complex between **3** and methyl elaidate in methanol-d_4 at 25 ºC.

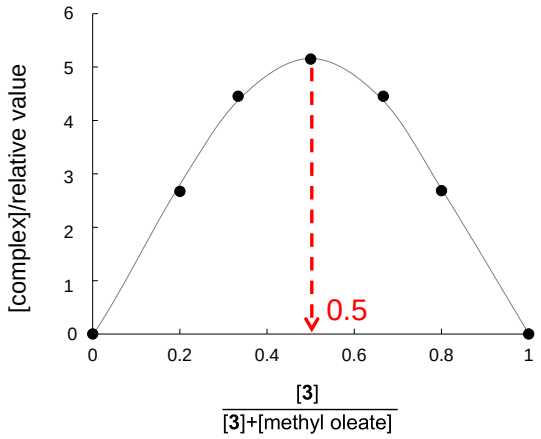

Figure 2-24. Job plot for complex between **3** and methyl oleate in methanol-d_4 at 25 ºC.

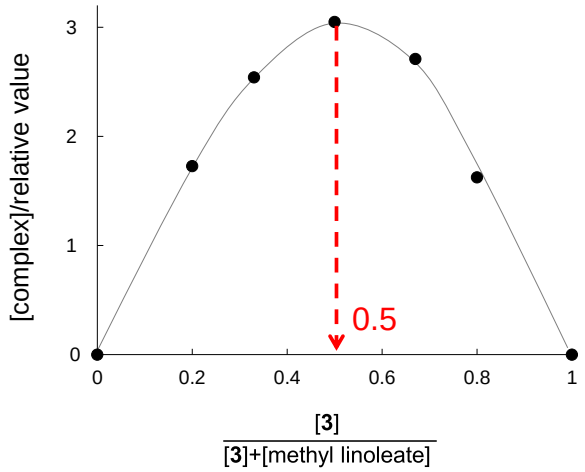

Figure 2-25. Job plot for complex between **3** and methyl linoleate in methanol-d_4 at 25 ºC.

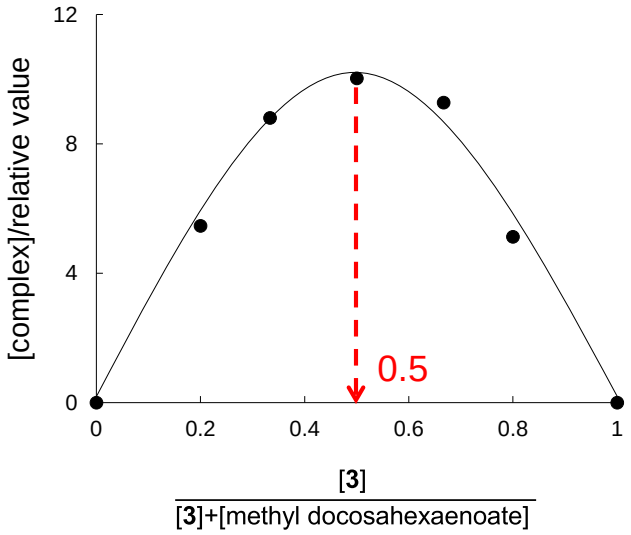

Figure 2-26. Job plot for complex between **3** and methyl docosahexaenoate in methanol-d_4 at 25 ºC.

2.4.9 ^{1}H-NMR Spectral Changes Observed for 3 or 4 upon Addition of Long- Chain Fatty Acid Esters in Methanol-d_4/DMSO-d_6 (7/3) and Titration Curves for Their Complex Formation

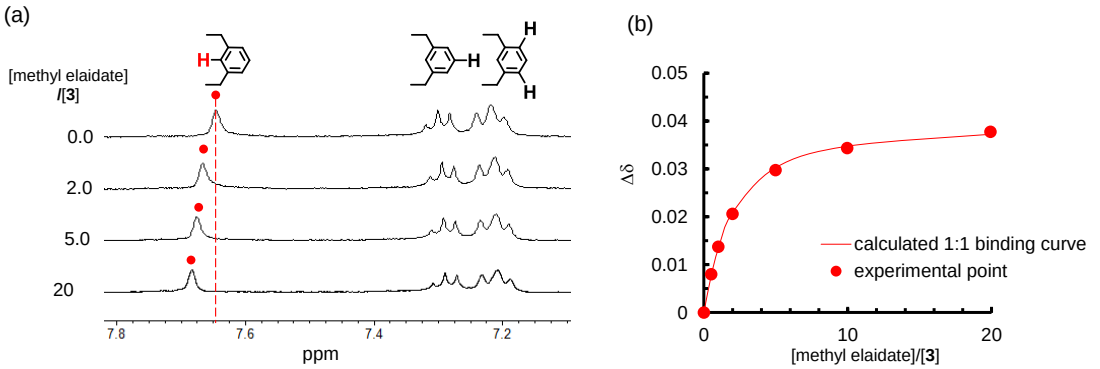

Figure 2-27. (a) ^{1}H NMR spectral changes observed for **3** (5.0×10^{-4} M) upon addition of methyl elaidate in methanol-d_4/DMSO-d_6 (7/3) at 25 ºC. (b) ^{1}H NMR titration curve observed for **3** (5.0×10^{-4} M) upon addition of methyl elaidate in methanol-d_4/DMSO-d_6 (7/3) at 25 ºC. The proton signal of **3** at 7.6-7.7 ppm was used for titration.

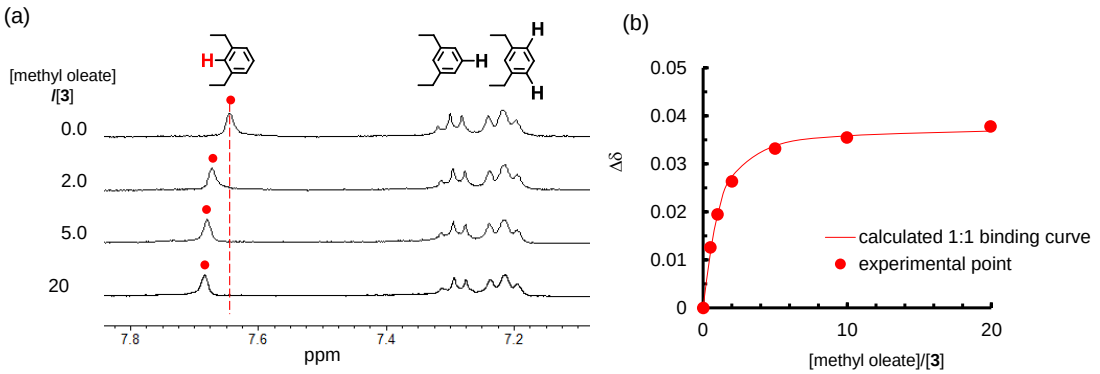

Figure 2-28. (a) ^{1}H NMR spectral changes observed for **3** (5.0×10^{-4} M) upon addition of methyl oleate in methanol-d_4/DMSO-d_6 (7/3) at 25 ºC. (b) ^{1}H NMR titration curve observed for **3** (5.0×10^{-4} M) upon addition of methyl oleate in methanol-d_4/DMSO-d_6 (7/3) at 25 ºC. The proton signal of **3** at 7.6-7.7 ppm was used for titration.

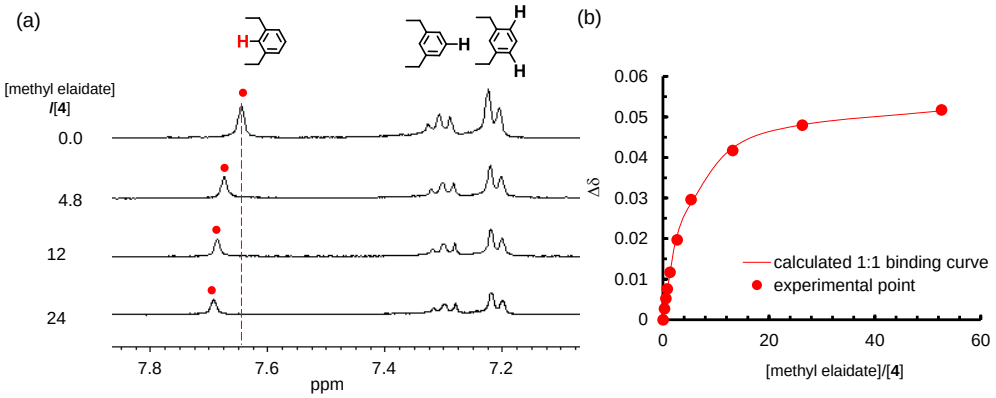

Figure 2-29. (a) ^{1}H NMR spectral changes observed for **4** (5.0×10^{-4} M) upon addition of methyl elaidate in methanol-d_4/DMSO-d_6 (7/3) at 25 ºC. (b) ^{1}H NMR titration curve for complex formation between **4** and methyl elaidate in methanol-d_4/DMSO-d_6 (7/3) at 25 ºC. The proton signal of **4** at 7.6-7.7 ppm was used for titration.

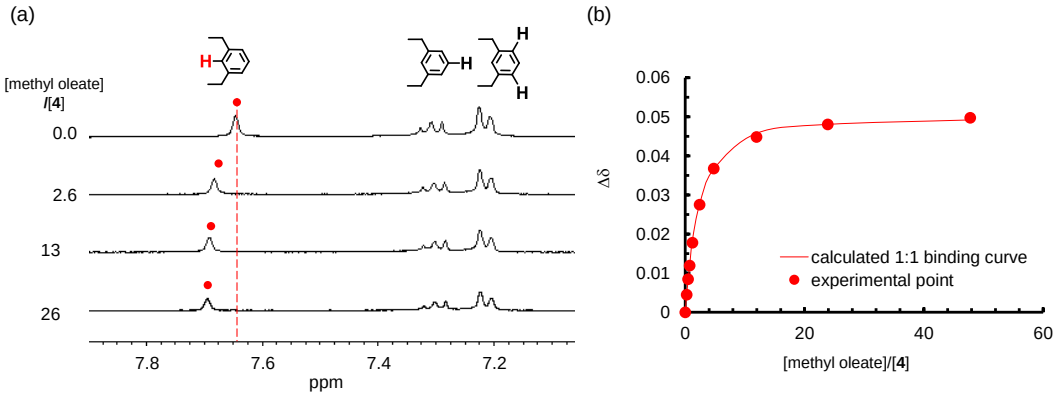

Figure 2-30. (a) ^{1}H NMR spectral changes observed for **4** (5.0×10^{-4} M) upon addition of methyl oleate in methanol-d_4/DMSO-d_6 (7/3) at 25 ºC. (b) ^{1}H NMR titration curve for complex formation between **4** and methyl oleate in methanol-d_4/DMSO-d_6 (7/3) at 25 ºC. The proton signal of **4** at 7.6-7.7 ppm was used for titration.

2.4.10 Job Plots for Complexes between 4 and Long-Chain Fatty Acid Esters in Methanol-d_4/DMSO-d_6 (7/3)

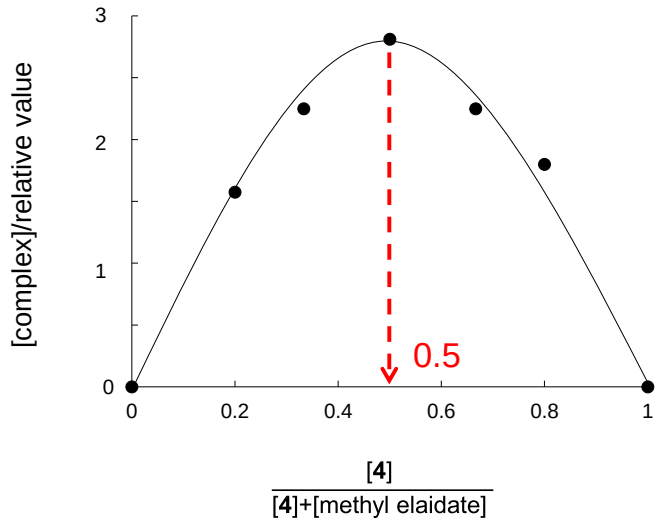

Figure 2-31. Job plot for complex between **4** and methyl elaidate in methanol-d_4/DMSO-d_6 (7/3) at 25 ºC.

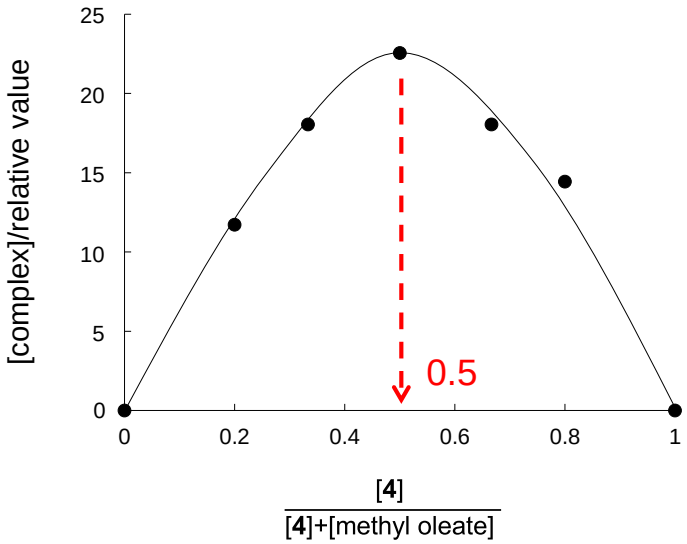

Figure 2-32. Job plot for complex between **4** and methyl oleate in methanol-d_4/DMSO-d_6 (7/3) at 25 ºC.

References

1) a) L. Krejčí, M. Buděšínský, I. Císařováb, T. Kraus, *Chem. Commun.* **2009**, 3557–3559. b) A. Wang, W. Li, P. Zhang, C.C. Ling, *Org. Lett.* **2011**, *13*, 3572–3575.
2) S. Ito, C. Kogame, M. Akashi, T. Kida, *Tetrahedron Lett.* **2016**, *57*, 5243–5245.
3) R. S. Lewis, C. J. Garza, A. T. Dang, T. K. A. Pedro, W. J. Chain, *Org. Lett.* **2015**, *17*, 2278–2281.
4) a) K. Takeo, K. Uemura, H. Mitoh, *J. Carbohydr. Chem.* **1988**, *7*, 293–308; b) K. Takeo, H. Mitoh, K. Uemura, *J. Carbohydr. Chem.***1989**, *187*, 203–221.
5) a) K. O. Christe, W. W. Wilson, R. D. Wilson, R. Bau, J. A. Feng, *J. Am. Chem. Soc.* **1990**, *112*, 7619–7625; b) M. Y. Kobayashi, K. Inamoto, Y. Kondo, *Chem. Lett.* **2014**, *43*, 477–479.
6) a) R. M. Claramunt, F. Herranz, M. D. Santa Maria, C. Jaime, M. d. Federico, J. Elguero, *Biosens. Bioelectron.* **2004**, *20*, 1242–1249; b) K. Samanta, W. Sicking, C. Schmuck, *Eur. J. Org. Chem.* **2018**, 6515–6518.
7) I. Tabushi, K. Shimokawa, N. Shimizu, H. Shirakata, K. Fujita, *J. Am. Chem. Soc.* **1976**, *98*, 7855–7856.

Chapter 3

Terminal Trialkylsilyl Substituent Effect of Janus-type β-CD Dimers on Inclusion of Unsaturated Fatty Acid Esters

3.1 Introduction

The terminal TBDMS substituents of the Janus-type CD dimer **3** play an important role in enhancing the guest inclusion ability of the tubular host possibly through changing the internal environment of the tubular cavity (Chapter 2). This interesting finding prompted us to examine the inclusion ability of the molecular tubes with different terminal substituents and to study the mechanism for enhanced guest inclusion.

There are several reports on shape recognition of fatty acids by synthetic host molecules.[1] For example, Glass et al. reported fluorescent sensors composed of four naphthol units, which allow selective sensing of linear long-chain fatty acids over the corresponding branched- or short-chain fatty acids.[1d] Yoshizawa et al. reported that a polyaromatic molecular tube selectively includes methyl elaidate bearing a *trans*-double bond over the corresponding *cis*-isomer.[1b] The control of inclusion ability of these hosts toward the fatty acids has been attained by changing the host skeleton such as the ring size and shape. On the other hand, inclusion ability control by changing the terminal substituent of the tubular host without changing the skeleton has not been reported yet.

Under these backgrounds, we report herein the synthesis of Janus-type β-CD dimer bearing 6-*O*-triisopropylsilyl (TIPS) groups at one end and the inclusion complex formation with unsaturated fatty acid esters. A comparison of the inclusion ability of this Janus-type β-CD dimer with the previous β-CD dimer bearing TBDMS substituents demonstrated that the molecular size of the terminal substituents remarkably affects the inclusion ability towards unsaturated fatty acid esters.

3.2 Results and Discussion

3.2.1 Synthesis

First, we synthesized TIPS-β-CD dimer **5**, in which two TIPS-β-CD molecules are connected with seven *m*-xylylene linkers through the C-2 hydroxyl groups via a reaction of TIPS-β-CD with five equivalents of *m*-xylylene bromide in the presence of sodium hydride according to Chapter 2 on the synthesis of TBDMS-β-CD dimer (Scheme 3-1). Similar to the case of TBDMS-β-CD dimer, dimerization gave desired dimer **5** in 24% isolated yield. The structure of

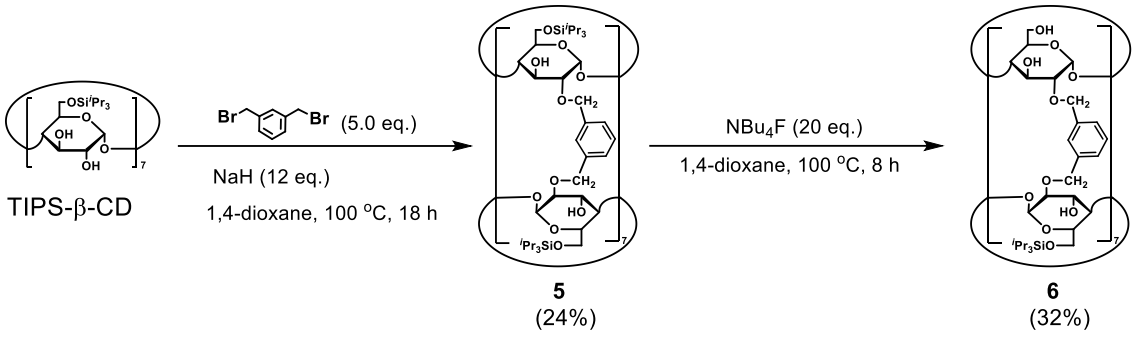

Scheme 3-1. Synthesis of TIPS-β-CD dimer **5** and Janus-type CD dimer **6**.

dimer **5** was confirmed by NMR (^{1}H, ^{13}C, NOESY) and TOF-MS analyses. Interestingly, in the NOESY spectrum of TIPS-β-CD dimer **5** in cyclohexane-d_{12} (Fig. 3-16a), the methyl protons of the isopropyl groups of the TIPS substituents and both the H_5 and H_3 protons of the CD units are clearly correlated. Since the H_5 and H_3 protons of CD are directed inside the cavity, this observation reveals that one or some of the TIPS groups are self-included in the CD cavity. Based on the optimized structure of **5** by a Macromodel calculation,[2] we can confirm that one TIPS group at both ends is self-included in the CD cavity (Fig. 3-17a). The TBDMS-β-CD dimer **2**, which was synthesized as a control, exhibits similar correlations between both the *t*-butyl and methyl protons of the TBDMS substituents and both the H_5 and H_3 protons of CD units (Fig. 3-16b). The optimized structure of **2** confirms that one of the seven TBDMS groups at each end is self-included in the CD cavity (Fig. 3-17b), similar to **5**.

Next, we examined selective removal of the TIPS groups from one end of **5**. In Chapter 2, reacting a TBDMS-β-CD dimer **2** with tetramethylammonium fluoride (TMAF, 21 eq.) in 1,4-dioxane for 8 h at 100 °C gave a Janus-type TBDMS-β-CD dimer **3**. The mechanism of the selective elimination of TBDMS groups from one side of the two CD rings with TMAF is due to the steric hindrance created by seven TBDMS groups on the CD rings. The bulky TBDMS groups sterically inhibit the attack of the F^- ion on the Si atom of TBDMS groups in the early stage of the reaction, but once one or two on the Si atom are removed by a successful attack of the F^- ion, the generated space decreases the steric hindrance and then the F^- ion easily attacks the next Si atom on the same CD ring to give a Janus-type TBDMS-β-CD dimer **3**. Following the previous method, treatment of **5** with TMAF as a desilylation agent for 8 h at 100 °C yielded a considerable amount of unreacted **5** in the MALDI-TOF MS spectra of the reaction products. Extending the reaction time to 3 days produced a complex mixture of the random desilylation products (Fig. 3-1a). These results suggest that the TIPS-β-CD dimer is less reactive for desilylation with TMAF than the TBDMS-β-CD dimer because the TIPS group is bulkier than the TBDMS group.[3] The desired Janus-type dimer **6** was successfully synthesized when tetra(*n*-butyl)ammonium fluoride (TBAF), which has a more reactive fluoride anion than TMAF,[4] was used (Fig. 3-1b). The

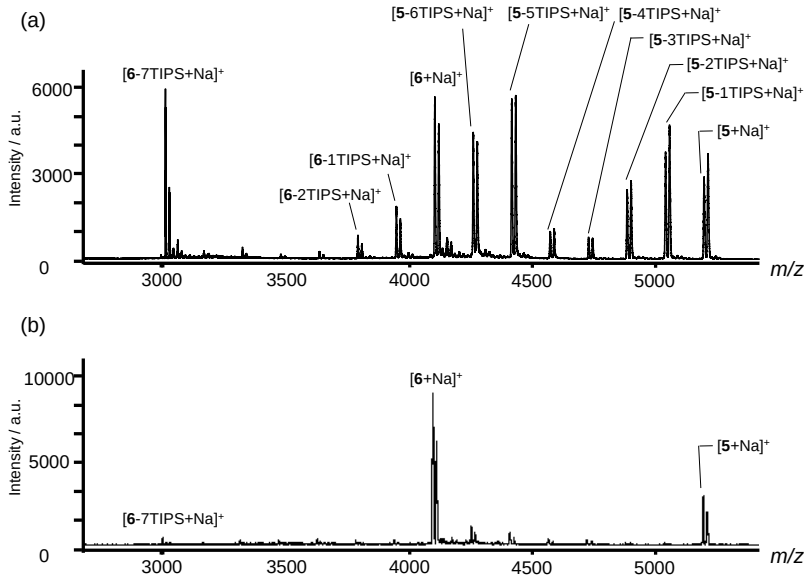

Figure 3-1. MALDI-TOF MS spectra of the products of desilylation of **5** with (a) TMAF in 1,4-dioxane at 100 °C for 3 days and (b) TBAF in 1,4-dioxane at 100 °C for 8 hours.

selective desilylation from one end can be explained by the same mechanism as the case of TBDMS-β-CD dimer. Although seven bulky TIPS groups suppress the attack of F^- ion on the Si atom of TIPS groups in the early stage, the desilylation on the same CD ring proceeds smoothly once one or two silyl groups are removed. After removal of the ammonium salt from the reaction mixture using Dowex 50WX-8-400 (H^+-form) and calcium carbonate followed by the solvent evaporation, the residue was purified by silica gel column chromatography using chloroform/methanol (in a gradient 10:1 to 6:1) as an eluent and recrystallized by slow diffusion of methanol vapor into the chloroform solution. The integral ratio of peaks of isopropyl protons on the Si atoms (around 1.0 ppm) to peaks of H_1 and $H_{1'}$ (around 4.9 ppm) in the ^{1}H NMR spectrum indicates the elimination of seven TIPS groups from **5** (Fig. 3-8). In addition, the ^{1}H NMR spectrum of **6** contains a set of CD and linker proton peaks, which are observed in **5**, as well as another set of CD and linker proton peaks whose integral ratio with the former set is 1:1. These results confirm that **6** is composed of two types of CD rings in different chemical environments. That is, **6** contains TIPS-β-CD and unmodified β-CD. The elimination of seven TIPS groups was also confirmed by the MALDI-HRMS spectrum, which has a monoisotopic peak for the sodium adduct of molecular ion at *m/z* 4098.9854 $[M + Na]^+$, which corresponds to the theoretical molecular weight of desired Janus-type dimer **6** ($C_{203}H_{322}O_{70}Si_7Na$) (Fig. 3-10). These results demonstrate that the selective elimination of the TIPS groups from one end of the TIPS-β-CD dimer occurs to give the Janus-type structure.

3.2.2 Inclusion of Unsaturated Fatty Acid Esters

We evaluated the inclusion ability of **6** toward *cis*- and *trans*-fatty acid esters (Fig. 3-2) by the ^{1}H NMR titration method using methanol-d_4 as a solvent. Methyl oleate and methyl elaidate were chosen as *cis*- and *trans*-fatty acid esters, respectively. Oleic acid and elaidic acid are common fatty acid contained in various animal and vegetable fats and oil. Although selective recognition of these *cis-trans* isomers by synthetic receptors is important in the food industry[5], it remains a challenging subject.

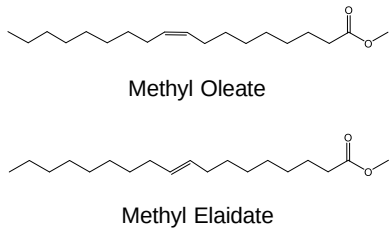

Figure 3-2. Unsaturated fatty acid esters used in this study.

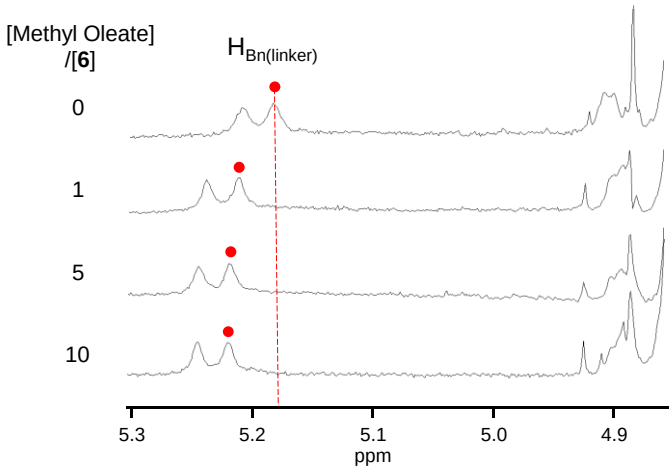

Figure 3-3. ^{1}H NMR spectral changes observed for **6** (5.0×10^{-4} M) upon the addition of methyl oleate in methanol-d_4 at 25 ˚C.

Figure 3-3 shows the changes in the ^{1}H NMR signals of **6** induced by the addition of methyl oleate in methanol-d_4 at 25 °C. Adding the guest shifts the peak of the methylene protons of the xylylene linker of **6**, suggesting the formation of an inclusion complex between **6** and methyl oleate in methanol-d_4. In the case of methyl elaidate, the peak of methylene protons of the xylylene linker of **2** also shifts upon the addition of the guest. (Fig. 3-13). The Job plots using the NMR method has a maximum at a [**6**]/[guest] molar ratio of 1:1, indicating that **6** forms a 1:1 inclusion complex with these guests in methanol-d_4 (Figs. 3-14, 3-15).

Table 1 summarizes the association constants between **6** and the guests along with those between the Janus-type β-CD dimer bearing seven TBDMS groups (Janus-type TBDMS-β-CD dimer **3**)

and the guests. The association constant with methyl oleate is 2.5 times higher than that with methyl elaidate. Thus, **6** exhibits a selective inclusion ability for the *cis*-fatty acid ester over the corresponding *trans*-fatty acid ester. Although this tendency is similar to the case of **3**, **6** shows an increased *cis*/*trans* selectivity. Notably, **6** shows a two-fold higher association with these guests compared to the Janus-type TBDMS-β-CD dimer **3**, suggesting that the molecular size of the terminal substituents affects the inclusion ability of CD dimers.

A simple comparison of inclusion ability or selectivity between our results and the previous results[1] is difficult because the solvent is different. All the previous reports use water or solutions containing water as a medium in which the inclusion of fatty acid derivatives by host molecules is evaluated. On the other hand, we use methanol-d_4 as a medium for the evaluation of the host-guest binding.

Table 3-1. Association constants between **3** or **6** and unsaturated fatty acid methyl esters in methanol-d_4 at 25 °C.

Host	Guest	K (M^{-1})	K_{cis}/K_{trans}
6	Methyl elaidate	$(5.2\pm0.43)\times10^3$	2.5
	Methyl oleate	$(1.3\pm0.15)\times10^4$	
3	Methyl elaidate	$(3.0\pm0.46)\times10^3$	2.2
	Methyl oleate	$(6.7\pm0.71)\times10^3$	

3.2.3 Studies on the Structure of Janus-type CD Dimers

In the NOESY spectrum of **6** in methanol-d_4 (Fig. 3-4a), the methyl protons of isopropyl groups of the TIPS substituents are clearly correlated with both the H_5 and H_3 protons of CD units. Similar to the case of TIPS-β-CD dimer **5**, the optimized structure of **6** by a MacroModel calculation confirms that one of the TIPS groups is self-included in the CD cavity (Fig. 3-5a). Using the Janus-type TBDMS-β-CD dimer **3** as a control, the results of the NOESY spectrum (Fig. 3-4b) and the MacroModel calculation (Fig. 3-5b) demonstrate that one of the TBDMS groups is self-included in the CD cavity. These structures suggest that the self-included trialkyl silyl group may be involved in the enhanced guest inclusion ability by constructing a more hydrophobic inner space. In fact, we previously observed that the Janus-type TBDMS-β-CD dimer shows a higher inclusion ability toward unsaturated fatty acid esters than the corresponding β-CD dimer without substituents at both ends (Chapter 2). In addition, the bottom views of the structures of Janus-type β-CD dimers indicate that the TIPS groups more effectively block the opening at the end of the tube through dense packing (Fig. 3-5c). Compared with the TBDMS groups, this provides a more hydrophobic inner space to the tubular host. For the Janus-type TBDMS-β-CD dimer **3**, some small gaps appear to be created, which may be because the TBDMS group is not large enough to fill the space (Fig. 3-5d). This observation can explain the higher inclusion ability of **6** bearing

TIPS substituents compared to the corresponding CD dimer bearing TBDMS substituents. Moreover, it indicates that changing the molecular size of the terminal hydrophobic substituents may control the inclusion ability of the CD dimer.

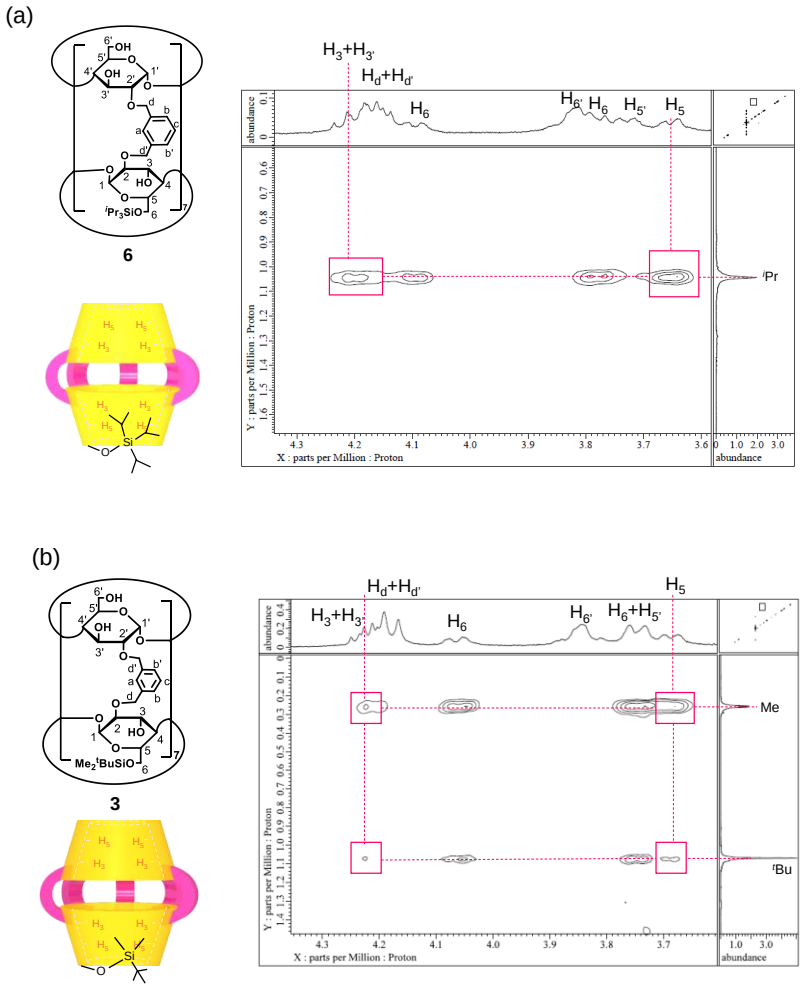

Figure 3-4. NOESY spectra and proposed self-inclusion structures of (a) **6** and (b) **3** in mehtanol-d_4.

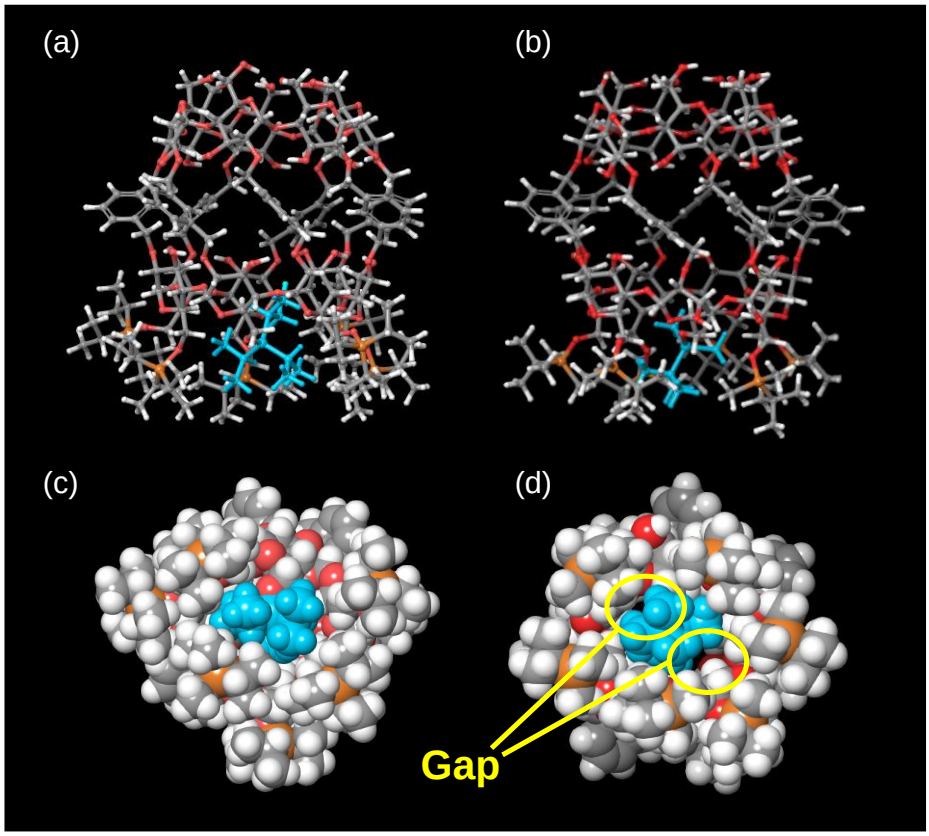

Figure 3-5. Optimized structure of (a, c) **6** and (b, d) **3** as obtained from Macromodel calculations (Monte Carlo Conformational Search, OPLS 2005 force fields). (a, b) Side views are shown with a ball-and-stick representation, (c, d) Bottom views are shown with a space-filling representation. Color labels: gray, carbon; red, oxygen; orange, silicon; white, hydrogen, except for a self-included trialkylsilyl group which is shown with blue label.

3.3 Conclusions

In conclusion, a new Janus-type CD dimer bearing seven TIPS groups at one end is successfully synthesized from the TIPS-β-CD dimer through the selective removal of seven TIPS groups at one end with TBAF. This Janus-type CD dimer exhibits a two-fold higher inclusion ability for unsaturated fatty acid esters compared with the corresponding CD dimer bearing seven TBDMS groups at one end. This enhanced inclusion ability can be explained by the more effective blocking of the opening at the end of the tube by the TIPS groups, leading to the formation of a more hydrophobic inner space. Changing the terminal trialkylsilyl groups to other substituents with a different size and hydrophobicity should allow the inclusion ability and inclusion selectivity of the Janus-type tubular host to be tuned freely. We offered novel possibilities for the inclusion behavior of cyclodextrin, which had been considered difficult to achieve selective recognition of unsaturated fatty acids.

3.4 Experimental Section

3.4.1 Materials and Methods

Sodium hydride (60%) and tetrabutylammonium fluoride (ca. 1 mol/L in tetrahydrofuran) were purchased from Tokyo Chemical Industry (Japan). 1,4-Dioxane was purchased from Wako Pure Chemical Industries (Japan). These reagents were used without further purification. TIPS-β-CD,[5] the TBDMS-β-CD dimer,[6] and the Janus-type β-CD dimer bearing TBDMS substituents[7] were prepared according to our previously reported method. ^{1}H and ^{13}C NMR spectra were recorded on a JEOL NMR system (400 MHz).

The following abbreviations were used for chemical shift multiplicities: s = singlet, d = doublet, t = triplet, q = quartet, m = multiplet. NMR signal assignments were based on additional 2D-NMR spectroscopy (e.g., COSY and HSQC). Infrared (IR) spectra were obtained with a Spectrum 100FT-IR spectrometer (Perkin Elmer). MALDI-TOF MS spectra were measured by Bruker Autoflex III. MALDI-HRMS spectra were measured by JEOL Spiral TOF/TOF JMS-S3000. Melting points were measured with BUCHI Melting point B-545. Elemental analysis was performed with Perkin Elmer 240C. HPLC was performed using a Shimadzu Prominence HPLC system equipped with a Soft 400 ELSD detector.

3.4.2 Synthesis of TIPS-β-CD dimer 5

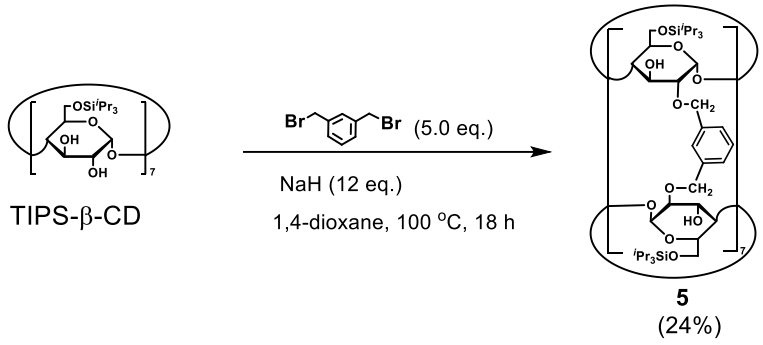

Scheme 3-2. Synthesis of **5**.

Under a N_2 atmosphere, dried TIPS-β-CD (300 mg, 0.14 mmol) and sodium hydride (60% content, 65 mg, 1.6 mmol), which was washed with hexane twice to remove the oil before use, were dissolved in 1,4-dioxane (10 mL) and the reaction mixture was refluxed for 1 hour. Then α,α'-dibromo-*m*-xylene (180 mg 0.67 mmol) dissolved in 1,4-dioxane (2 mL) was added dropwise, and the mixture was stirred overnight under reflux conditions. The reaction was quenched with methanol (4 mL) and the solvent was evaporated in vacuo. The residue was dissolved in chloroform (20 mL) and washed with brine (15 mL). After the solvent was removed in vacuo, the resulting solid was purified by silica gel column chromatography (hexane/ethyl acetate, in a gradient 15:1 to 10:1) to give compound **5** (83 mg, 24% yield). R_f 0.7 (*n*-hexane/ethyl acetate = 4/1); mp: 238 °C (decomp); ^{1}H NMR (400 MHz, chloroform-*d*): δ 1.02 (s, 294H), 3.33 (dd, *J* = 10, 3.2 Hz, 14H), 3.43-3.48 (m, 14H), 3.61 (m, 16H), 3.62 (d, *J* = 7.6 Hz, 14H), 3.74 (d, *J* = 10.8 Hz, 14H), 4.00 (d, *J* = 7.6 Hz, 14H), 4.13-4.19 (m, 28H), 4.85 (d, *J* = 3.2 Hz, 14H), 5.01 (s, 14H), 5.21 (d, *J* = 10.4 Hz, 14H), 7.10 (d, *J* = 7.2 Hz, 14H), 7.26 (d, 7H), 7.73 (s, 7H) ^{13}C NMR (100 MHz, chloroform-*d*): δ 12.26, 18.05, 62.34, 72.01, 73.57, 76.05, 82.20, 82.65, 101.97, 128.11, 128.57, 130.49, 137.74; MALDI-TOF MS: *m/z* = 5196 $[M+Na]^+$; Anal. Calcd for $C_{266}H_{462}O_{70}Si_{14}•7H_2O$: C, 60.28; H, 9.05. Found: C, 60.38; H, 9.09; FT-IR (cm^{-1}): 3423, 2939, 2890, 2865, 1462, 1384, 1361, 1326, 1158, 1087, 1041, 919, 881, 781, 679, 565, 527.

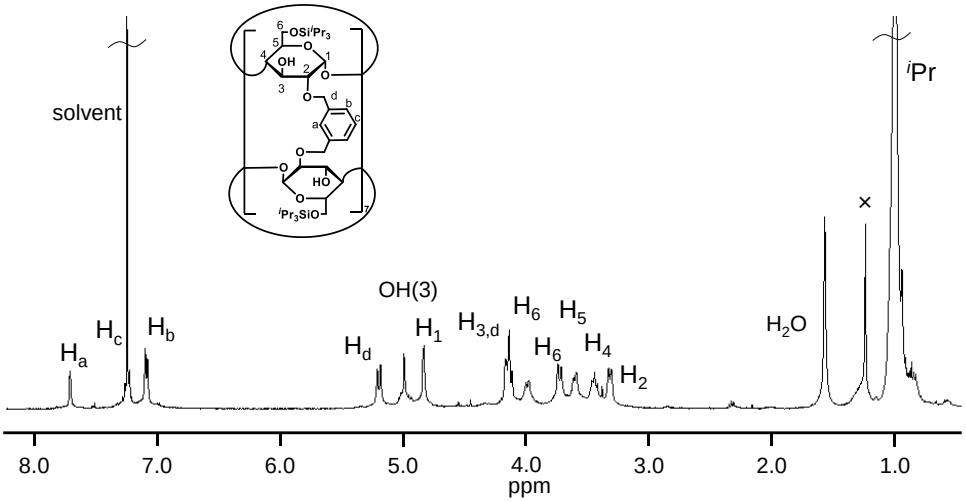

Figure 3-6. ^{1}H NMR spectrum of **5** in chloroform-*d* at 25 °C.

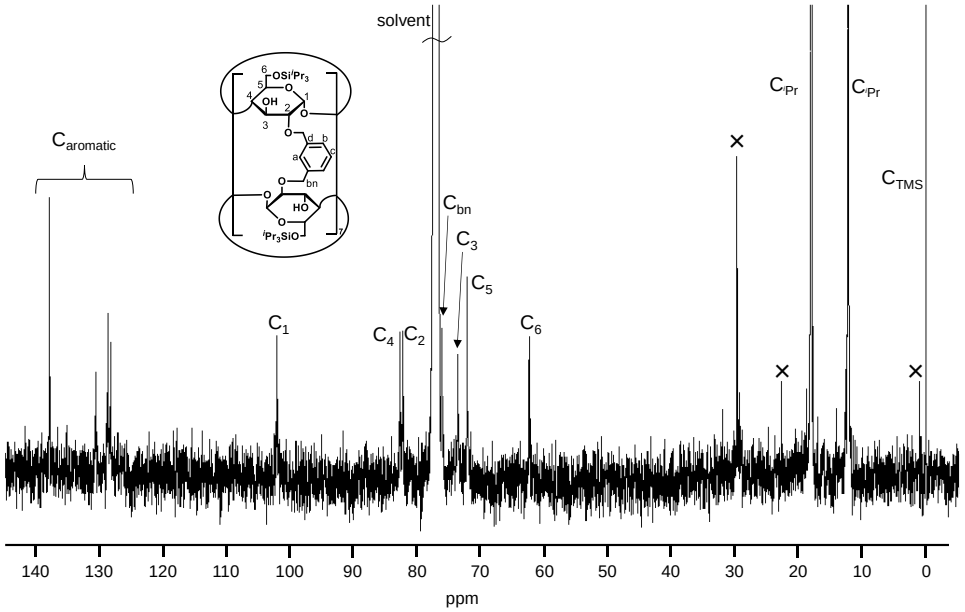

Figure 3-7. ^{13}C NMR spectrum of **5** in chloroform-*d* at 25 °C.

3.4.3 Synthesis of Janus-type TIPS-β-CD dimer 6

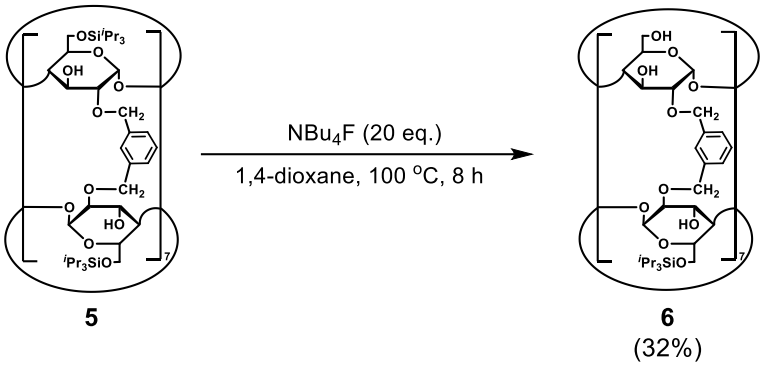

Scheme 3-3. Synthesis of **6**.

5 (40 mg, 7.9 μmol) and tetrabutylammonium fluoride (ca. 1 mol/L in tetrahydrofuran, 160 μL, ca. 160 μmol) were dissolved in 1,4-dioxane (6.0 mL). The reaction mixture was stirred for 8 h at 100 °C. After the solvent was removed in vacuo, the resulting solid was dissolved in methanol (10 mL), followed by the addition of DOWEX 50WX8-400 (H^+-form, excess) and calcium carbonate (powder, excess). DOWEX 50WX8-400 and calcium carbonate were removed by filtration and the solvent was removed in vacuo. The resulting solid was purified by silica gel column chromatography (chloroform/methanol, in a gradient 10:1 to 6:1). The residual solid was recrystallized by slow diffuse of methanol vapor into the chloroform solution to give **6** (10.3 mg, 32% yield). R_f 0.6 ($CHCl_3$/MeOH = 4/1); mp: 271 °C (decomp); ^{1}H NMR (400 MHz, acetone-d_6): δ 1.07 (m, 147H), 3.36-3.39 (d, 14H), 3.50-3.54 (m, 14H), 3.77-3.85 (m, 28H), 4.15-4.28 (m, 42H), 4.87 (d, J = 4.0 Hz, 7H), 4.93 (d, J =4.0 Hz, 7H), 5.23 (d, J =10.4 Hz, 7H), 5.28 (d, J =10.4 Hz, 7H), 7.15 (t, J = 6 Hz, 14H), 7.23 (t, J = 7.6 Hz, 7H), 7.68 (s, 7H); ^{13}C NMR (100 MHz, chloroform-*d*): δ 11.32, 17.11, 61.31, 70.39, 71.23, 73.05, 75.30, 80.35, 81.46, 81.82, 101.22, 127.23, 127.78, 129.47, 136.49, 136.81; HRMS (MALDI) : calcd. for $C_{203}H_{322}O_{70}Si_7Na$: 4098.99139 $(M + Na)^+$, found 4098.9854.

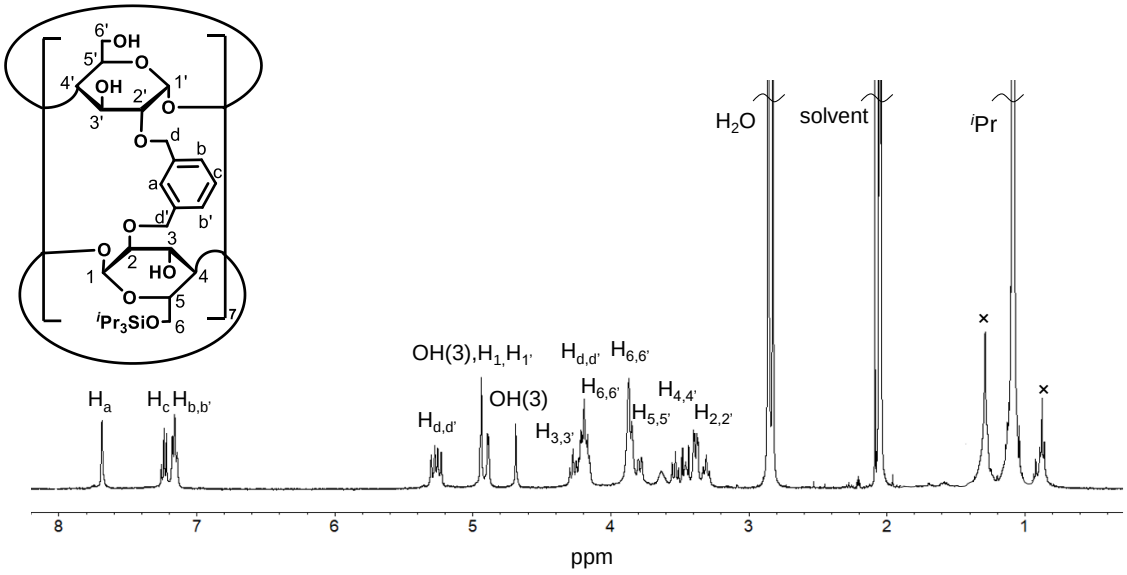

Figure 3-8. ^{1}H NMR spectrum of **6** in acetone-d_6 at 25 °C.

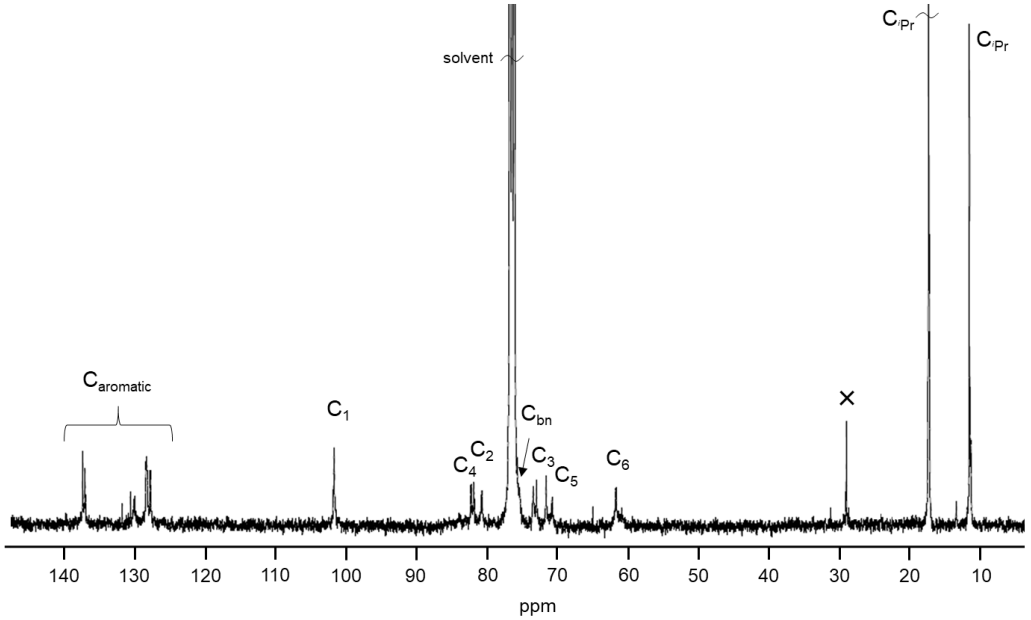

Figure 3-9. ^{13}C NMR spectrum of **6** in chloroform-*d* at 25 °C.

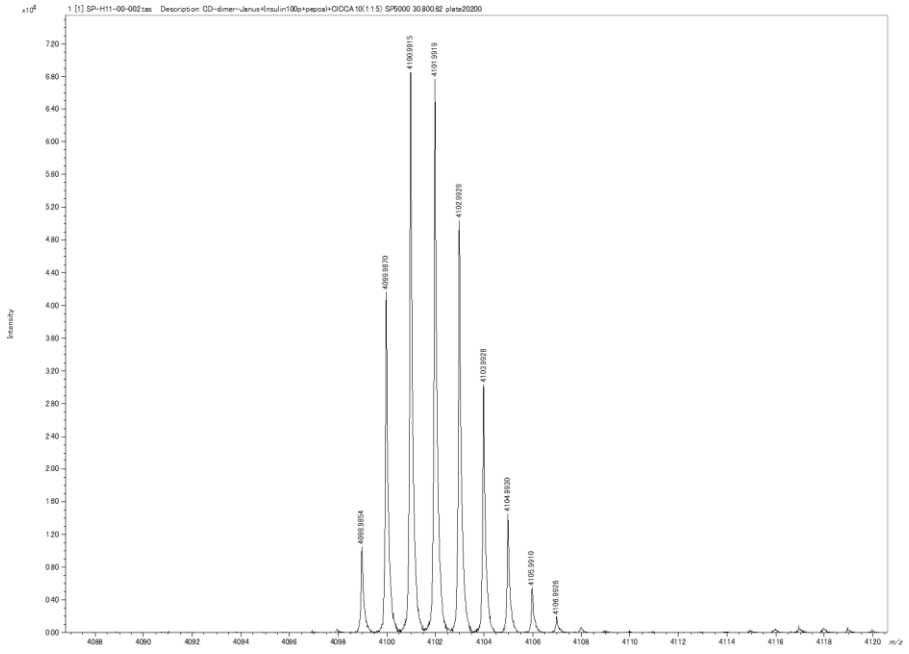

Figure 3-10. HRMS (MALDI) spectrum of **6**.

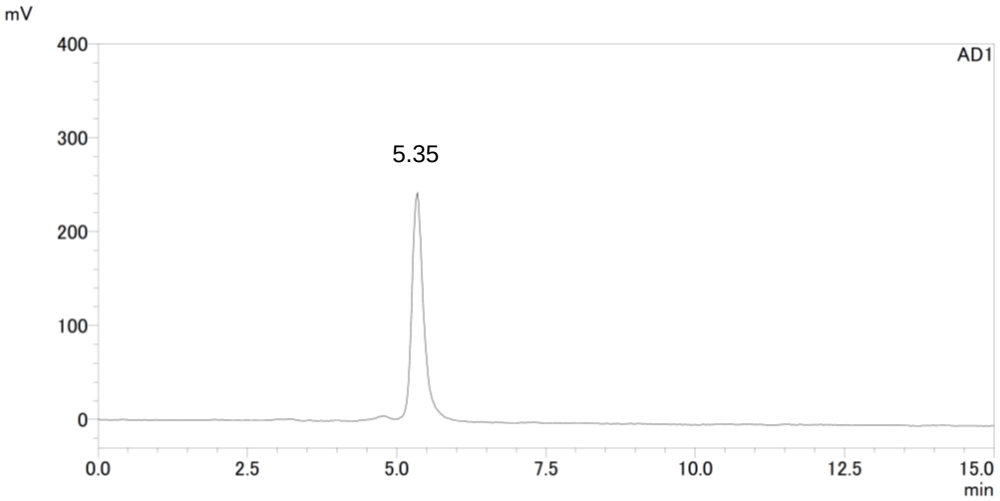

Figure 3-11. HPLC chromatogram of **6**. Column: NACALAI TESQUE, COSMOSIL 5SL-II Packed Column (250 mm × 4.6 mm i.d.); mobile phase: chloroform/methanol = 2/1 (v/v); flow rate: 1.0 ml min^{-1}; temperature: 25 °C; detector: ELSD.

3.4.4 ^{1}H NMR Spectral Changes Observed for 6 upon Addition of Unsaturated Fatty Acid Esters in Methanol-d_4 and Titration Curves for Their Complex Formation

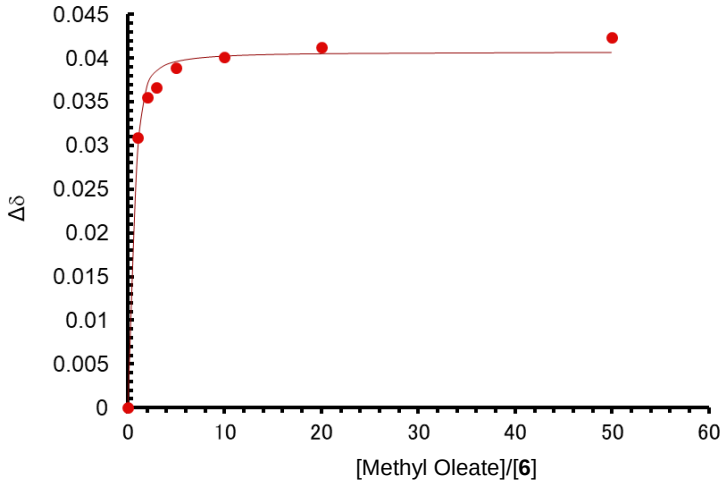

Figure 3-12. ^{1}H NMR titration curve for complex formation between **6** and methyl oleate in methanol-d_4 at 25 ºC. The proton signal of **6** around 5.2 ppm was used for titration.

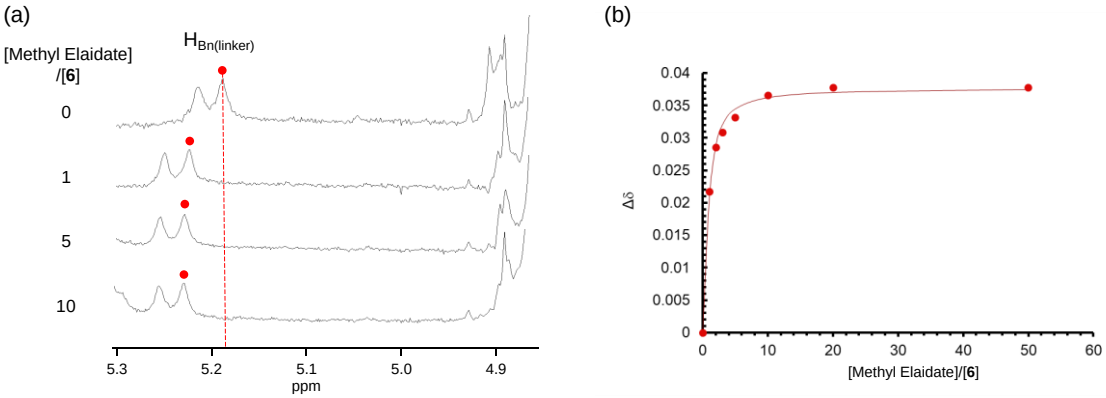

Figure 3-13. (a) ^{1}H NMR spectral changes observed for **6** (5.0×10^{-4} M) upon addition of methyl elaidate in methanol-d_4 at 25 ºC. (b) ^{1}H NMR titration curve for complex formation between **6** and methyl elaidate in methanol-d_4 at 25 ºC. The proton signal of **6** around 5.2 ppm was used for titration.

3.4.5 Job Plots for Complexes between 6 and Unsaturated Fatty Acid Esters in Methanol-d_4

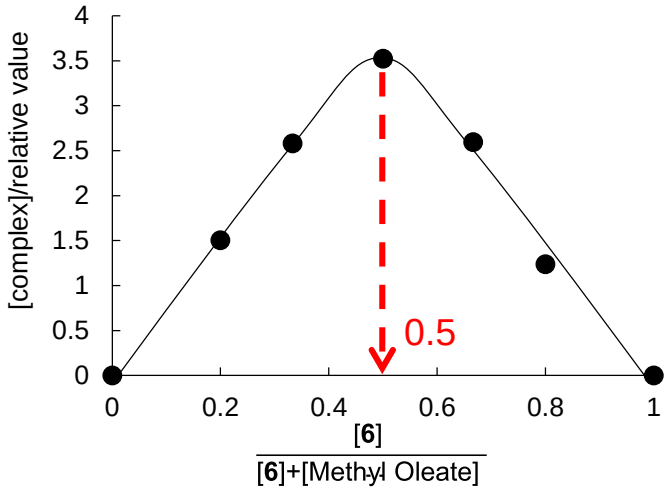

Figure 3-14. Job plot for complex between **6** and methyl oleate in methanol-d_4 at 25 ºC.

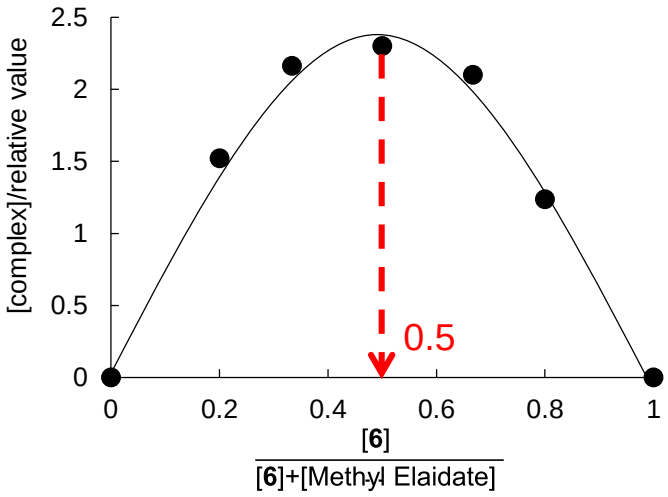

Figure 3-15. Job plot for complex between **6** and methyl elaidate in methanol-d_4 at 25 ºC.

3.4.6 NOESY spectra of TIPS-β-CD dimer 5 and TBDMS-β-CD dimer 2

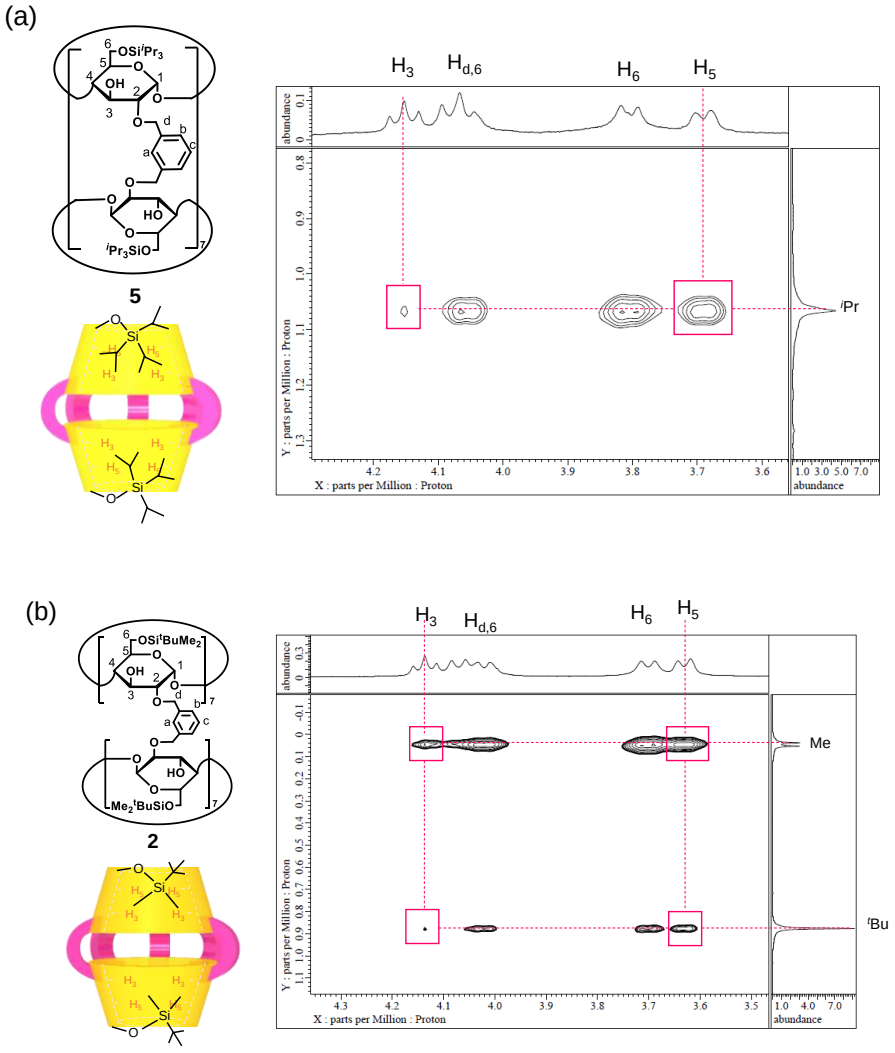

Figure 3-16. NOESY spectra and proposed self-inclusion structures of (a) **5** and (b) **2** in cyclohexane-d_{12}.

3.4.7 Optimized Structure Obtained from Calculations

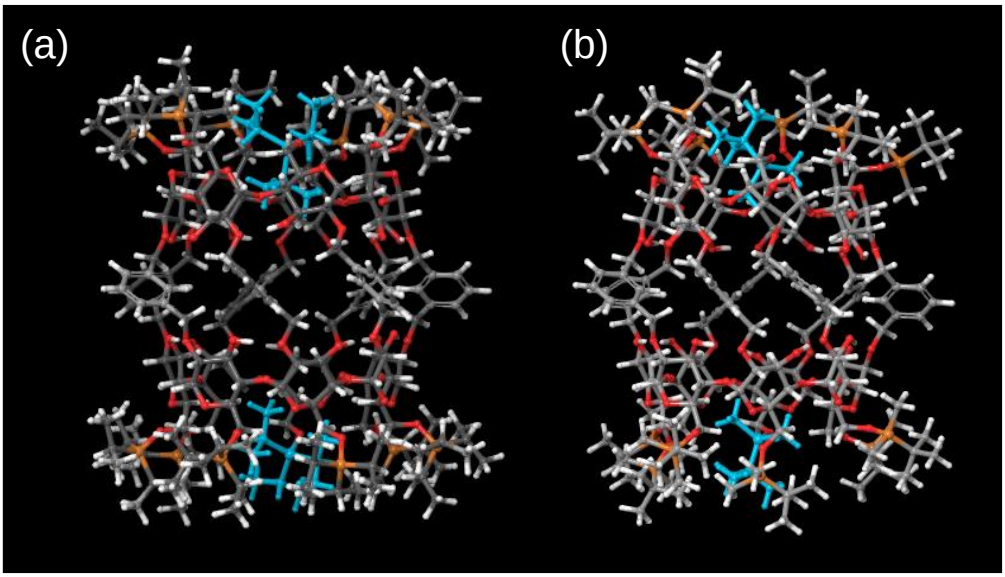

Figure 3-17. Optimized structure of (a) **5** and (b) **2** as obtained from Macromodel calculations (Monte Carlo Conformational Search, OPLS 2005 force fields) with a ball-and-stick representation. Color labels: gray, carbon; red, oxygen; orange, silicon; white, hydrogen, except for a self-included trialkylsilyl group which is shown with blue label.

References and Notes

8) a) C. T. Avetta, B. J. Shorthill, C. Ren, T. E. Glass, *J. Org. Chem.* **2012**, *72*, 851–857. b) K. Yazaki, Y. Sei, M. Akita, M. Yoshizawa, *Nat. Commun.* **2014**, *5*, 5179. c) K. Fujimoto, S Yamada, M. Inouye, *Chem. Commun*. **2009**, 7164–7166. d) B. J. Shorthill, C. T. Avetta, T. E. Glass, *J. Am. Chem. Soc*. **2004**, *126*, 12732–12733. e) S. Mosca, D. Ajami, J. Rebek, Jr. *Proc. Natl. Acad. Sci. USA* **2015**, *112*, 11181–11186. f) K. Niki, T. Tsutsui, M. Yamashina, M. Akita, M. Yoshizawa, *Angew. Chem. Int. Ed.* **2020**, *59*, 10489–10492. g) K. Wang, J. H. Jordan, B. C. Gibb, *Chem. Commun*. **2019**, *55*, 11695‑11698.

9) a) R. M. Claramunt, F. Herranz, M. D. Santa Maria, C. Jaime, M. d. Federico, J. Elguero, *Biosens. Bioelectron.* **2004**, *20*, 1242–1249; b) K. Samanta, W. Sicking, C. Schmuck, *Eur. J. Org. Chem.* **2018**, 6515–6518.

10) M. Bols, C. M. Pedersen, *J. Org. Chem.* **2017**, *13*, 93–105.

11) (a) K. O. Christe, W. W. Wilson, R. D. Wilson, R. Bau, J. A. Feng, *J. Am. Chem. Soc.* **1990**, *112*, 7619–7625. (b) M. Y. Kobayashi, K. Inamoto, Y. Kondo, *Chem. Lett.* **2014**, *43*, 477–479.

12) T. Kida, T. Iwamoto, Y. Fujino, N. Tohnai, M. Miyata, M. Akashi, *Org. Lett.* **2011**, *13*, 4570−4573.

13) S. Ito, C. Kogame, M. Akashi, T. Kida, *Tetrahedron Lett.* **2016**, *57*, 5243–5245.
14) Janus-type β-CD dimer bearing TBDMS substituents were prepared according to Chapter 2.

Conclusions

In this study, we succeeded in developing novel β-CD dimers (β-CD dimer capsules and β-dimer tubes) with various numbers of linkers and various types of substituents at the 6-*O*-position. We achieved high chiral recognition of naphthalene derivatives and selective inclusion of *cis*-unsaturated fatty acid esters in organic solvents, which were not realized by conventional CD dimers.

In Chapter 1, the synthesis of β-CD dimer in which two 6-*O*-modified β-CD are connected by a single linker, its inclusion ability and chiral recognition ability for aromatic guests in organic solvents was described. The β-CD dimer bearing a single *m*-xylylene linker showed high recognition ability toward pyrene and high chiral recognition ability toward 1-NEA due to effective cooperation of the two CD rings in guest inclusion. Moreover, by utilizing chiral recognition with the β-CD dimer in cyclohexane, a kinetic resolution of racemic 1-NEA via enantioselective *N*-benzoylation is attained with an enantiomer excess of up to 87%.

In Chapter 2, a Janus-type TBDMS-β-CD dimer with one end fully modified and the other end unmodified is facilely synthesized from the TBDMS-β-CD dimer by controlling the elimination conditions of the TBDMS groups. The Janus-type TBDMS-β-CD dimer exhibits inclusion selectivity for *cis*-unsaturated fatty acid esters over the corresponding *trans* isomers and saturated fatty acid esters. In particular, the CD molecular tube shows an extremely high inclusion ability toward DHA ester in methanol-d_4.

In Chapter 3, a new Janus-type CD dimer bearing seven TIPS groups at one end is successfully synthesized from the TIPS-β-CD dimer through the selective removal of seven TIPS groups at one end with TBAF. This Janus-type CD dimer exhibits a two-fold higher inclusion ability for unsaturated fatty acid esters compared with the corresponding CD dimer bearing seven TBDMS groups at one end synthesized in Chapter 2. This enhanced inclusion ability can be explained by the more effective blocking of the opening at the end of the tube by the TIPS groups, leading to the formation of a more hydrophobic inner space. Changing the terminal trialkylsilyl groups to other substituents with a different size and hydrophobicity should allow the inclusion ability and inclusion selectivity of the Janus-type tubular host to be tuned freely.

Based on the findings obtained in this study, it is possible to design a tailor-made CD dimer host that fits the structure of the target guest molecule well by appropriately choosing the type of CD, the type and number of linkers, and the type of terminal substituents. The CD dimers synthesized in this way will realize precise molecular recognition that is not expressed by conventional host molecules and greatly contribute to the development of supramolecular chemistry, separation/analytical chemistry, organic synthesis, and biochemistry.

List of publications

1) Effective Guest Inclusion by a 6-*O*-Modified β-Cyclodextrin Dimer in Organic Solvents
Chizuru Asahara, Takuya Iwamoto, Mitsuru Akashi, Hajime Shigemitsu, and Toshiyuki Kida
ChemPlusChem **2018**, *83*, 868–873.

2) Novel Molecular Tube Fully Modified at One End: Selective Inclusion of *cis*-Unsaturated Fatty Acid Esters
Chizuru Kogame-Asahara, Shogo Ito, Hitomi Iguchi, Ai Kazama, Hajime Shigemitsu, and Toshiyuki Kida
Chem. Commun. **2020**, *56*, 1353–1356.

3) Remote Substituent Effect of Janus-type Molecular Tubes on Inclusion of Unsaturated Fatty Acid Esters
Chizuru Kogame-Asahara, Hitomi Iguchi, Kenichiro Honda, Hajime Shigemitsu, and Toshiyuki Kida
ACS Omega **2021**, *6*, 3227–3231.

Supplementary publications

1) Unique Cation Binding Capability of Cyclic Oligo(L-lactic acid) (L-COLA)
Chizuru Kogame, Toshiyuki Kida, Tomoko Fujiwara, and Mitsuru Akashi
Tetrahedron Lett. **2015**, *56*, 1675–1678.

2) Facile Synthesis of Novel Cyclodextrin Dimer Capsules and Their Inclusion Ability towards Aromatic Guests in a Nonpolar Solvent
Shogo Ito, Chizuru Kogame, Mitsuru Akashi, and Toshiyuki Kida
Tetrahedron Lett. **2016**, *57*, 5243–5245.

3) Control of Guest Inclusion and Chiral Recognition Ability of 6-*O*-Modified β-Cyclodextrins in Organic Solvents by Aromatic Substituents at the 2-*O* Position
Justine M. Kalaw, Ryusuke Yamamoto, Chizuru Kogame-Asahara, Hajime Shigemitsu, and Toshiyuki Kida
ChemPlusChem **2020**, *85*, 1928–1933.